

IODP Proposal Coversheet

Hyuga-Nada Observatory	Received for: 2020-10-01
------------------------	--------------------------

Title

Drilling and monitoring in Hyuga-Nada: Unveiling effects of ridge subduction on slow earthquakes

Proponents

Rie Nakata, Masataka Kinoshita, Yoshitaka Hashimoto, Yohei Hamada, Laura Wallace, Tianhaozhe Sun, Eiichiro Araki, Yusuke Yamashita, Aitaro Kato, Patrick Fulton, Hiroko Kitajima, Serge Lallemand, Seiichi Miura, Kimihiko Mochizuki, Kazushige Obara, Demian Saffer, Yuzuru Yamamoto, Yusuke Yokota, Takashi Tonegawa, Miкия Yamashita

Keywords

slow earthquake, seamount, subduction

Area

Hyuga-Nada offshore Kyushu Japan

Proponent Information

Proponent:	Rie Nakata
Affiliation:	University of Tokyo
Country	Japan

Permission granted to post the coversheet/site table on www.iodp.org

No

Abstract

Shallow slow earthquakes, which last minutes to years, are important indicators of subduction megathrust slip behavior and future seismic and tsunami potential. Subducting plate roughness and seamounts have been proposed to promote slow earthquakes by inducing local geomechanical and hydrogeological anomalies. The Hyuga-Nada region offshore Kyushu, Japan is an outstanding locale for drilling and observatory experiments to investigate these effects.. In this region, slow earthquakes are repeatedly observed on and near the subducting Kyushu-Palau-Ridge, KPR, chain of seamounts thus providing excellent opportunities to explore the effects of seamounts on geomechanical/hydrological/thermal properties, and ultimately seismic coupling. Long-term monitoring enabled by a planned permanent network (N-net) will allow subsurface processes during frequent (~1 year) periodical slow earthquakes and ~M7 earthquakes (~20-30 year interval) to be captured with high fidelity. Drilling, logging, and coring will provide key constraints on stress state, hydrological processes, and sediment physical properties in the region above the ridge.

We propose to drill and install observatories at three primary locations in Hyuga-Nada to address two hypotheses: 1) Seamount subduction modulates stress and pore pressure, creates fracture networks and influences the thermal and hydrological state of the margin. 2) The spatiotemporal distribution of slow earthquakes is strongly influenced by seamount subduction through the processes outlined in Hypothesis 1. We will drill three primary holes at three distinct sites relative to the seamount, to (1) measure physical properties, and (2) describe deformation by LWD, APCT-3, and core analysis to characterize in-situ stress state, fracture density, heat flow, and pore fluid flow. Spatial variations in the upper plate disruption caused by seamount subduction will be revealed by comparing results from holes in the leading and lateral edges, and top of the currently subducting seamount; and these will constrain geomechanical, hydrological, and thermal models. At two of the sites, we will install a "Fiber-CORK" observatory equipped with conventional pressure and temperature sensors and cutting-edge fiber-optic sensors. One site will be connected to the N-net node for real-time data streaming. The combination will fill a gap in slip durations currently observable in this region with seismic and geodetic instrumentation. Fully characterizing slow earthquakes will reveal the degree to which they accommodate plate motion, and whether strain is accumulated for future earthquakes.

Scientific Objectives

We drill, core, and install observatories at three primary drill sites to address scientific questions;

(1) What is the stress and consolidation state? Do they differ between the leading side, the lateral side and the top of the seamount? Do they vary azimuthally around the subducting Toi Seamount?: How is the seamount disrupting the upper plate?: How does the shallow state relate to the state of the deep plate interface?

(2) Is temperature on the plate interface anomalously lower or higher where the KPR subducts?: What is the hydrological state? Does subduction of seamount enhance advective fluid transfer, ultimately affecting the thermal state?

(3) Does Slow Slip Event (SSE) happen prior, concurrently or after tremors and Very Low Frequency Earthquakes (VLFE)?: When VLFEs and tremors migrate from the NS to EW segments, do SSEs also migrate in a similar manner? Do SSEs occur in the NS segment even when only the VLFEs and tremors occur in the EW segment, and vice versa? Does the SSE in the NS segment occur even when only the VLFEs and tremors occur in the EW segment? Do subsurface elastic structures change over time associated with slow earthquake activities?

Non-standard measurements technology needed to achieve the proposed scientific objectives

Proposal History

Submission Type:

Resubmission from previously submitted proposal

Review Response:

Thank you very much for reviewing our proposal. We are thrilled to hear positive and encouraging comments. We have organized an online international workshop (Sep 9, 11, 13, 2020) along with proponent meetings and have refined our proposal.

The major revisions from the proposal are

- Our two hypotheses focus on the seamount subduction (Hypothesis 1), the slow earthquake events and their relationships (Hypothesis 2) to simplify our drilling plan. The segmentation of the Philippine Sea Plate into the Shikoku and West-Philippine Basins is now treated as an important background information.
- We fully reviewed the drill sites and selected the sites that best addresses our objectives (Section 6.1). Due to the increased focus on the seamount subduction, we added SKP-14A (top of the seamount) as a new primary to evaluate the 3D effects of the seamount subduction. To fit our program in an allocated cruise time, we unfortunately have to remove SKP-03A from the list. We also removed the contingency sites.
- Our observatory is now called "fiber-CORK" rather than DAS to emphasize the versatile capability of fiber cable sensing.
- We reviewed seismic sections with other seismological, geophysical and geological information to clarify the role of the drill sites.
- We added Section 8 "Operational Options" to fully describe potential issues when one or both of observatories are not successful, along with potential issues in coring and LWD.
- As pointed out, Challenge 14 is the correct one. We fixed it. Also we expanded the descriptions about the hydrological effects throughout the proposal.
- We improved the descriptions of SSEs, tremors and VLFEs in the Hyuga-Nada region in Section 3.2 and Figure 5 and more clearly associated with our site selection and observatory plan in Section 5.3, 6.1 and 6.3.
- We added Section 2 to clearly express the uniqueness of Hyuga-Nada and what we can add and complement the works in other margins especially in Hikurangi, Nankai and Costa Rica.

Proposed Sites

(Total proposed sites: 7; pri: 3; alt: 4; N/S: 0)

Site Name	Position (Lat, Lon)	Water Depth (m)	Sed	Bsm	Total	Brief Site-Specific Objectives
SKP-11A primary	31.512 132.2959	1980	700	0	700	Core and log sedimentary section in middle slope of wedge in the leading side of a subducting seamount for lithology and physical properties. Establish a borehole observatory to measure time series of pore fluid pressure, temperature and strain.
SKP-01B alternate	31.5388 132.3542	2090	700	0	700	Core and log sedimentary section in middle slope of wedge in the leading side of a subducting seamount for lithology and physical properties. Establish a borehole observatory to measure time series of pore fluid pressure, temperature and strain.
SKP-12A alternate	31.5797 132.322	2000	700	0	700	Core and log sedimentary section in middle slope of wedge in the leading side of a subducting seamount for lithology and physical properties. Establish a borehole observatory to measure time series of pore fluid pressure, temperature and strain.
SKP-13A primary	30.9057 132.2435	2690	800	0	800	Core and log sedimentary section in middle slope of wedge in the western side of a subducting seamount for lithology and physical properties. Establish a borehole observatory to measure time series of pore fluid pressure, temperature and strain.
SKP-02A alternate	30.9152 132.2612	2815	800	0	800	Core and log sedimentary section in middle slope of wedge in the western side of a subducting seamount for lithology and physical properties. Establish a borehole observatory to measure time series of pore fluid pressure, temperature and strain.
SKP-14A primary	31.0144 132.4401	2940	900	0	900	Core and log sedimentary section in a middle slope of wedge at the top of a subducting seamount for lithology and physical properties.
SKP-15A alternate	30.9434 132.4925	2880	900	0	900	Core and log sedimentary section in a middle slope of wedge at the top of a subducting seamount for lithology and physical properties.

Contact Information

Contact Person:	Rie Nakata
Department:	Earthquake Research Institute
Organization:	University of Tokyo
Address:	1-1-1 Yayoi Bunkyo Tokyo 113-0032 Japan
Email/Phone:	rnakata@eri.u-tokyo.ac.jp; Phone: 81358411767

Proponent List

First Name	Last Name	Affiliation	Country	Role	Expertise
Rie	Nakata	University of Tokyo	Japan	Principal Lead and Data Lead	Seismic imaging
Masataka	Kinoshita	University of Tokyo	Japan	Other Lead	Heat flow, Observatory
Yoshitaka	Hashimoto	Kochi University	Japan	Other Lead	Tectonics, Geomechanics
Yohei	Hamada	Japan Agency for Marine-Earth Science and Technology	Japan	Other Lead	Logging
Laura	Wallace	GNS	New Zealand	Other Lead	Geodesy
Tianhaozhe	Sun	Geological Survey of Canada	Canada	Other Lead	Geomechanics, Observatory
Eiichiro	Araki	Japan Agency for Marine-Earth Science and Technology	Japan	Other Lead	Observatory
Yusuke	Yamashita	University of Kyoto	Japan	Other Lead	Seismology
Aitaro	Kato	University of Tokyo	Japan	Other Proponent	Seismology
Patrick	Fulton	Cornell University	United States	Other Proponent	Hydrogeology, Heat flow, Geomechanics
Hiroko	Kitajima	Texas A&M University	Japan	Other Proponent	Hydrogeology, Geomechanics
Serge	Lallemand	Université Montpellier	France	Other Proponent	Geodynamics, Subduction zone
Seiichi	Miura	JAMSTEC	Japan	Other Proponent	Seismic imaging and acquisition
Kimihiro	Mochizuki	University of Tokyo	Japan	Other Proponent	Seismology, Seismic imaging
Kazushige	Obara	University of Tokyo	Japan	Other Proponent	Seismology

1. Introduction and Motivation

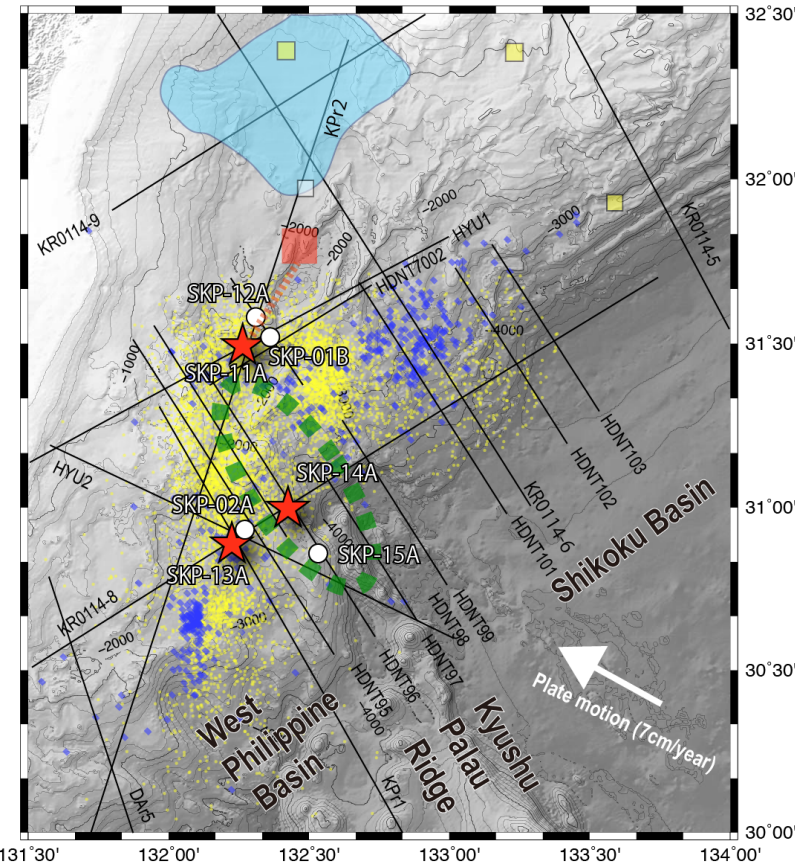
Slow earthquakes are important indicators of subduction megathrust slip behavior and future seismic and tsunami potential of these plate boundary faults (e.g. Obara and Kato 2016; Kano and Kato 2020). Slow earthquake (including slow slip) events are characterized by a long duration lasting from seconds to years. The recent recognition of shallow (<10 km) slow earthquakes highlights the importance of slip processes on subduction faults near the trench (Araki et al. 2017; Nakamura and Sunagawa, 2015; Davis et al. 2015; Wallace et al. 2016). Although underlying mechanisms behind slow earthquakes are not fully understood (Ikari et al. 2013; Obara and Kato 2016; Bürgmann 2018), subducting seamounts, a type of subducting plate roughness, are proposed to play a key role by inducing local geomechanical and hydrogeological anomalies (Barnes et al. 2020; Collot et al. 2017; Saffer and Wallace 2015; Sun et al. 2020b). This proposed drilling and monitoring plan (Figure 1) is clearly aimed to deepen our understanding of the impacts of seamounts on subduction zone processes including the occurrence of slow earthquake events.

The Hyuga-Nada region is located south of Japan, at a transition between the Nankai Trough and the Ryukyu Trench (Figure 2). Hyuga-Nada is an outstanding natural laboratory to explore the effects of seamounts on megathrust behavior and seismic coupling. Episodic shallow slow earthquake events occur around a currently subducting seamount (**Toi Seamount**, Figure 3), which is a part of the Kyushu-Palau-Ridge (KPR), a chain of seamounts. Remarkable details in the observed spatiotemporal migration patterns of the slow earthquake events clearly set Hyuga-Nada apart from the other subduction zones with similar settings (e.g., Hikurangi, Nankai and Costa-Rica). The target seamount is close to the trench and at much shallower depths than those targeted by the previous IODP projects. Hence, their effects will be evident even with our shallow drilling targets (< 1 km). The slow earthquake events repeatedly occur in the same area with a short recurrence interval (1-2 years), making detection and monitoring promising.

We will perform drilling, coring, logging and long-term monitoring at Hyuga-Nada in order to test the following hypotheses to address the effects of seamount subduction on megathrust mechanical, thermal, and hydrological state, and ultimately on its slip behavior:

- 1. Seamount subduction modulates stress fields, creates fracture networks and influences the thermal and hydrological state of the subduction margin.**
- 2. The majority of plate motion at Hyuga-Nada is accommodated by episodic slow earthquakes. The spatiotemporal distribution of slow earthquakes is strongly influenced by seamount subduction through the process outlined in Hypothesis 1.**

Our drilling sites are selected to address these interconnected phenomena. Three primary sites are located at distinct positions relative to the Toi Seamount; on the landward leading side (**SKP-11A** with **SKP-01B, 12A** as alternate), the lateral side (**SKP-13A** with **SKP-02A** as alternate) and the top of the seamount (**SKP-14A** with **SKP-15A** as alternate). Between these three sites, we expect significant contrast in geomechanical, hydrological and thermal states that are disrupted by the KPR. The leading (**SKP-01B, 11A, 12A**) and lateral (**SKP-02A, 13A**) sides situated within a seismically active region hosting many slow earthquakes, and the installation of observatories at these site will illuminate the entire sequence of slow earthquake events both in time and space. By combining the proposed logging, coring and monitoring program with high-quality seismic sections and seismological information already obtained, we will deepen understanding of seamount subduction effects on subduction fault slip behavior. The aims of our proposal dovetail with the IODP theme of “Earth-in-Motion”, and our investigations will contribute to understanding the mechanisms of earthquakes (Challenge 12) and the fluid flow controlled by the complexity of thermal and geomechanical conditions (Challenge 14).



Primary site	Location relative to Seamount	Tremor/VLFE	N-Net	Observatory	Coring	LWD	Alternate sites
SKP-11A	Leading	Rich	Yes	Yes	full	full	SKP-01B,12A
SKP-13A	West	Rich		Yes	full	full	SKP-02A
SKP-14A	Top	Sparse			full	full	SKP-15A

Figure 1 Bathymetry map of the proposed Hyuga-Nada drill sites. Our three primary sites (**SKP-11A**, **13A** and **14A**) are indicated by red stars, and the alternate sites by white circles. Black lines indicate existing seismic survey lines. The direction of the plate motion is shown by an arrow (DeMets et al. 2010). Light blue shaded area indicates the rupture area of 1968 Mw 7.5 earthquake (Yagi et al. 1999). Tremors (yellow dots) and very-low-frequency events (VLFEs; blue squares) migrated around the Toi Seamount (green dashed ellipse) from south to north on the West Philippine Basin side, and then from west to east to the Shikoku Basin side (Yamashita et al. 2015, 2019b; Tonegawa et al. 2020). Slow slip events (SSEs) were detected at GNSS-A stations indicated by yellow squares, but not at a station close to the tremor-VLFE clouds (Yokota and Ishikawa 2020). Red square is a planned N-Net node that the observatory at Site **SKP-11A** will be connected to. The N-net will be installed by the National Research Institute for Earth Science and Disaster Resilience by 2024, (<https://www.jishin.go.jp/main/suishon/honbu18b/cable20180710.pdf> in Japanese).

2. Why Hyuga-Nada and Relationships to Previous Drilling Projects

Hyuga-Nada provides exceptional opportunities to reveal relationships between slow earthquakes and structural/geomechanical/hydrological heterogeneities at the plate interface (seamounts) and the upper plate. Our scientific and drilling plan are focused on the role of subducting topography of a near-trench seamount to test hypotheses about stress and hydrological effects and their relationships with megathrust fault slip behaviors and slow earthquakes.

Although subducting seamounts are present in the region of IODP drilling at Costa Rica and Hikurangi, the influence of these seamounts on subduction processes were not a focus of either of these previous efforts, and nor were these experiments designed to address these features. In this proposal, we target a specific near-trench subducting seamount, which we refer to as the “**Toi Seamount**”, clearly imaged as a magnetic anomaly (Figure 3b) and as a topographic high in the seismic sections (Figure 4). We have positioned the primary sites, **SKP-11A**, **SKP-13A** and **SKP-14A**, to investigate three-dimensional variations in upper-plate properties associated with seamount subduction (Figure 1). The large dimensions of the seamount (at least 4-5 km high and 30-80 km wide) and its proximity to the trench ensure that shallow drilling (< 1 km) can capture the geomechanical and hydrological effects of the subducting seamount. In particular, the seamount is at 4 km below the seafloor (kmbsf) at **SKP-14A** and the associated deformation is clear in the seismic sections.

Hyuga-Nada is one of the best studied regions for seismicity related to shallow slow earthquakes thanks to dense seafloor seismic deployments (Yamashita et al. 2015). Compared with other subduction zones hosting shallow slow slip events (SSEs) (Hikurangi, Costa Rica, and Ecuador), the remarkable spatio-temporal migration of slow earthquakes has been suggested based on

studies of tremors and very low frequency earthquakes (VLFEs). However, geodetic measurements of seafloor deformation during the SSEs themselves are sparse (and based on datasets with high levels of noise; Yokota and Ishikawa 2020), greatly limiting our understanding of the occurrence of tremors and VLFEs in relation to slow slip events on the subduction interface. The migration appears to be controlled by the position of the Toi Seamount (Figures 3b, 5d). These provide outstanding monitoring opportunities in Hyuga-Nada to obtain in-depth understanding of slow earthquakes. We propose to install observatories at two locations (SKP-11A and 13A) above the documented area of rich slow earthquake activities to capture this temporal evolution (typically, slow earthquakes migrate from **SKP-02A** to **SKP-11A** within a few days). The short recurrence interval of tremor/VLFE episodes (1-2 years) and the high plate convergence rate (> 7 cm/year) ensure that a rich range of observations will be recorded in a proposed subseafloor network. Moreover, periodic occurrence of large plate-boundary earthquakes (Mw6.5-7.6, approximately every 25 years) is another strong motivation to install subseafloor observatories to investigate f the evolution of slow earthquake behaviour throughout the seismic cycle. A distinct advantage of this area is the planned permanent seafloor network, N-net, provides opportunities in streaming the observatory data in real time that are not readily available in most subduction zones outside of Japan. The proposed observatories at the Hyuga-Nada region will also be able to leverage co-located, continuous seafloor observations of the N-net to better resolve the spectrum of seismic to aseismic deformation processes in this region of seamount subductions.

2.1 Relationship to previous IODP drilling projects

Hyuga-Nada is located to the west of the Nankai subduction zone that has a long history of scientific drilling starting in 1973 and more frequently since 1990s with a total 13 ODP legs and IODP expeditions performed up to today (e.g. Taira et al. 1991; Kinoshita et al. 2009; Tobin et al. 2019). As part of recent drilling in the NanTroSEIZE project, observatories were installed during three IODP Expeditions (319, 365 and 380) and connected to a seafloor observatory

network (DONET). Formation pressure observations captured crustal deformation related to previously undetected slow slip events (Araki et al. 2017). The Nankai Trough has hosted past Great earthquakes and is currently strongly coupled interseismically. This is in contrast to the Hyuga-Nada region which is largely creeping and undergoing slip in episodic slow slip events. The drilling results and related research from the Nankai Trough serve as an important counterpoint to the weakly-coupled Hyuga-Nada region, which has not been drilled previously. The ability to contrast Nankai with Hyuga-Nada may explain why some subduction zones lock-up and slip in Great megathrust earthquakes, while others (like Hyuga-Nada) are dominated by creep, slow slip, and moderate to large earthquakes.

The Circulation Obviation Retrofit Kit (CORK) observatories installed during ODP Leg 205 successfully depicted triggered slow slip events offshore Nicoya Peninsula, Costa Rica, which are associated with tremors (Davis et al. 2015). There is some evidence for the role of seamounts in modulating interface slip behaviour (Ikari 2019). The drilling did not address the physical, hydrological or thermal effects of seamount subduction. The results from our focused drilling and observatory plan will help illuminating the processes in Costa Rica. IODP Expeditions 334 and 344 (Costa Rica Seismogenesis Project, CRISP) demonstrated that paleoseismic activities and deformation history of the incoming oceanic and upper plates in depth have been potentially caused by the ridge subduction into the erosional margin (e.g., Vannucchi et al. 2013; Hamahashi et al. 2017). Our drilling and coring results may serve as a good counterpart to the rough-surface subduction into the erosional margin.

The Hikurangi margin is a good counterpart to the Hyuga-Nada region in terms of slow earthquake activity and seamount subduction (Wallace et al. 2016; Todd et al. 2018). Hikurangi drilling projects (Expeditions 372 and 375) aimed to investigate the processes and in situ conditions that underlie SSEs at northern Hikurangi through coring, logging and monitoring *along the subduction axis* covering frontal thrusts, the upper plate and the incoming sedimentary succession. Barnes et al. (2020) documented complex and heterogeneous subducting inputs and

active splay faults clearly associated with the seamount subduction. However, the Hikurangi margin drilling project was not designed to investigate the effects of subducting seamounts nor their spatial (azimuthal) effects on upper plate or megathrust state, or ultimately on SSEs. ***Our proposal is specifically designed to understand 3D effects of the Toi seamount. The installation method and monitoring data analysis will be essential in carrying out/calibrating the Hyuga-Nada drilling monitoring plan. Comparing the results between the Hikurangi and Hyuga-Nada will definitely shed light on questions about how characteristics of seamounts (size, depth, and composition) affect characteristics of slow earthquakes and slips (duration, location, etc.) and eventually determine different seismic cycles.***

3. General setting

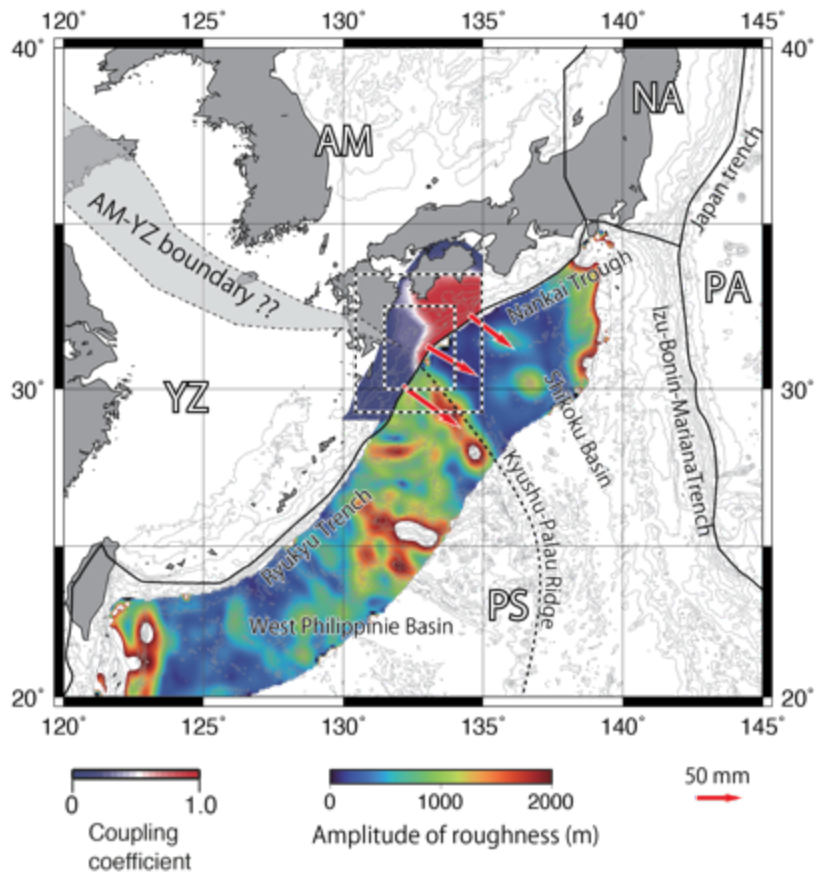


Figure 2 Tectonic setting around Hyuga-Nada; PA: Pacific Plate, PS: Philippine Sea Plate, NA: North American Plate, AM: Amurian Plate, YZ: Yangtze Plate; Ambiguous AM-YZ boundary is shown by a gray area. The coupling ratio in the Hyuga-Nada region is shown by a color scale from blue to red (Wallace et al. 2009). Red arrows represent relative motions of AM and YZ to PS based on the long-term GPS data. Low-frequency roughness (80-100 km of wavelength) of PS is represented by a rainbow color scale (Lallemand et al. 2018). A small rectangle with a broken line at the center indicates the map area of Figure 3, and a large rectangle shows the area of Figure 1.

Hyuga-Nada is situated along the convergent margin between the Philippine Sea Plate and the Amurian/Yangtze Plate (Sella et al. 2002), and is a transition zone between the Nankai Trough and the Ryukyu Trench (Figure 2). The KPR (trending N60W) divides the Philippine Sea Plate

(subducting in a NW direction) into the West Philippine and Shikoku Basins. The KPR is an aseismic remnant arc separated from the Izu-Bonin-Mariana arcs during the opening of the Shikoku Basin at 27~15 Ma (Ishizuka et al. 2011; Haraguchi et al. 2003). The basement of the West Philippine Basin is much older (>50 Ma) in the northernmost part (e.g., Hall et al. 1995; Deschamps and Lallemand 2002). Since ~5 Ma, the KPR subduction has been intercepting with the Nankai Trough and migrating southwestwards along the margin to its current position, following the movement of a trench-trench-trench triple junction at east between the Japan Trench, the Nankai Trough and the Izu-Bonin-Mariana Trench (Hall et al. 1995; Wu et al. 2016; Faccenna et al. 2018).

Sharp transition across the KPR in seismic coupling, characteristics of the incoming Philippine Sea Plate (age, heat flow and roughness), and wedge structures makes Hyuga-Nada a unique setting (Figures 2, 3, Wallace et al. 2009; Nishimura et al. 2018). The Shikoku Basin basement has a smooth surface, high heat flow, the plate interface hosts historic great subduction earthquakes, whereas the West Philippine Basin and KPR have a rough surface, very low heat flow, and low coupling with no history of great earthquakes (Ashi et al. 1999; Lallemand et al. 2018). Typical accretionary prisms develop east of the KPR, but there are faint internal structures in the region west of the KPR (Yamashita et al. 2019a).

3.1 KPR subduction

The obliquely subducting KPR extends northwest, and a strong positive magnetic anomaly (Figure 3b) and a mound-like structure in the seismic profiles (Figures 4g, h) indicate a currently subducting seamount, the Toi Seamount. The NW extension of the KPR was observed as a low-velocity belt by seismic tomography (Yamamoto et al. 2013; Figure 3b). Shallow deformed structures are recognized in the accretionary wedges in seismic images (Yamashita et al. 2019a). Advective hydrothermal circulation due to the subduction of the Toi Seamount is suggested to

cause an anomalously low local heat flow above the KPR estimated based on depths of Bottom Simulating Reflectors (BSRs) in the seismic sections (Figures 3a, 4a, b, Kinoshita et al. 2020).

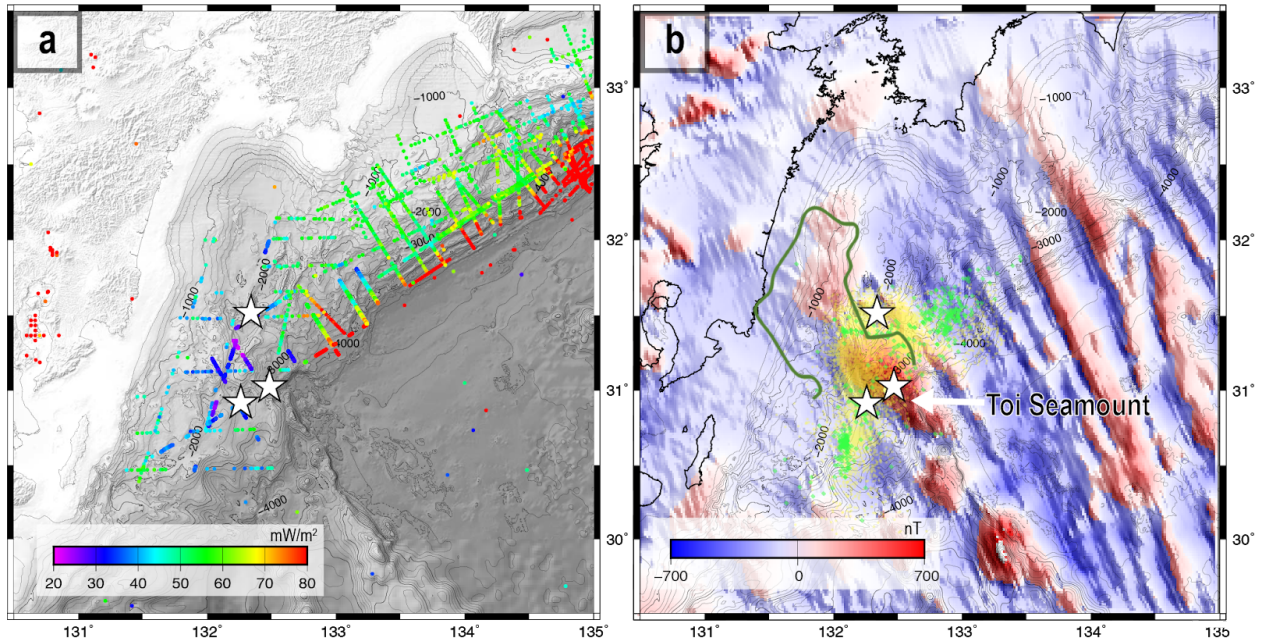


Figure 3 (a) Heat-flow and (b) total magnetic anomaly map in Hyuga-Nada. Contours in (a,b) are the seafloor depth. Stars indicate the proposed primary drill sites (see Figure 1). Yellow and green dots in (b) indicate the tremors (Yamashita et al. 2015, 2019b) and VLFEs (Tonegawa et al. 2020), respectively. Area in thick green curve in (b) is the subducted KPR inferred from the low velocity zone of the subducting slab (Yamamoto et al. 2013). The heat flow map was created based on the bottom simulating reflector (BSR) depths in seismic sections.

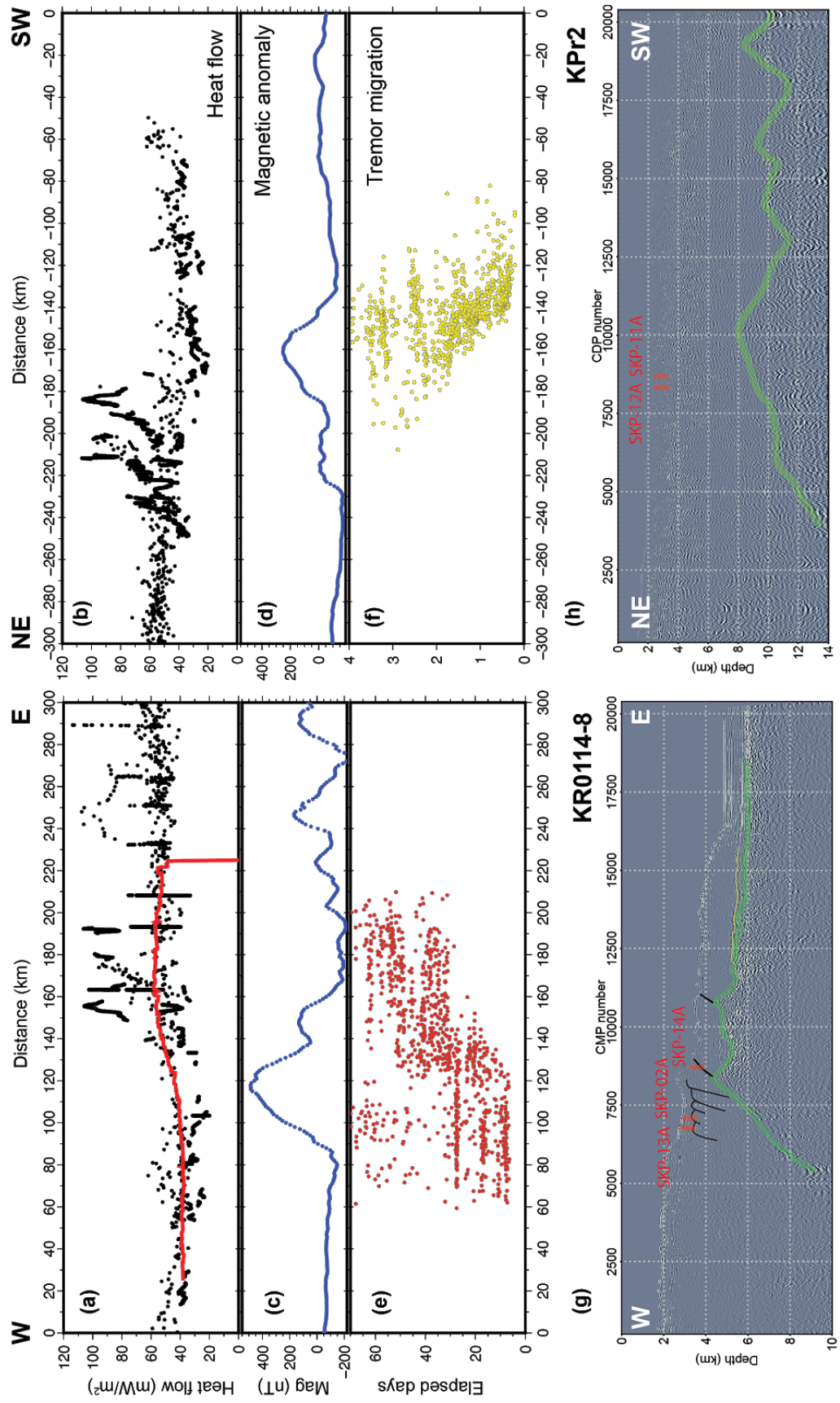


Figure 4 (previous page): Geophysical profiles along the seismic line (left) KR0114-8 of Park et al. (2009) and (right) KPr2 of Nishizawa et al. (2008). (a,b) Heat flow data estimated from BSR depths within 100 km of the seismic line are shown with black dots. Solid red curve shows the heat flow at 13 Ma predicted by 3D thermal conduction modeling with subduction of Shikoku and West-Philippine basins (Kinoshita et al. 2020). The regional trend reflects the ~20 Ma age difference between the subducting two segments (Ashi et al. 1999). Lowest heat flow at $x=80\sim140$ km is potentially associated with the advective heat flow caused by the KPR subduction. (c,d) Total magnetic anomaly within 10 km of the line. (e,f) Spatiotemporal distribution of tremors in 2015 within 20 km from the line (Yamashita et al. 2015, 2019b). (g,h) pre-stack seismic section modified from Park et al. (2009) shown with the location of the drill sites (red lines). Close up of the drill sites is available in Figure 10.

3.2 Slow earthquakes in Hyuga-Nada

Unlike regular earthquakes, slow earthquakes last minutes to years and can be categorized as non-volcanic tremors lasting 0.1-10 seconds, very-low-frequency earthquakes (VLFEs) lasting 10-100 seconds, and slow slip events (SSEs) lasting days to years (Figure 5a). Various types of seismic and geodetic observations are required to detect all of them. In Hyuga-Nada, the seismic activities along the weakly coupled subducting plate are well characterized to the depth, including repeating earthquakes and deep slow earthquakes (Figures 5b, c, Takemura et al. 2020; Uchida et al. 2019; and Kano and Kato 2020). Spatiotemporal correlation between the repeating tremors/VLFEs and the subducting KPR are established (Figures 3b, 4, 5d, Asano et al. 2015; Yamashita et al. 2015, 2019b; Tonegawa et al. 2020). The tremor and VLFEs are collocated (Yamashita et al. 2015; Tonegawa et al. 2020) and occur coincidentally for all previous episodes (Figure 1). The migration occurs within two segments along NS and EW (Figures 4e,f, 5d), which we refer to as the “NS segment” and the “EW segment”. For instance, during the 2013 episode, the tremors migrated northward in 30 km/day and then changed directions to westward in 60 km/day (Figure 5d). During other episodes, they migrated within either one of the NS or EW segments. The major activities occur every two years with minor activities every few months to a year. The concurrency of the tremors and VLFEs may suggest the existence of undetected SSEs (Davis et al. 2015; Todd et al. 2018), but their relationship remains unclear as only sparse SSE observations have been made using seafloor GNSS-A stations (Figure 1, Yokota and Ishikawa 2020).

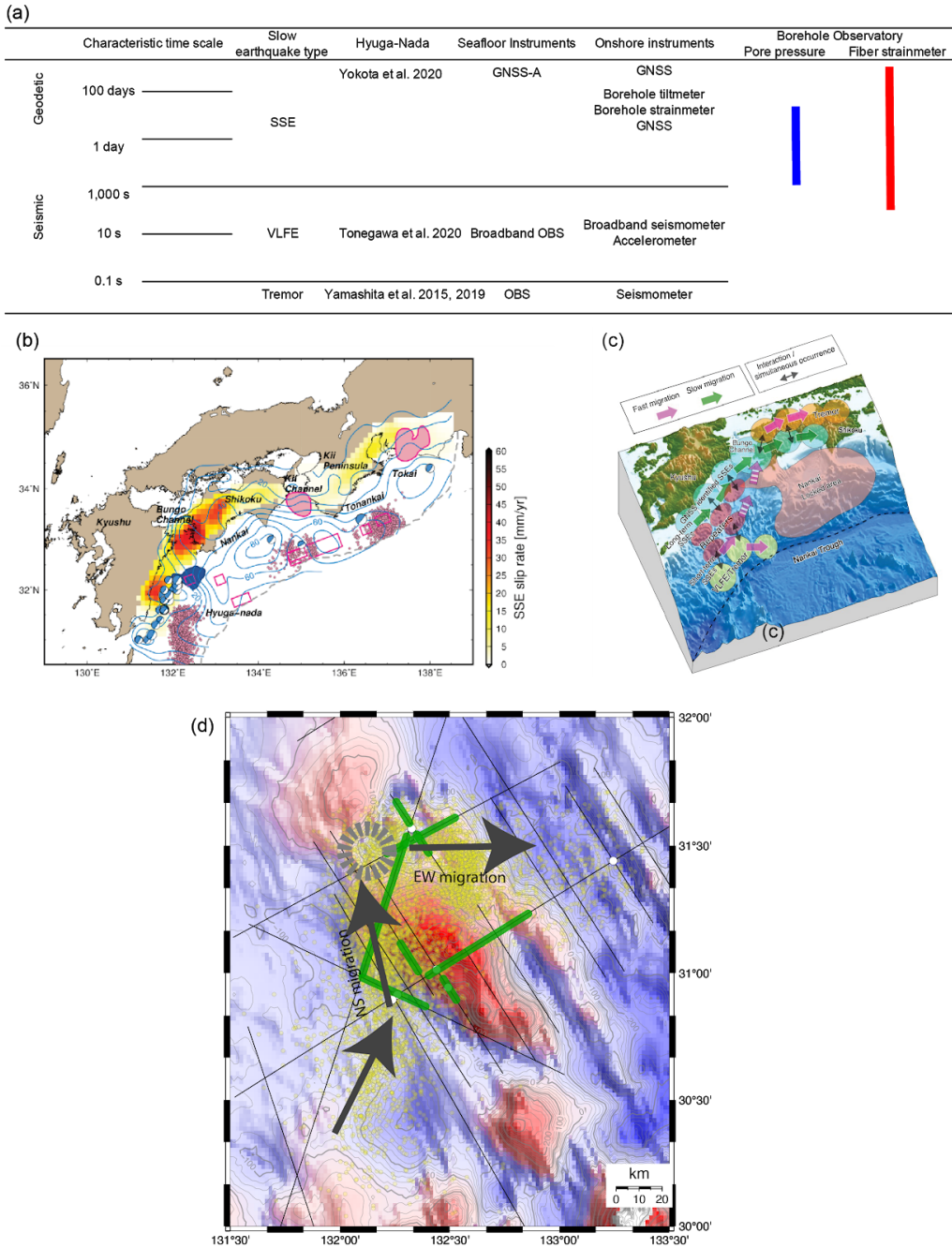


Figure 5 (a) Classification of slow earthquakes (modified from Obara and Kato 2016) (b) Seismic activities in the Nankai subduction zone (Takemura et al. 2020). The dark blue shade indicates the 1968 earthquake, pink circles shallow tremors and VLFEs, pick shaded areas and rectangles the slip area of SSEs, and blue concours indicate the slip deficit rates [mm yr⁻¹]. (c) Interaction between deep and shallow slow earthquakes and repeating earthquakes in Hyuga-Nada (Uchida et al. 2019) (d) Zoom up of the magnetic anomaly in Figure 3b and tremors (yellow circles). Green lines indicate topographic high indicated in seismic sections. Arrows indicate two major tremor migration segments along NS and EW directions (Yamahisa et al. 2015). The gray dashed circle indicates the location where the NS migration turns.

4 .Hypothesis

4.1 Hypothesis 1: Seamount subduction modulates stress, hydrological and thermal states of the subduction margin

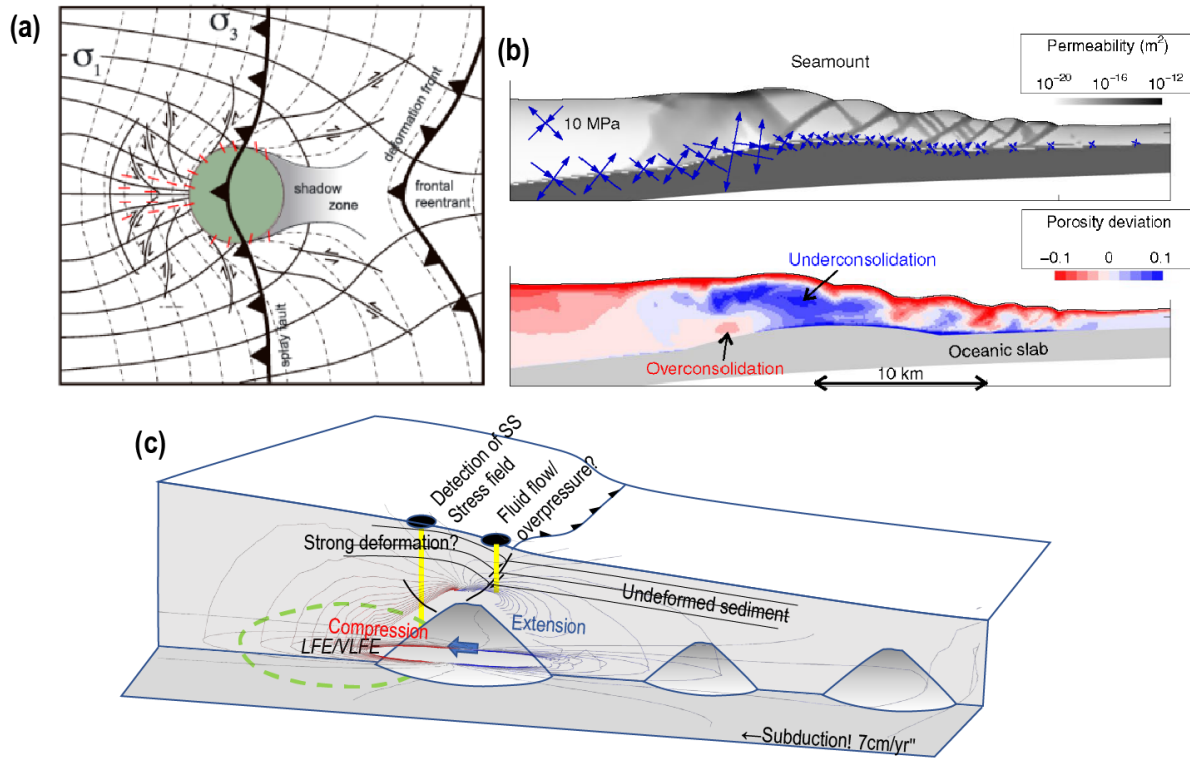


Figure 6 Predicted stress, deformation and consolidation anomaly triggered by seamount subduction. (a) Stress field and deformation of the accretionary wedge (Kimura et al. 2014, modified from Dominguez et al. 2000). Note the development of strike-slip faults and the bent of frontal thrusts. (b) Simulation results from Sun et al. (2020b): (top) Maximum and minimum principal stress (blue arrows) and permeability (gray image); (bottom) Porosity deviation (c) Schematic view of 3D elastic model, where a certain amount of landward displacement is given to a subducting seamount (Kinoshita et al. in prep.).

4.1.1 Stress state

Subducting seamounts and geometrical irregularity of the incoming plate affect the coupling ratio, magnitude of earthquakes and slip behaviors (Figure 6, Lallemand et al. 2018). Many studies of field observations (von Huene and Scholl 1991; Kopp 2013), laboratory analogue experiments (Dominguez et al. 2000; Martinod et al. 2013; Van Rijsingen et al. 2019) and numerical modeling (Ruh et al. 2016; Morgan and Bangs 2017; Ding and Lin 2016; Sun et al. 2020b) suggest that subducting seamounts severely fracture the upper plate and disturb the stratigraphy, modulating in-situ stress state and fluid flow patterns. Seismological and geodetic observations also suggest that subducting roughness commonly causes dominant fault creep (Wang and Bilek, 2011, 2014; Wallace and Beavan, 2010), abundant small earthquakes of complex rupture history (e.g., Bilek et al. 2003; Mochizuki et al. 2008) and/or slow slip events (e.g., Yamashita et al. 2015), potentially via its impacts on deformation, stress and fluid pressure distributions.

Numerical modelling of Sun et al. (2020a,b) demonstrated the interconnected deformation and fluid flow processes associated with seamount subduction. Their results support earlier studies and further highlight the hydro-mechanical impacts of seamount subduction on in-situ stress, pore pressure, and sediment consolidation patterns. Enhanced compression, fluid drainage and compaction are expected at the downdip leading edge of a subducting seamount, whereas reduced stresses (less compression) and relatively unconsolidated sediment are preserved above and in the wake of the seamount. Ground-truth observations, such as those provided by logging and coring, are urgently needed to test these speculations and to enhance our understanding of the effects of subducting roughness on megathrust slip behavior and the associated tsunami potential.

In Hyuga-Nada, we expect the KPR (e.g., the subducting Toi Seamount) to modify regional stress state, physical properties of sediments and deformation features, leading to a favorable

environment for the documented SSEs, very-low-frequency earthquakes and tremors (Yamashita et al. 2015). We propose three drilling sites at the upper plate, penetrating through the shallow cover sediment layer into the old-sedimentary complex below, with their distribution maximizing our opportunity to observe the spatially contrasting compaction and stress states due to the Toi seamount subduction.

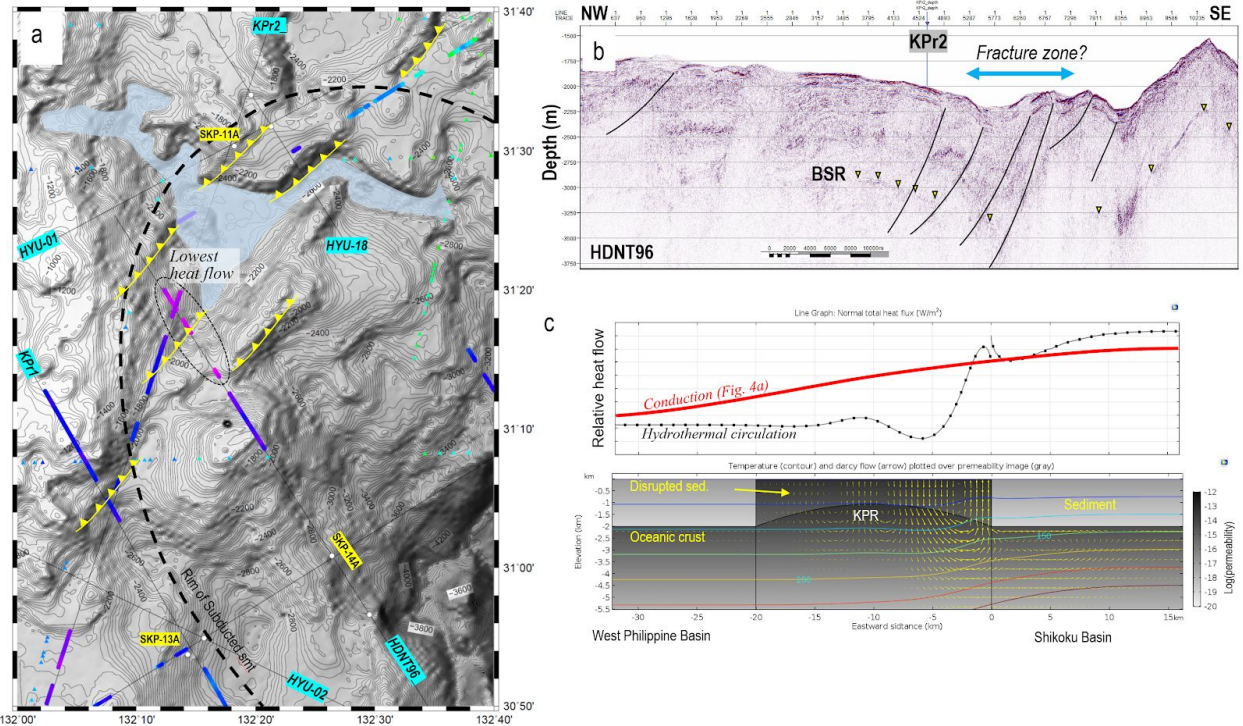


Figure 7 (a) Bathymetry map with preliminary interpretation of faults (yellow) and a submarine canyon (cyan) around the proposed drill sites. Colored dots indicate the heat flow as shown in Figure 3a. The lowest heat flow area is indicated by the black ellipsoid. The large dashed curved line indicates a rim of the subducted seamount inferred from geomagnetic anomaly (Figures 3b, 5d). (b) Preliminary interpretation of the seismic line HDNT96 (V.E.=10). Thick cyan arrow suggests the fracture zone. The BSRs, inversely proportional to the heat flow, are indicated by triangles. See (a) for the location of HDNT96. (c) (Top) Simulated heat flow profile (red, thermal conduction in Figure 4a; black, hydrothermal circulation model as shown below). (Bottom) temperature (contour) and fluid flow section (small yellow arrows) obtained by 2D heat flow modeling with Darcian flow across the KPR.

4.1.2 Thermal and hydrological state

Temperature is one of the major factors modulating pore pressure and plate interface rock types by governing physico-chemical processes (e.g., dehydration through clay mineral alteration). Yoshioka (2007) hypothesized that delayed dehydration due to low temperature has created apparently stable sliding near the trench at Hyuga-Nada. In contrast, Gao and Wang (2014) hypothesized that rough crust subduction causes substantial frictional heating and high temperatures at the interface (and elevated surface heat flow), and plate interface creep. Fluid circulation along the subducting plate interface or within the frontal wedge alters the thermal

structure, being evident as extremely high-heat flow close to the trench axis in the Shikoku Basin (e.g., Yamano et al. 2003; Spinell and Harris 2011; Harris et al. 2013).

We hypothesize that a subducting seamount induces hydrological heterogeneities (i.e., permeability variations), creates local thermal and pressure disturbances and affects effective stress along a plate interface or in an upper plate (e.g. Saffer and Tobin, 2011, Harris et al. 2010). We further hypothesize that the hydrological heterogeneities contribute to creating a favorable condition for the occurrence of the slow earthquakes near the seamount. The locally enhanced permeability surrounding a seamount (Sun et al. 2020a,b) should encourage the drainage of deep warm fluid through the upper plate and increase the heat flow. However, the heat flow is lowest on the leading side of the Toi Seamount (Figures 3a, 7a) indicated by the deepest BSRs (Figure 7b; Kinoshita et al. in prep.). The observation may suggest the entrainment of seawater into the upper plate through fractures and/or permeable layers (e.g. cyan arrow zone in Figure 7b) potentially combined with other phenomena (e.g., thermal refraction, rapid sedimentation, fluid flow associated either with basement relief as in Antriasian et al. 2019).

In the Hyuga-Nada, we expect that the presence of subducting seamounts enhances the fluid transport within the upper plate. In addition to the pressure-driven fluid drainage/entrainment, a background hydrothermal circulation exists between the young hot Shikoku and old cold West Philippine Basins. Using a 2D time-dependent model based on the permeability estimates of Sun et al. (2020a), we confirmed that a low heat flow can be reproduced above the seamount (Figure 7c; Kinoshita et al. in prep.). Vigorous pore fluid circulation occurs between the Shikoku Basin and KPR (at distance ~ 0 km in Figure 7c) and significantly decreases the heat flow on the eastern side of KPR. The result suggests that the lowest heat flow be a proxy for the fluid supply into depth, and thus the existence of highly permeable (i.e., active fault/fracture) zones on the leading edge of the seamount.

4.2 Hypothesis 2: The majority of plate motion at Hyuga-Nada is accommodated by episodic slow earthquakes. The spatiotemporal distribution of slow earthquakes is strongly influenced by seamount subduction through the process outlined in Hypothesis 1.

Slow earthquakes have been identified at both deeper and shallower ends of the seismogenic zone (Obara and Kato 2016; Uchida et al. 2019; Kano and Kato 2020). Shallow (<10 km) slow earthquakes have increased importance in deducing seismic behaviors near the trench as more observations are being made in subduction zones including Nankai (e.g., Araki et al. 2017), Ryukyu (e.g., Nakamura and Sunagawa 2015), Costa Rica (e.g. Davis et al. 2015) and Hikurangi (e.g. Wallace et al. 2016) margins.

The Hyuga-Nada has not hosted any great ($M_w > 8.0$) earthquakes but are characterized by regular (M_w 6-7) and repeating earthquakes and a range of slow earthquakes (Figures 5b,c). We posit that the vast majority of plate motion is accommodated via episodic slow earthquakes as in the Hikurangi margin (Todd et al. 2018). We expect that a range of all shallow slow earthquakes (tremors, VLFEs and SSEs) occur in the shallow subduction zones near the trench. They may occur in isolated adjacent patches with contrasting frictional properties, and the resulting stress changes may induce complex interactions between these slip behaviors (Shelly et al. 2006; Obara and Kato, 2016; Kano and Kato 2020). There are two competing hypotheses: the VLFEs and tremors are collocated at the edge of SSEs and triggered by the SSE activity. Alternatively, all of these slow earthquakes are collocated and simultaneously activated (Yamashita et al. 2015).

In a regional scale, fluid migration from deeper slow slip events may activate shallower slow earthquake activities (Figure 5c; Uchida et al. 2019, Kano and Kato 2020) which would result in north to south migration of tremors and VLFEs. However, tremors and VLFEs tend to migrate from south to north over a horizontal distance of 70–80 km along the strike direction (Figure 5d; Yamashita et al. 2015, 2019b). We hypothesize that the local spatiotemporal distribution of slow

earthquakes is significantly affected by the combination of spatially heterogeneous geomechanical, hydrological, thermal and frictional states due to the rough seamount subduction as described in Hypothesis 1.

At Hyuga-Nada, detecting SSEs and resolving their spatiotemporal evolution in the tremor-VLFE cloud (Figure 5d) is the first step. This requires filling the time-scale gap (the order of hours and months) that exist between seismological and seafloor geodetic (GNSS-A) observations (Figure 5a). Continuous borehole monitoring enables to accurately detect the onset of SSE events, in contrast to GNSS-A measurements that only measure a few times per year and whose time-resolution is quite limited. Monitoring volumetric strain will constrain slip models for offshore SSEs and suggest the degree to which these episodic events accommodate plate motion. Refined VLFE-tremor-SSE relationships and detailed (re-)interpretation of past and future seismic sections for spatial variations in physical properties will enable resolving the relationship between the subducting features and slow earthquakes, and the complex interplay between these various flavors of plate interface slip style.

5. Scientific objectives and Methods

We design the drilling and monitoring program in order to achieve three scientific objectives.

5.1 Objective 1: Characterize the stress regime, temperatures, rock properties, shallow sedimentary strata that are potentially deformed by the Toi seamount subduction

The objective aims to test the geomechanical part of *Hypothesis 1* described in Section 4.1.1. We further decompose the objective into three questions.

Question 1-1: “What is the stress, consolidation and hydrological state? Do they differ between the leading side , the lateral side and the top of the seamount? Do they azimuthally vary around the subducting Toi Seamount ? “

Answering the questions starts from documenting the current stress from **borehole breakouts** and drilling induced tensile fractures in **LWD resistivity images**. **Paleo-stress using fault analysis** in core description and LWD resistivity images reveals the history of stress evolution which is good to compare the current setting whether current and paleo stresses are consistent or not. Estimating **porosity- and velocity-depth curves** from LWD and also on core samples to build an empirical relationship between the parameters is essential to relate to the consolidation state which is needed to be combined with the laboratory experiments in the post cruise science. Comparing between sites, we depict the azimuthal variations of the stress, consolidation and hydrological states with respect to the subducting seamount.

Question 1-2: How is the seamount disrupting the upper plate?

To answer the question, we compare the relationship between fracture density and depth among the sites. **Lithology and age** of cover sediments, unconformity and old-sedimentary complex is the basic geological background for the interpretations of the fracture distribution. The origin of the old-sedimentary complex (an accretionary prism, a sedimentary basin or others unexpected) is also examined with **lithology and age**. **Strength** is also another expression of deformation of the upper plate. Combining the fracture and strength distribution with the geological background, we extract the effect of the subducting seamount on the deformation of the upper plate.

Question 1-3: How does the shallow state relate to the state of the deep plate interface?

Proposed target depths are relatively shallow around 700-900 mbsf. To understand the nature of the deeper plate boundaries where tremors and VLFEs occur, we need to extract the shallow properties into the deeper setting. Combining the physical properties with the seismic velocity model (Tsuji et al. 2014) or combining the depth variations in physical properties with 2D

modeling, we infer the spatial variations including the deeper portion around the subducting seamount.

5.2 Objective 2: Characterize the temperatures and hydrological parameters that are potentially altered by the Toi seamount subduction

The objective aims to test the hydrological and thermal part of *Hypothesis 1* described in Section 4.1.2. We further decompose the objective into two questions.

Question 2-1: Is temperature on the plate interface anomalously lower or higher where the KPR subducts?

The previous heat flow data are highly uncertain due to shallow penetration of probes and subjective interpretation of BSRs. Having “deep” determinations of thermal gradient and heat flow via the observatories is crucial to establish temperatures at the plate interface in the Hyuga-Nada region. The heat flow is estimated by combining **temperature-depth curves** and **thermal conductivity**. The conductivity will be measured on core samples or estimated from P-wave velocity or porosity using empirical relationships (e.g., Martin et al. 2004; Brigaud and Vesseur 1989). The effect of rapid sedimentation/erosion will be corrected from seismic profiles to estimate the heat flow from the old basement. The **in-situ temperature** data acquisition via advanced piston corer temperature (**APCT-3**) tool (Heesemann et al. 2006) and **monitoring** using the thermometer in the observatory are fundamental combined with the diagenesis status revealed from **clay mineral mineralogy** of core samples. The observation will improve the temperature estimation along the plate interface and complement temperatures at locations where BSR is not apparent.

Question 2-2: What is the hydrological state? Does subduction of seamount enhance advective fluid transfer affecting the thermal state?

The influence of the subducting seamount on permeability, pressure-driven fluid discharge, and hydrothermal circulation in the upper plate must be assessed to develop robust thermal models. Permeabilities will be measured on core samples or estimated from fracture networks through the descriptions of LWD resistivity image or CT scan of cores. **Geochemical anomalies** (e.g., chlorinity, hydrocarbon, isotope ratios) on pore fluids can constrain their origin and flux, refining the model significantly.

The **temperature and pressure data** can provide key information on subsurface fluid flow. Temporal changes caused by the current on the seafloor can be removed by monitoring temperatures at depth (> 100 m). Tidal modulations will be removed with pressure data on the seafloor. We use further excursions in **temperature and pressure monitoring data** as a proxy for subseafloor fluid flow, either steady-state or transient (Fulton and Brodsky 2013; Davis et al. 2006; Davis and Villinger 2006).

These pieces of borehole information will be integrated with the seismic profiles to better constrain the effective strength along the plate interface and to construct a reliable 3D thermal/hydrological model as performed in Section 4.1.2.

5.3 Objective 3: Monitor slow earthquake activities and subsurface changes by installing cutting-edge observatories equipped with conventional and advanced sensors

Accomplishing the objectives directly contributes to *Hypothesis 2* described in Section 4.2. We further decompose the objective to three questions.

Question 3-1: Does SSE happen prior, concurrently or after tremors and VLFEs?

Question 3-2: When VLFEs and tremors migrate from the NS to EW segments, do SSEs also migrate in a similar manner? Do SSEs occur in the NS segment even when only the VLFEs and

tremors occur in the EW segment, and vice versa? Does the SSE in the east segment occur even when only the VLFEs and tremors occur in the west segment?

The most effective way to detect SSEs is with **in-situ, continuous monitoring** of subsurface deformation via **pore pressure** changes as a proxy for volumetric strain in a quiet borehole environment (e.g., Araki et al. 2017). In order to expand the frequency range and lower the detection limit (Figure 8), we explore frontier **broadband fiber-optic strain sensing** based on **Optical Fiber Strainmeter (OFS)**; DeWolf et al. 2015; Zumberge et al. 2018; Araki et al., 2019). The combination of OFS and pore pressure will enable us to distinguish between crustal strain changes and hydrological events. OFS will also enable us to observe SSE events with duration over a year, which could be difficult to detect using pore pressure relaxation over such a period. Tremors and VLFEs will be detected and their migration pattern will be tracked by a temporary OBS network. The timing and spatial locations will be compared with SSEs detected at the installed observatories.

Question 3-3: Do subsurface elastic structures change over time associated with slow earthquake activities?

Temporal changes in physical conditions (e.g. pore pressure) cause time-lapse changes in subsurface elastic properties (e.g. velocity, attenuation). Seismic monitoring is a powerful tool to detect such changes either using earthquakes (Nakata and Snieder 2011), noise (Ikeda and Tsuji 2018) and controlled sources (Kamei et al. 2016). As the changes in elastic properties tend to be small both in terms of magnitude and spatial extent, sensors need to be densely placed. **Distributed Acoustic Sensing (DAS)**; Lindsey et al. 2019), another fiber sensing technique, allows to measure seismic signals in extremely high spatial and temporal resolution along a fiber cable even compared to conventional array of seismographs. We may be able to resolve changes of elastic parameters along the cable (Williams et al. 2019) and potentially at/near the plate boundary (Nakata and Shelly 2018).

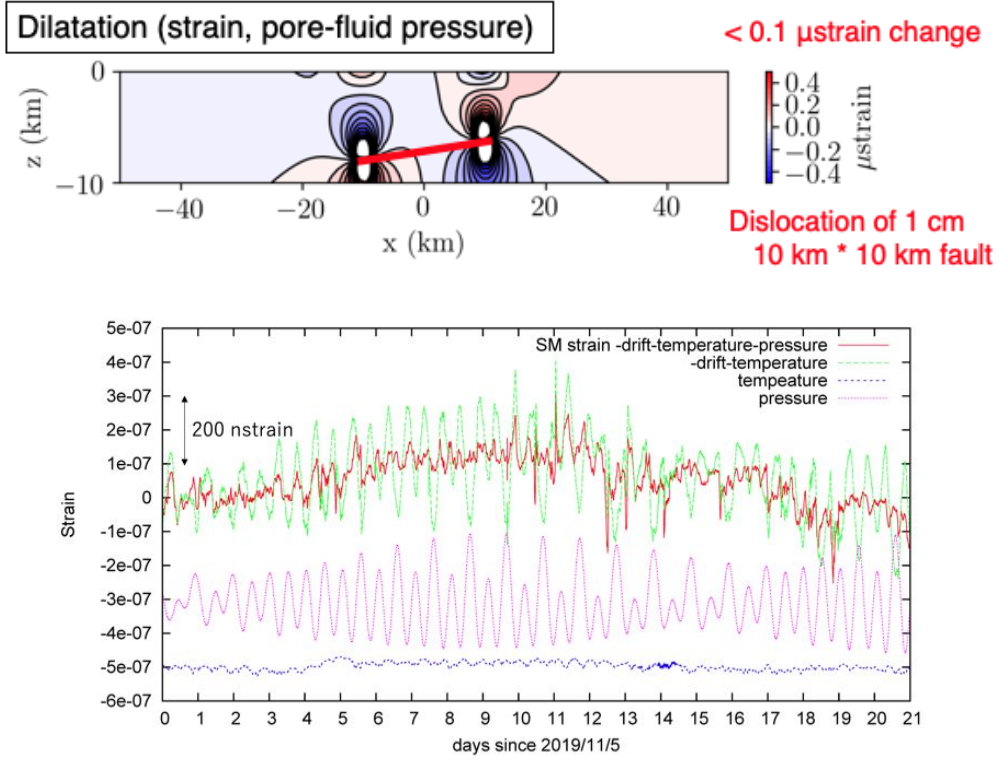
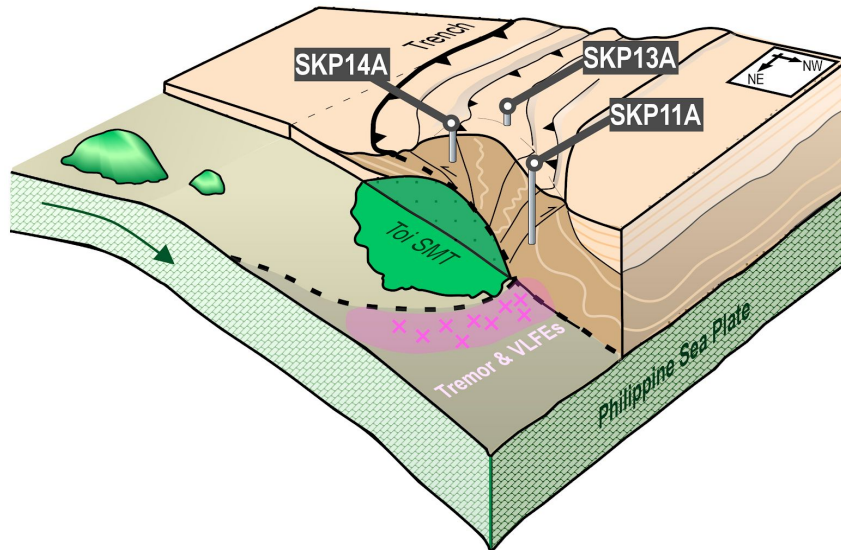


Figure 8 (Top) Expected strain change (Okada 1985) when 1cm dislocation occurs along the 10 km x 10 km fault (red line). The dislocation corresponds to the smallest SSE discovered in the Nankai Trough (Araki et al. 2017). (Bottom) Nankai Trough seafloor fiber optic strainmeter records for three weeks. The red trace shows time series where temperature contribution (blue), seafloor pressure loading contribution (pink), and linear trend removed from the original record (green) (Araki et al. 2019b)

6. Proposed Drilling and Monitoring Program

We optimize our drill sites to evaluate the two hypotheses related to the seamounts and slow earthquakes (Section 4) by accomplishing scientific objectives (Section 5). Based on the discussions with JRSO, we propose three primary sites (**SKP-11A, 13A** and **14A**, see Figure 9 for schematic illustrations). We plan to conduct LWD and coring at all three sites and install obsservatories at two of them (**SKP-11A** and **13A**). The primary sites are selected based on their scientific significance and whether the sites have cross-seismic sections and have at least one already fully-processed and interpreted seismic sections. We also identify four alternate sites

(**SKP-01B, 12A, 02A** and **15A**). We show the map and the summary of our drilling plan in Figure 1 and representative seismic sections of the primary sites in Figure 10.



	Method	SKP-11A	SKP-13A	SKP-14A
Location relative to seamount		Leading	Lateral	Top
Fracture density	core description, LWD resistivity image	moderately intense due to the concentration of compressional stress	less intense than the axial transect of the central part of subducting seamount.	most intense due to a past compression as on a leading site overprinted by a current extensional deformation
Present stress	LWD resistivity iamge	Oriented as in Figure 6b		
Paleo stress	core description, LWD resistivity image	Consistent with the present stress above. Or as the paleo-stress indicates integrated stress history, we may infer the change in paleo-stress with seismic cycle		
Consolidation state	porosity-depth curve and acoustic velocity log	lower porosity corresponding to the over-consolidation state and low fluid pressure	between SKP11A and SKP-14A	higher porosity corresponding to the under-consolidation state and high fluid pressure
Strength	drilling parameters, triaxial tests in laboratory experiments	relatively high due to the expected states with over-consolidation and low fluid pressure	between SKP11A and SKP-14A	low due to the expected states with under-consolidation and high fluid pressure
Heat flow	APCT-3	low. Fluid flow may locally either increase or decrease the value.	low consistent with the BSR-derived one	high due to the fluid upwelling along the thrust fault
Fluid flow footprint	pore-fluid chemistry and precipitated mineral of core	anomalous due to fracture network in pore fluid chemistry and precipitated mineral.	very small due to low heat	expected along a major thrust detached from the edge of seamount
Cementation	LWD parameters, chemical analysis of core	may be very small. If the active fluid flow exists in the fracture network, cementation may be observed due to the circulation of exotic fluid	very small due to low heat	
Dehydration and diagenesis	clay mineralogy, LWD parameters, chemical analysis of core	very small due to low heat	very small due to low heat	may detect upwelling fluid from deep along the fault related to the dehydration and diagenesis in the deeper portion

Figure 9 (Top) Schematic illustration of the drill sites with respect to the seamount and tremor/VLFs network. Note that it is drawn from the north. (Bottom) Summary of the LWD-coring plan.

6.1 Site selection

Objective 1: Deformation and stress associated with seamount subduction

We ideally locate drill sites on the leading, lateral sides and top of the subducting seamount and cover entire azimuths (360 degrees) relative to the seamount in order to understand their spatially varying geomechanical, hydrological and thermal effects. As the seamount is located at a very close proximity to the trench, identifying the trailing side is deemed not realistic. We thus identify potential sites

- on the leading side of the seamount (**SKP-11A** with alternatives at **SKP-01B** and **SKP-12A**),
- on the west-lateral side of the seamount (**SKP-13A** with alternative at **SKP-02A**),
- above the seamount (**SKP-14A** with alternative at **SKP-15A**).

On the leading side, **SKP-01B**, **11A**, **12A** are located in the north of the seamount above the plate boundary of 10-12 km depths (Figure 1). The shallow sections are occupied by cover sediments underlain by the old-sedimentary complex. We expect that both covering sediments and the old-sedimentary complex record the disturbances due to the seamount subduction. At **SKP-11A**, the cover sediments are the thinnest, and we will be able to sample sediments of the cover and old-sedimentary complex. At **SKP-01B** and **12A**, thick cover sediments may preclude the penetration into the old-sedimentary complex, and thus the locations are considered as alternatives.

The **SKP-13A** and **02A** are located on the west lateral side of the seamount, positioned to the west of the KPR. The depth of the plate boundary is 10-12 km, similar to that on the leading-side sites. At the **SKP-13A** and **02A**, we sample the cover sediments and the old-sedimentary complex. We expect substantial differences in the mechanical properties (e.g., stress orientation)

from the leading side (**SKP-01B, 11A, 12A**), which provides insights into the angle variations of the seamount subduction.

SKP-14A and **15A** are located above the seamount as indicated by the magnetic anomaly and confirmed by the seismic sections. The plate boundary is at the depths of 2-3 km, much shallower than those at **SKP-01A, 11A, 12A** and **13A**, and more prominent effects of the seamount will be seen in the cores and LWD data. In addition, at **SKP-14A**, we identify a clear imbricated thrust system that can be associated with the topographic high of the seamount. We interpret that the fault is associated with the seamount subduction.

Our proposed LWD and coring at each site do not reach the basaltic basement or a depth comparable to the summit of the subducted seamount. Nonetheless, the prevalent effect of a large subducting geometrical anomaly is still expected to be observed at shallow depths. Site comparison between the leading side and the top of the seamount likely captures the locally greatest contrast between enhanced tectonic compression (and consolidation) and reduced compression (and even possibly widespread horizontal tension at shallow depths) (Figure 6b; Sun et al. 2020b). The in-situ wedge properties inferred from the rich set of coring and logging data at our drilling sites will be interpreted together with high-resolution seismic images and velocity models to better demonstrate spatial variations. Geodynamics modeling is eventually needed to integrate all the drilling and seismic observations, with the objective of illuminating the nature of the greater depths (beyond our drilling capability) where slow slip events, tremors, and VLFEs take place.

Objective 2: Thermal and hydrological state modifications due to the seamount subduction

All proposed sites are in the region of the low heat flow and suitable for testing *Objective 2*. The very low heat flow area (the black circle in Figure 7a) resides in a series of NE-SW-trending elongated ridges associated with faults. Unfortunately, the area is within the US Navy Corps training area where we deem too challenging to drill. **SKP-01B, 11A** and **12A** are at a distance

of approximately 20 km to the north of the very low heat flow area (Figure 7a) and in the same fault system. The faults are probably a westward continuation of the frontal thrust group of the Nankai Trough, may have been (re)activated by the subducting KPR and play a role as a fluid pathway between the plate interface and the seafloor (the cyan arrow in Figure 7b). As for *Objective 1*, by comparing with the west lateral drill sites (**SKP-02A, 13A**), azimuthal thermal and hydrological variations of the seamount subduction effects. We expect that the splay fault (Figure 4f) may act as the fluid conduit. The shallow depth of the seamount and confirmed low heat flow from the BSR analysis makes **SKP-14A** an optimal site.

Objective 3: Monitor slow earthquake activities and subsurface changes by installing cutting-edge observatories equipped with conventional and advanced sensors

Tremors and VLFs have migrated within the two segments (Figure 5d). The dense deployment of temporal OBSs have been able to locate these seismological events, but the geodetic slow slip events are not well characterized in the region. We limit the number of the observatories to two to fit the allocated 2-month period and select sites i) to have experienced rich VLFE and tremor activities, ii) to cover the NS and EW segments of the tremor/VLFE clouds, and iii) to have at least one observatory connected to the N-net node for real-data streaming capability. We identify **SKP-01B, 11A, 12A, 02A** and **13A** fulfill the first two requirements (Figure 5d). **SKP-01B, 11A** and **12A** can be connected to the N-net node located at the distance of 10-20 km.

Our decision not to place the two observatory wells at a close distance (< 10-20 km) may limit the ability to detect downdip migration of SSEs as done in Davis et al. (2015) and Araki et al. (2017) and potentially undermine the ability to cross check results. The observed tremors and VLFEs spatially cover a large area (>100 km x 100 km) and we prioritize resolving the regional relationships between SSEs, tremors and VLFEs rather than a local SSE movement within the 10-20 km distance. In this manner, we plan to utilize N-net sensors and temporal OBS networkss to infer the spatiotemporal migration of slow earthquake events.

6.2 Primary sites

SKP-11A (leading side of the seamount)

Surface topography at this site shows a small mound. Although an unconformity is not clear, surface cover sediments are at least 300-m-thick and show continuous layering structures parallel to the surface topography (Figure 10 top). A moderately-deformed old-sedimentary complex exists below the cover sediments. Some faults associated with the seamount subduction are indicated by the discontinuous reflectors. The fault types, though not very clear, are most likely thrusts as being consistent with the mounded surface topography. The faults in the old-sedimentary complex do not apparently penetrate the cover sediments. We also note that displacements, although much smaller, continue from the faults and are faintly observed in the cover sediments. Hence, by targeting both the cover sediments and the old-sedimentary complex, we sample sedimentary units experienced deformation activities. In order to sample deformed sediments both in the cover sediments and the old-sedimentary complex, we set the target depths as 700 mbsf. **SKP-01B** and **12A** are alternate sites for this site, located about 5.5 km NE and about 7.1 km NEN away from this site, respectively.

SKP-13A (west-lateral side of the seamount)

Cover sediments (about 600 m thick) overlay the old-sedimentary complex (Figure 10 middle). The old-sedimentary complex is relatively transparent in the seismic section. Some thrust faults are visible in the body of the old-sedimentary complex and apparently truncate at the unconformity. Bedding are also slightly folded with the reliefs of the unconformity, although the thrust faults seem not to penetrate through the unconformity. These features suggest that the uplifting is still active at the surface. Target depth here is 800 mbsf penetrating both the covering sediments and the old-sedimentary complex where the structures with horizontal compression

(fold and thrust) are visible in the seismic profile. An alternate site, **SKP-02A** is specified at another cross point of the seismic lines.

SKP-14A (top of the seamount)

An unconformity is not clearly visible at this site, but the segmented layers represented by slightly strong reflectors show anastomosed texture in the shallow portion (Figure 10 bottom). Below the cover sediments (400 mbsf), the reflectors get faint in the old-sedimentary complex. The old-sedimentary complex is sie transparent seismically, but a long continuous reflector is a thrust fault from the edge of the seamount. Faint reflectors around the fault in the old-sedimentary complex are mostly parallel to the fault. These reflectors are either thrust faults related to the major thrust fault or landward tilted bedding in the old-sedimentary complex. The target depth of **SKP-14A** is 900 mbsf penetrating the anastomosed cover sediments, the old-sedimentary complex and the thrust fault. **SKP-15A** is the alternate site for **SKP-14A** and located at the top of another topographic high.

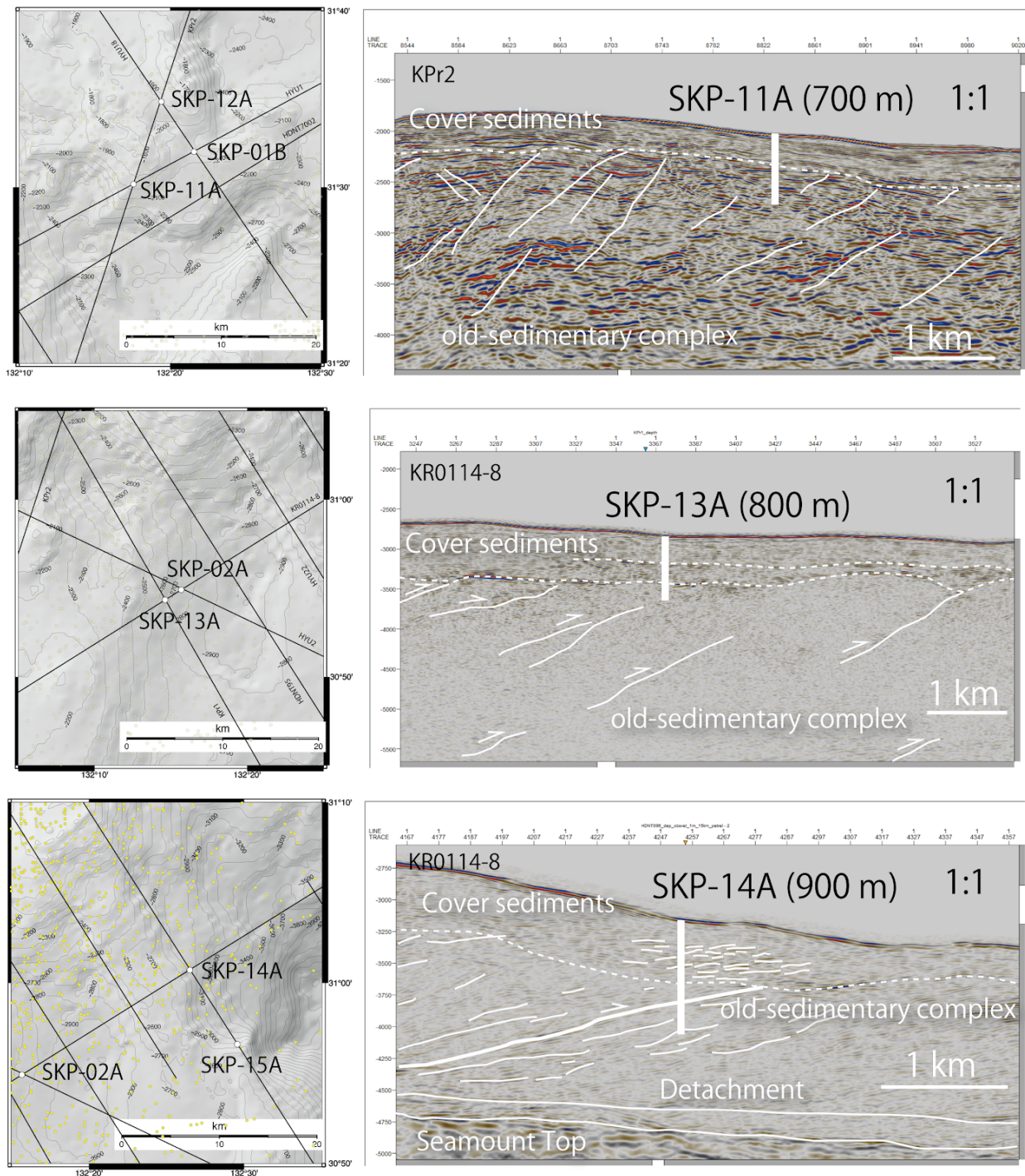


Figure 10 Seismic sections near the primary sites of (top) SKP-11A, (middle) 13A, and (bottom) 14A. Locations for each site are represented in the bathymetry map. Vertical axes of seismic images indicate depth (m). Name of the seismic line is shown in the upper left of each seismic image. Broken lines indicate possible unconformities between cover sediments and old-sedimentary complex. Thrust faults are shown by lines with arrows. Other lines are faults with an unknown sense, bedding, or seamount top (basement).

6.3 LWD and Coring plan

LWD and coring are planned for all sites to accomplish *Objectives 1 and 2* (Section 5) to test the **Hypotheses 1** (Section 4.1). We will illustrate the effects of seamount on deformations, stress, and physical properties of sediments (*Objective 1*) and evaluate the fluid flow due to different distribution of fracture networks among the sites and heat flow contrast between Shikoku Basin and West Philippine Basin (*Objective 2*). The comparisons in key parameters among these three sites can provide clues to understand the effect of seamount and heat flow distribution.

The key parameters and methodologies are:

- Lithology and age by core description as basic geological backgrounds (*Objective 1*)
- Fracture density by core description and LWD resistivity image (*Objectives 1 and 2*)
- Present stress by LWD resistivity image (*Objective 1*)
- Paleo stress by core descriptions and LWD resistivity image (*Objective 1*)
- Consolidation state and fluid pressure by physical properties from core and LWD (*Objective 1,2*)
- Strength by drilling parameters or internal friction angle by triaxial tests in laboratory experiments (*Objective 1*)
- In-situ temperature measured by APCT-3 tool (*Objective 2*)
- Footprint of fluid flow from chemical signature on core samples (*Objective 2*)
- Cementation by physical properties or chemical analysis from LWD and core (*Objective 2*)
- Dehydration and diagenesis by clay mineralogy, physical properties and chemical signature from LWD and core samples (*Objective 2*).

Lithology and age are basic important information on the geological setting and foundation for answering *Objectives 1 and 2*. Lithology and age in covering sediments provide the uplift events

in active basin sedimentation. Age of unconformity gives the timing of exhumation of the old-sedimentary complex. The other key parameters will vary among the sites systematically as summarized in the table in Figure 9

6.4 Observatory planning

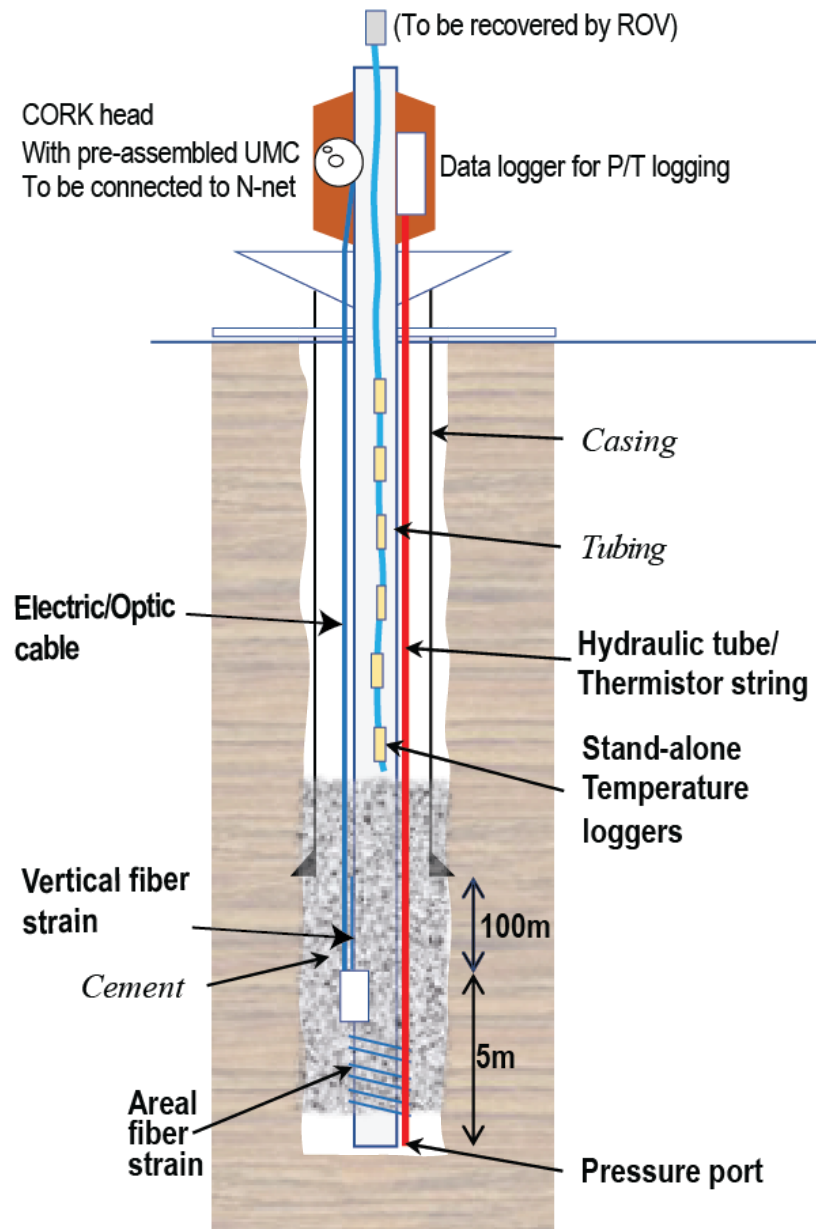


Figure 11 Schematic design of Fiber-CORK Observatory. See text for details.

Primary roles of the observatories is to monitor strain and pressure to detect SSEs (*Objective 3*), temperature to improve accuracy of the plate interface temperature and to detect changes associated with slow earthquakes (*Objective 2*). Furthermore, we aim to detect changes in elastic properties (e.g., velocity) related to slow earthquakes and seismic cycles (*Objective 3*). We

install two observatories based on CORK equipped with fluid pressure gauge, thermometer, and optical fiber cables, which we refer to as “Fiber-CORK” (Figure 11). The target depths of **SKP-11A** and **SKP-13A** are adequate for detecting small strain changes in high accuracy. The porosity of the sediments at these depths is expected to be less than a critical porosity (approximately 40 %) from the analysis of the Nankai accretionary margins. The target depths may be shortened if the borehole environment satisfies the stability condition for observatories after performing LWD.

The overall design of pressure and temperature sensors are based on Davis et al. (1992) and past ODP/IODP experiences in the Nankai Trough (Mikada et al. 2001; Expedition 332 Scientists 2011; Kinoshita et al. 2018), Cascadia (e.g. Davis et al. 2013) and Hikurangi (Wallace et al. 2019). Pressure ports will be installed in an open-hole section beneath a cemented interval and monitor variations in formation pore fluid pressure that is treated as a proxy for volumetric strain variation due to a near-field fault slip. A thermistor string will be attached on the tubing for long-term temperature monitoring. A series of independent temperature loggers (Fulton et al. 2013; Morono et al. 2017) will be installed within the tubing to complement the accuracy of the thermistor string. The temperature loggers will be retrieved by the ROV. The accuracy of the thermistor string and temperature loggers are $\sim 0.1\text{K}$ and $\sim 1\text{mK}$, respectively.

We will deploy two independent optical fiber measurement systems, OFS based on Michelson interferometry and DAS based on Rayleigh scattering. We use OFS to monitor strain changes with extremely high sensitivity as an average over dedicated fibers at the bottom of the borehole and DAS to measure strain and temperature changes in high spatial density along fibers installed from the wellhead to the bottom of the hole.

For OFS, two sets of dedicated optical fibers are cemented: a spiral wound optical fiber for detecting areal strain and a vertical optical fiber for detecting vertical strain at a sensitivity of 5 picostrain. Strain change will be separated from the temperature changes by using parallel optical fibers with different temperature coefficients (Zumberge et al. 2018). The measurement results

from the fiber optic strainmeter are transmitted to the UMC (Under Water Mating Connector) attached to the CORK head via the cable in the borehole. Initially, the continuous strain observation is possible over a year or two supported by battery packs.

Fiber cables for DAS are embedded along with the optical fibers for the areal strain and for the data transmission to cover from the wellhead to the bottom of the hole. Initially DAS observation requires connecting the cables to the onboard instruments via UMC. By connecting to a N-net node, continuous and real-time, high-density array seismic observations will be made possible from the seafloor. DAS can also be used to detect changes in hydrological conditions in the borehole and to observe tremors.

After one year after the installation, we plan to deploy an ROV to collect these data, analyze the wellbeing of the observatories and explore potential SSE activities. Once the N-net node becomes available and funding is secured, we plan to connect them and start real-data streaming of pressure, temperature and strain data. The connection also enables continuous power supplies over the network. As the N-net installation is currently planned in 2023-2024, we may possibly start streaming right after the installation.

6.5 Funding

To supplement the budget of LWD and Fiber-CORK operations, we plan to acquire funding from JSPS/JAMSTEC/MEXT. As our target and seawater depths are moderate, the proposed project can be undertaken by either the JOIDES Resolution or Chikyu.

7. Outcomes and Subsequent Work

The LWD and coring plan will shed light on the geomechanical, thermal and hydrological disturbances created by the seamount subduction. By combining detailed topography of the seamount illustrated by seismic and magnetic data, we envision to perform more detailed and

realistic analogue and numerical modeling of the seamount and to determine the state of the upper plate fundamental for understanding slip behaviours at the plate boundary.

The observatories with well-tested pressure/temperature sensing and cutting-edge fiber cable monitoring provides opportunities in confidently obtaining slow slip signals to fulfil primary science objectives and in challenging experimental limits. By combining with dense temporary OBS network and GNSS stations to supplement surface deformation extent, the monitoring data will enlighten an entire spectra of the slow earthquake events. We thrive to see that newly developed geomechanical, thermal and hydrological models will eventually be used to reveal the underlying physical phenomena of the slow earthquake events. Finally, we envision deep penetration holes in future to reach the plate interface to record a whole sequence of the seamount disturbance.

8. Operational options

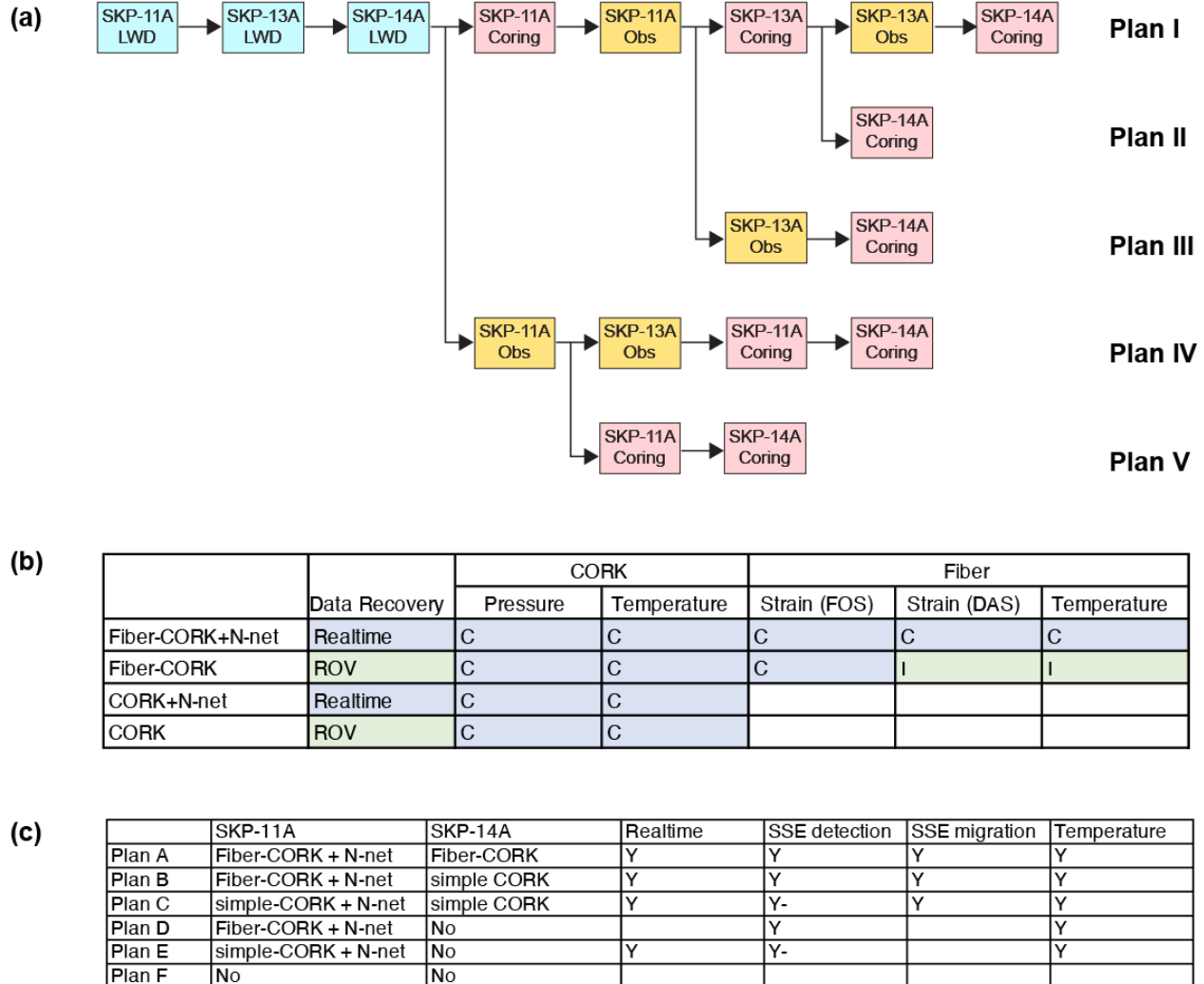


Figure 12 (a) Decision tree, (b) types of observatories and (c) observatory plans. In (b), “C” indicates continuous recording and “I” indicates intermittent recording that requires onboard systems. In (c), “Y” indicates that the category (e.g. SSE migration) can be observed with the plan. “Y-” indicates that year-long SSEs may be difficult to detect, while “Y” in SSE detection indicates that a range of SSEs can be detected at least one of the observatories.

Time estimation from JRSO is approximately 50 days for the scenario with previously assumed 700 m depths of LWD and entire coring and two observatory installations. Based on this

estimate, we propose our operation plan and decision plan as in Figure 12a. Our priority plan (Plan I) is to conduct

1. LWD at **SKP-11A, 13A and 14A**,
2. Entire coring and observatory installation at **SKP-11A**,
3. Entire coring and observatory installation at **SKP-13A**,
4. Entire coring at **SKP-14A**.

Performing LWD first makes the subsequent operation plan more flexible. For example, we may select coring intervals or even skip coring. We may install an observatory prior to coring, which is critical to ensure achieving *Objective 3 (detecting SSEs)* within the allocated time frame. The priority after LWD is to complete at least one observatory at **SKP-11A** to ensure detect SSEs (*Objective 3*), and to perform coring at the top of the seamount at **SKP-14A** to ensure comparisons of two contrasting sites, i.e., the leading and top of the seamount (*Objective 1*). In our decision tree in Figure 12a, we propose four alternative plans (Plan II, III, IV and V) in the order of our preference.

Our proposed observatory (Fiber-CORK) is the advanced version of CORK accompanying optical fiber installations. JRSO advised us that adding the proposed optical fiber cables in Figure 11 will not complicate the operation much and hence will not increase the operational time. However, as the design is new, we have prepared several scenarios to accommodate potential issues in our budget, unforeseen technical issues and operational time. We consider five scenarios for both CORK and Fiber-CORK installations, and their scientific contribution is summarized in Figure 12b-c. The preferred plan is to install two observatories with the Fiber-CORK design (Plan A), since the Fiber-CORK option edges the CORK option in detecting long-term deformations including SSEs. When installing two Fiber-CORKs becomes difficult, we first substitute the Fiber-CORK with the CORK in **SKP-13A** and keep the Fiber-CORK for **SKP-11A** to utilize data transfer capability of the N-net (Plan B). Ultimately, we may adopt the

CORK designs in both holes (Plan C). Even with this, if we may determine the only one installation is possible, we install the Fiber-CORK (Plan D) or CORK (Plan E) in **SKP-11A**.

We recognize that the observatory installation may not be possible either due to the funding or due to the operational challenges. Our diligently-created LWD and coring plan ensures to satisfy *Objective 1* and a part of *Objective 2*. In this case, we may not be able to supplement SSE information (*Objective 3*), but the determined in-situ nature unique to the seamount subduction will contribute to constraining the physical models of slow earthquake events.

We also recognize the proposed coring of the entire section may turn out too challenging during the operation. We first aim to obtain spot coring of two intervals where APCT-3 is possible; an interval in the cover sediments and the other in the old-sedimentary complex. Even when coring is not at all obtainable, the combination of seismic and LWD data allows us to discuss heat flow, hydrology and stress to still satisfy *Objectives 1 and 2*. However, a lack of age information precludes revealing the tectonic evolution related to the seamount.

We may encounter additional operational challenges arising from training areas of the US navy and of the Japanese defense force and from high fishery activities. The N-net cables planned by NIED may induce additional restrictions. We are currently cooperating with NIED to facilitate the issue.

9. Existing data

Many 2D seismic MCS and wide-angle OBS data have been acquired by JAMSTEC (e.g. Nakanishi et al. 2018; Yamashita et al. 2019a) and Japanese Coast Guard (e.g. Nishizawa et al. 2009) over the past 20 years (Figure 1). All of these data have been processed and the depth-converted migrated sections are available to us. The dense shallow penetration seismic surveys conducted in 2016 (HDNT96-102) provide detailed shallow upper-crust structures essential for planning drilling. In August 2020, four new seismic reflection and OBS profiles

were acquired along four lines jointly by JAMSTEC and University of Tokyo, and now six of seven proposed sites have cross sections. The seismic data are being processed to provide both high-resolution PSTM/PSDM sections and detailed P-wave velocity structures via full waveform inversion. Dredge sampling data are available. The regional gravity and magnetic survey data are available from AIST and the heat flow data are estimated from BSR in the seismic sections.

10. Pre-drilling data acquisition

We recognize the seamount subduction influences the structures in a complex and 3D manner. Performing 3D seismic surveys in the region is most ideal. The planning is ongoing, however, at least a few years will be required to complete the planning and to secure the funding. Instead, we plan to conduct additional 2D reflection lines in 2021 with JAMSTEC, to supplement three-dimensional structures of the area and refine our drilling targets. We also have submitted another proposal to the University of Tokyo to conduct heat flow and piston coring, as well as multi-channel seismic survey at locations at/close to the proposed drill site in order to validate the predicted temperatures from the BSRs and to identify lithological properties.

Reference

- Antriasian, A., R. N. Harris and 7 others (2019). Thermal regime of the Northern Hikurangi margin, New Zealand. *Geophys. J. Int.*, (2019) 216, 1177–1190. <https://dx.doi.org/10.1093/gji/ggy450>
- Araki, E., Saffer, D., Kopf, A., Wallace, L., Kimura, T., Machida, Y., Ide, S., Davis, E., scientists, (2017). Recurring and triggered slow-slip events near the trench at the Nankai Trough subduction megathrust. *Science*, 356(6343), 1157-1160. <https://dx.doi.org/10.1126/science.aan3120>
- Araki, E., Yokobiki T., Kimura, T., Zumberge, M. (2019a) Development of Fiber Optic Strain Observatory in Convergent Nankai Trough Seafloor and Verification Tests in Kamioka-Mine, IEEE Underwater Technology Conference, Taiwan.
- Araki, E., Zumberge, M. A., Yokobiki, T., Nishida, S., Kimura, T., Machida, Y., Kodaira, S. (2019b). Observation of slow crustal deformation by seafloor fiber optic strainmeter connected to DONET seafloor cable observation, AGU Fall Meeting.
- Asano, Y., Obara, K., Matsuzawa, T., Hirose, H., Ito, Y. (2015). Possible shallow slow slip events in Hyuga-nada, Nankai subduction zone, inferred from migration of very low frequency earthquakes. *Geophysical Research Letters*, 42(2), 331-338. <https://dx.doi.org/10.1002/2014gl062165>
- Ashi, J., Tokuyama, H., Ujiie, Y. and Taira, A. (1999). Heat flow estimation from gas hydrate BSRs in the Nankai Trough: Implications for thermal structures of the Shikoku Basin. *Eos Transactions AGU*, 80, Fall Meeting Supplement, Abstract.

Barnes, P. M., Wallace, L. W., Saffer, D. M., Bell, R. E., Underwood, M. et al. (2020). Slow slip source characterized by lithological and geometric heterogeneity, *Science Advances*, 6, eaay3314.

Bilek, S. L., Schwartz, S. Y., DeShon, H. R. (2003). Control of seafloor roughness on earthquake rupture behaviour. *Geology* 31, 455–458

Brigaud, F., Vasseur, G. (1989). Mineralogy, porosity and fluid control on thermal conductivity of sedimentary rocks. *Geophys. J.*, 98:525-542.

Bürgmann, R. (2018). The geophysics, geology and mechanics of slow fault slip. *Earth and Planetary Science Letters* 495, 112-134. <https://dx.doi.org/10.1016/j.epsl.2018.04.062>

Collot, J., Sanclemente, E., Nocquet, J., Leprêtre, A., Ribodetti, A., Jarrin, P., Chlieh, M., Graindorge, D., Charvis, P. (2017). Subducted oceanic relief locks the shallow megathrust in central Ecuador. *Journal of Geophysical Research*, 122(5), 3286-3305. <https://dx.doi.org/10.1002/2016jb013849>

Davis, E. E., K. Becker, K. Wang, K. Obara, Y. Ito, M. Kinoshita (2006). A discrete episode of seismic and aseismic deformation of the Nankai trough subduction zone accretionary prism and incoming Philippine Sea plate. *Earth and Planetary Science Letters* 242, 73–84, doi:10.1016/j.epsl.2005.11.054

Davis, E. E., Heesemann, M., IODP Expedition 328 Scientists and Engineers (2013). IODP Expedition 328: Early Results of Cascadia subduction zone ACORK Observatory. *Scientific Drilling*, 13, 12-18, doi:10.2204/iodp.sd.13.02.2011.

Davis, E. E., Mottl, M. J., Fisher, A. T., et al. (1992). CORK: A HYDROLOGIC SEAL AND DOWNHOLE OBSERVATORY FOR DEEP-OCEAN BOREHOLES, Proc. ODP, Init. Repts., 139:43-53. College Station, TX (Ocean Drilling Program).

Davis, E.E., Villinger, H. (2006). Transient formation fluid pressures and temperatures in the Costa Rica forearc prism and subducting oceanic basement: CORK monitoring at ODP Sites 1253 and 1255. *Earth and Planetary Science Letters* 245, 232–244, doi:10.1016/j.epsl.2006.02.042

Davis, E., Villinger, H., Sun, T. (2015). Slow and delayed deformation and uplift of the outermost subduction prism following ETS and seismogenic slip events beneath Nicoya Peninsula, Costa Rica. *Earth and Planetary Science Letters* 410(), 117-127. <https://dx.doi.org/10.1016/j.epsl.2014.11.015>

DeMets, C., Gordon, R., Argus, D. (2010). Geologically current plate motions. *Geophysical Journal International* 181(1), 1 80. <https://dx.doi.org/10.1111/j.1365-246x.2009.04491.x>

Deschamps, A., Lallemand, S. (2002). The West Philippine Basin: An Eocene to early Oligocene back arc basin opened between two opposed subduction zones *Journal of Geophysical Research: Solid Earth* (1978–2012) 107(B12), EPM 1-1-EPM 1-24. <https://dx.doi.org/10.1029/2001jb001706>

DeWolf, S., Wyatt, F., Zumberge, M., Hatfield, W. (2015). Improved vertical optical fiber borehole strainmeter design for measuring Earth strain. *Review of Scientific Instruments*, 86(11), 114502. <https://dx.doi.org/10.1063/1.4935923>

Ding, M., Lin, J. (2016). Deformation and faulting of subduction overriding plate caused by a subducted seamount, *Geophysical Research Letter*, <https://doi.org/10.1002/2016GL069785>

Dominguez, S., Lallemand, S. E., Malavieille, J., von Huene, R. (1998). Upper plate deformation associated with seamount subduction, *Tectonophysics*, Volume 293, Issues 3–4, 15 August 1998, Pages 207-224, [https://doi.org/10.1016/S0040-1951\(98\)00086-9](https://doi.org/10.1016/S0040-1951(98)00086-9)

Dominguez, S., Malavieille, J., Lallemand, S. (2000), Deformation of accretionary wedges in response to seamount subduction: Insights from sandbox experiments. *Tectonics*, 19(1), 182–196, doi:10.1029/1999TC900055.

Expedition 332 Scientists, 2011. Site C0002. In Kopf, A., Araki, E., Toczko, S., the Expedition 332 Scientists, Proc. IODP, 332: Tokyo (Integrated Ocean Drilling Program Management International, Inc.). doi:10.2204/iodp.proc.332.104.2011

Faccenna, C. , Holt, A. F., Becker, T. W., Lallemand, S., Royden, L. H. (2018), Dynamics of the Ryukyu/Izu-Bonin-Marianas double subduction system. *Tectonophysics*, 746, 229-238, <http://dx.doi.org/10.1016/j.tecto.2017.08.011>.

Fulton, P. M., Brodsky, E. (2016). In situ observations of earthquake-driven fluid pulses within the Japan Trench plate boundary fault zone. *Geology*, 44, 851-854. doi:10.1130/G38034.1

Fulton, P. M., Brodsky, E. E., Kano, Y., Mori, J., Chester, F. , Ishikawa, T., Harris, R. N., Lin, W., Eguchi, N., Toczko, S., Expedition 343, 343T, and KR13-08 Scientists (2013). Low coseismic friction on the Tohoku-Oki fault determined from temperature measurements: *Science*, v. 342, p. 1214– 1217, doi:10.1126/science.1243641.

Gao, X., Wang, K. (2014). Strength of stick-slip and creeping subduction megathrusts from heat flow observations. *Science*, 345(6200), 1038-1041. <https://dx.doi.org/10.1126/science.1255487>

Hall, R., Ali, J. R., Anderson, C. D., Baker, S. J. (1995) Origin and motion history of the Philippine Sea Plate. *Tectonophysics*, 251, 229–250.

Haraguchi, S., Ishii, T., Kimura, J., and Obara, Y. (2003), Formation of tonalite from basaltic magma at the Komahashi-Daini Seamount, northern Kyushu-Palau Ridge in the

Philippine Sea, and growth of Izu-Ogasawara (Bonin)-Mariana arc crust. *Contrib Mineral Petrol*, 145: 151–168, DOI 10.1007/s00410-002-0433-y.

Harris, R. N., I. Grevemeyer, C. R. Ranero, H. Villinger, U. Barckhausen, T. Henke, C. Mueller, and S. Neben (2010), Thermal regime of the Costa Rican convergent margin: 1. Along-strike variations in heat flow from probe measurements and estimated from bottom-simulating reflectors, *Geochem. Geophys. Geosyst.*, 11, Q12S28, doi:10.1029/2010GC003272

Harris, R., M. Yamano, M. Kinoshita, G. Spinelli, H. Hamamoto, and J. Ashi (2013), A synthesis of heat flow determinations and thermal modeling along the Nankai Trough, Japan, *J. Geophys. Res. Solid Earth*, 118, 2687–2702, doi:10.1002/jgrb.50230.

Heesemann M, Villinger H, Fisher AT, Tréhu AM, White S (2006). Data report: testing and deployment of the new APCT-3 tool to determine in situ temperatures while piston coring. In: Riedel M, Collett TS, Malone MJ, the Expedition 311 Scientists (eds) Proc IODP, vol 311. Integrated Ocean Drilling Program Management International, Inc, Washington, DC, doi:10.2204/iodp.proc.311.108.2006

Ikari, M., Marone, C., Saffer, D. M., Kopf, A. (2013) Slip weakening as a mechanism for slow earthquakes. *Nature Geoscience*, 6, 468-472, doi: 10.1038/NGEO1818

Ikari, M. (2019). Laboratory slow slip events in natural geological materials. *Geophysical Journal International* 218(1), 354-387. <https://dx.doi.org/10.1093/gji/ggz143>

Ikeda, T., Tsuji, T. (2018). Temporal change in seismic velocity associated with an offshore MW 5.9 Off-Mie earthquake in the Nankai subduction zone from ambient noise cross-correlation. *Progress in Earth and Planetary Science*, 5(1), 62. <https://dx.doi.org/10.1186/s40645-018-0211-8>

Ishizuka, O., Taylor, R. N., Yuasa, M., Ohara, Y. (2011), Making and breaking an island arc: A new perspective from the Oligocene Kyushu-Palau arc, Philippine Sea. *Geochem. Geophys. Geosyst.*, 12, Q05005, doi:10.1029/2010GC003440.

Kamei, R., Jang, U-G, Lumley, D., Mouri, T., Nakatsukasa, M., Takanashi, M. (2016) Time-lapse seismic waveform inversion for monitoring near-surface microbubble injection, 2016 Fall meeting, AGU, San Francisco

Kano, M., Kato, A. (2020). Detailed Spatial Slip Distribution for Short-Term Slow Slip Events Along the Nankai Subduction Zone, Southwest Japan. *Journal of Geophysical Research: Solid Earth*, 125(7) <https://dx.doi.org/10.1029/2020jb019613>

Kimura, G., Hashimoto, Y., Kitamura, Y., Yamaguchi, A., Koge, H. (2014), Middle Miocene swift migration of the TTT triple junction and rapid crustal growth in southwest Japan: A review. *Tectonics*, 33, 1219–1238, doi:10.1002/2014TC003531.

Kinoshita, M., Becker, K., Toczko, S., Edgington, J., Kimura, T., Machida, Y., Roesner, A., Senyener, B., Sun, T. (2018). Expedition 380 methods. In Becker, K., Kinoshita, M., Toczko, S., and the Expedition 380 Scientists, NanTroSEIZE Stage 3: Frontal Thrust Long-Term Borehole Monitoring System (LTBMS). *Proceedings of the International Ocean Discovery Program*, 380: College Station, TX (International Ocean Discovery Program). <https://doi.org/10.14379/iodp.proc.380.102.2018>

Kinoshita, M., Nakata, R., Hashimoto, Y. (2020) Subduction of Kyushu-Palau Ridge can cause local thermal disturbance, as estimated from new heat flow data in the forearc in the eastern Kyushu, Japan, abstract accepted for 2020 JpGU/AGU Joint Assembly.

Kinoshita, M., Tobin, H., Ashi, J., Kimura, G., Lallement, S., Sreaton, E.J., Curewitz, D. Masago, H., Moe, K.T., and the Expedition 314/315/316 Scientists (2009). *Proc. IODP*

314/315/316: Washington, DC (Integrated Ocean Drilling Program Management International Inc.). doi:10.2204/iodp.proc.314315316.2009

Kopp, H. (2013). Invited review paper: The control of subduction zone structural complexity and geometry on margin segmentation and seismicity, Tectonophysics, 589, 18 March 2013, Pages 1-16, <https://doi.org/10.1016/j.tecto.2012.12.037>

Lallemand, S., Peyret, M., Rijsingen, E., Arcay, D., Heuret, A. (2018). Roughness Characteristics of Oceanic Seafloor Prior to Subduction in Relation to the Seismogenic Potential of Subduction Zone. Geochemistry, Geophysics, Geosystems, 19(7), 2121-2146. <https://dx.doi.org/10.1029/2018gc007434>

Lindsey, N., Dawe, T., Ajo-Franklin, J. (2019). Illuminating seafloor faults and ocean dynamics with dark fiber distributed acoustic sensing. Science, 366(6469), 1103-1107. <https://dx.doi.org/10.1126/science.aay5881>

Martin, V., Henry, P., Nouze, H., Noble, M., Ashi, J., Pascal, G. (2004), Erosion and sedimentation as processes controlling the BSR-derived heat flow on the Eastern Nankai margin, Earth Planet. Sci. Lett., 222(1), 131–144, doi:10.1016/j.Epsl.2004.02.020

Martinod, J., Guillaume, B. , Espurt, N., Faccenna, C., Funiciello, F. , Regard, V. (2013) Effect of aseismic ridge subduction on slab geometry and overriding plate deformation: Insights from analogue modeling. Tectonophysics, 588, 39-55, <http://dx.doi.org/10.1016/j.tecto.2012.12.010>

Mikada, H., K. Becker, J.C. Moore, A. Klaus, et al., (Eds.), Proc. ODP, Init. Repts., vol. 196, Ocean Drilling Program, College Station, TX, USA, 2002, pp. 1 –29.

Mochizuki, K., Yamada, T., Shinohara, M., Yamanaka, Y., Kanazawa, T. (2008). Weak Interplate Coupling by Seamounts and Repeating M7 Earthquakes. Science, 321(5893), 1194-1197. <https://dx.doi.org/10.1126/science.1160250>

Morgan, J. K., Bangs, N. L. (2017). Recognizing seamount-forearc collisions at accretionary margins: Insights from discrete numerical simulations, *Geology*, 45 (7): 635–638, <https://doi.org/10.1130/G38923.1>

Morono, Y., Inagaki, F., Heuer, V. B., et al. (2017). Expedition 370 methods. In Heuer, V.B., Inagaki, F., Morono, Y., Kubo, Y., Maeda, L., and the Expedition 370 Scientists, Temperature Limit of the Deep Biosphere off Muroto. Proceedings of the International Ocean Discovery Program, 370: College Station, TX (International Ocean Discovery Program). <https://doi.org/10.14379/iodp.proc.370.102.2017>

Nakanishi, A., Takahashi, N., Yamamoto, Y., Takahashi, T., Citak, S., Nakamura, T., Obana, K., Kodaira, S., Kaneda, Y. (2018). Three-dimensional plate geometry and P-wave velocity models of the subduction zone in SW Japan: Implications for seismogenesis. in Byrne, T., Underwood, M.B., Fisher, D., McNeill, L., Saffer, D., Ujiie, K., and Yamaguchi, A., eds., *Geology and Tectonics of Subduction Zones: A Tribute to Gaku Kimura: Geological Society of America Special Paper* 534, 69–86. [https://dx.doi.org/10.1130/2018.2534\(04\)](https://dx.doi.org/10.1130/2018.2534(04))

Nakata, N., Snieder, R. (2011). Near-surface weakening in Japan after the 2011 Tohoku-Oki earthquake. *Geophysical Research Letters*, 38(17), L17302. <https://dx.doi.org/10.1029/2011gl048800>

Nakata, N., Shelly, D. (2018). Imaging a Crustal Low-Velocity Layer Using Reflected Seismic Waves From the 2014 Earthquake Swarm at Long Valley Caldera, California: The Magmatic System Roof? *Geophysical Research Letters*, 45(8), 3481-3488. <https://dx.doi.org/10.1029/2018gl077260>

Nakamura, M., Sunagawa, N. (2015). Activation of very low frequency earthquakes by slow slip events in the Ryukyu Trench. *Geophysical Research Letters*, 42(4), 1076-1082. <https://dx.doi.org/10.1002/2014gl062929>

Nishimura, T., Yokota, Y., Tadokoro, K., Ochi, T. (2018). Strain partitioning and interplate coupling along the northern margin of the Philippine Sea plate, estimated from Global Navigation Satellite System and Global Positioning System-Acoustic data. *Geosphere*, 14(2), 535-551. <https://dx.doi.org/10.1130/ges01529.1>

Nishizawa, A., Kaneda, K., Oikawa, M. (2009). Seismic structure of the northern end of the Ryukyu Trench subduction zone, southeast of Kyushu, Japan. *Earth, Planets and Space*, 61(8), e37-e40. <https://dx.doi.org/10.1186/bf03352942>

Obara, K., Kato, A. (2016). Connecting slow earthquakes to huge earthquakes *Science* 353(6296), 253-257. <https://dx.doi.org/10.1126/science.aaf1512>

Okada, Y. (1985). Surface deformation due to shear and tensile faults in a half-space. *Bulletin of the Seismological Society of America*, 75(4), 1135-1154.

Park, J., Hori, T. Kaneda, Y. (2009) Seismotectonic implications of the Kyushu-Palau ridge subducting beneath the westernmost Nankai forearc. *Earth Planetary Science*, 61, 1013–1018. <https://doi.org/10.1186/BF03352951>

Ruh, J. B., Sallares, V., Ranero, C. R. , Gerya, T. (2016). Crustal deformation dynamics and stress evolution during seamount subduction: High-resolution 3-D numerical modeling, *JGR Solid Earth*, <https://doi.org/10.1002/2016JB013250>

Saffer, D., Kopf, A., Toczko, S., Araki, E., Carr, S., Kimura, T., Kinoshita, C., Kobayashi, R., Machida, Y., Rösner, A., Wallace, L.M. (2017). Expedition 365 methods. With contributions by S. Chiyonobu, K. Kanagawa, T. Kanamatsu, G. Kimura, and M.B. Underwood. In Saffer, D., Kopf, A., Toczko, S., and the Expedition 365 Scientists,

NanTroSEIZE Stage 3: Shallow Megasplay Long-Term Borehole Monitoring System. Proceedings of the International Ocean Discovery Program, 365: College Station, TX (International Ocean Discovery Program).
<https://doi.org/10.14379/iodp.proc.365.102.2017>

Saffer, D., Tobin, H. (2011). Hydrogeology and Mechanics of Subduction Zone Forearcs: Fluid Flow and Pore Pressure. *Annu. Rev. Earth Planet. Sci.* 2011. 39:157–86.
<https://doi.org/10.1146/annurev-earth-040610-133408>

Saffer, D., Wallace, L. (2015). The frictional, hydrologic, metamorphic and thermal habitat of shallow slow earthquakes. *Nature Geoscience* 8(8), 594-600.
<https://dx.doi.org/10.1038/ngeo2490>

Sella, G. F., Dixon, T. H., Mao, A. (2002). REVEL: a model for recent plate velocities from space geodesy, *J. geophys. Res.*, 107 (B4), doi:10.1029/2000JB000033.

Shelly, D., Beroza, G., Ide, S., Nakamura, S. (2006). Low-frequency earthquakes in Shikoku, Japan, and their relationship to episodic tremor and slip. *Nature*, 442(7099), 188-191.
<https://dx.doi.org/10.1038/nature04931>

Spinelli, G. A., Harris, R. N. (2011). Thermal effects of hydrothermal circulation and seamount subduction: Temperatures in the Nankai Trough Seismogenic Zone Experiment transect, Japan, *Geochem. Geophys. Geosyst.*, 12, Q0AD21,

Sun, T., Ellis, S., Saffer, D. (2020a). Coupled evolution of deformation, pore fluid pressure, and fluid flow in shallow subduction forearcs. *Journal of Geophysical Research: Solid Earth*, 125, e2019JB019101. <https://doi.org/10.1029/2019JB019101>

Sun, T., Saffer, D., Ellis, S. (2020b). Mechanical and hydrological effects of seamount subduction on megathrust stress and slip, *Nature geoscience*, <https://doi.org/10.1038/s41561-020-0542-0>

Taira, A., Hill, I., Firth, J.V., et al. (1991). Proceedings of the Ocean Drilling Program, Initial Reports, 131: College Station, TX (Ocean Drilling Program).
<http://dx.doi.org/10.2973/odp.proc.ir.131.1991>

Takemura, S., Okuwaki, R., Kubota, T., Shiomi, K., Kimura, T., Noda, A. (2020). Centroid moment tensor inversions of offshore earthquakes using a three-dimensional velocity structure model: slip distributions on the plate boundary along the Nankai Trough. *Geophysical Journal International*, 222(2), 1109-1125.
<https://dx.doi.org/10.1093/gji/ggaa238>

Tobin, H. J., Kimura, G., Kodaira, S. (2019). Processes governing giant subduction earthquakes: IODP drilling to sample and instrument subduction zone megathrusts. *Oceanography*, 32(1):80–93. <https://doi.org/10.5670/oceanog.2019.125>

Todd, E., Schwartz, S., Mochizuki, K., Wallace, L., Sheehan, A., Webb, S., Williams, C., Nakai, J., Yarce, J., Fry, B., Henrys, S., Ito, Y. (2018). Earthquakes and Tremor Linked to Seamount Subduction During Shallow Slow Slip at the Hikurangi Margin, New Zealand *Journal of Geophysical Research: Solid Earth* 123(8), 6769-6783.
<https://dx.doi.org/10.1029/2018jb016136>

Tonegawa, T., Yamashita, Y., Ito, A., Shinohara, M., Suetsugu, D., Takahashi, T., Ishihara, Y., Kodaira, S., Kaneda, Y. (2020). Spatial relationship between shallow very low frequency earthquakes and the subducted Kyushu-Palau Ridge in the Hyuga-nada region of the Nankai subduction zone, *Geophysical Journal International*, 222(3), 1542–1554, <https://doi.org/10.1093/gji/ggaa264>.

Tsuji, T., Kamei, R., Pratt, R. (2014). Pore pressure distribution of a mega-splay fault system in the Nankai Trough subduction zone: Insight into up-dip extent of the seismogenic zone. *Earth and Planetary Science Letters*, 396(C), 165-178.
<https://dx.doi.org/10.1016/j.epsl.2014.04.011>

Uchida, N., Takagi, R., Asano, Y., Obara, K. (2019). Migration of shallow and deep slow earthquakes toward the locked segment of the Nankai megathrust, *Earth and Planetary Science Letters*, 531, 115986. <https://dx.doi.org/10.1016/j.epsl.2019.115986>

von Huene, R., Scholl, D. W. (1991). Observations at convergent margins concerning sediment subduction, subduction erosion, and the growth of continental crust, *Review of Geophysics*, <https://doi.org/10.1029/91RG00969>

Wallace, L., Beavan, J. (2010). Diverse slow slip behavior at the Hikurangi subduction margin, New Zealand, *Journal of Geophysical Research*, 115, B12402.
<https://dx.doi.org/10.1029/2010jb007717>

Wallace, L. M., Ellis, S., Miyao, K., Miura, S., Beavan, J., Goto, J. (2009). Enigmatic, highly active left-lateral shear zone in southwest Japan explained by aseismic ridge collision, *Geology* 37, 143–146. <http://dx.doi.org/10.1130/G25221A.1>.

Wallace, L. M., Saffer, D. M., Barnes, P. M., Pecher, I. A., Petronotis, K. E., LeVay, L. J., the Expedition 372/375 Scientists (2019). Hikurangi Subduction Margin Coring, Logging, and Observatories. *Proceedings of the International Ocean Discovery Program*, 372B/375: College Station, TX (International Ocean Discovery Program).
<https://doi.org/10.14379/iodp.proc.372B375.2019>

Wallace, L., Webb, S., Ito, Y., Mochizuki, K., Hino, R., Henrys, S., Schwartz, S., Sheehan, A. (2016). Slow slip near the trench at the Hikurangi subduction zone, New Zealand, *Science*, 352(6286), 701-704. <https://dx.doi.org/10.1126/science.aaf2349>

Wang, K., Bilek, S. L. (2011). Do subducting seamounts generate or stop large earthquakes? *Geology* 39, 819–822. <http://dx.doi.org/10.1130/G31856.1>.

Wang, K., Bilek S. L. (2014). Invited review paper: Fault creep caused by subduction of rough seafloor relief, *Tectonophysics*, 610, 6 January 2014, Pages 1-24, <https://doi.org/10.1016/j.tecto.2013.11.024>

Williams, E., Fernández-Ruiz, M., Magalhaes, R., Vanthillo, R., Zhan, Z., González-Herráez, M., Martins, H. (2019). Distributed sensing of microseisms and teleseisms with submarine dark fibers, *Nature Communications*, 10(1), 5778. <https://dx.doi.org/10.1038/s41467-019-13262-7>

Wu, J., Suppe, J., Lu, R., Kanda, R. (2016), Philippine Sea and East Asian plate tectonics since 52 Ma constrained by new subducted slab reconstruction methods, *J. Geophys. Res. Solid Earth*, 121, 4670–4741, doi:10.1002/2016JB012923.

Yagi, Y., Kikuchi, M., Yoshida, S., Sagiya, T. (1999). Comparison of the coseismic rupture with the aftershock distribution in the Hyuga-nada Earthquakes of 1996, *Geophysical Research Letters*, 26(20), 3161-3164. <https://dx.doi.org/10.1029/1999gl005340>

Yamamoto, Y., Obana, K., Takahashi, T., Nakanishi, A., Kodaira, S., Kaneda, Y. (2013). Imaging of the subducted Kyushu-Palau Ridge in the Hyuga-nada region, western Nankai Trough subduction zone, *Tectonophysics*, 589, 90-102. <https://dx.doi.org/10.1016/j.tecto.2012.12.028>

Yamano, M., Kinoshita, M., Goto, S., Matsubayashi, O. (2003) Extremely high heat flow anomaly in the middle part of the Nankai Trough, *Phys. Chem. Earth*, 28, 487-497.

Yamashita, M., Nakanishi, A., Arai, R., Moore, G., Kodaira, S., Miura, S., Kaneda, Y. (2019a) Structural characteristics of the subducting Kyushu-Palau ridge around the Hyuga-nada

region in Nankai Trough revealed by seismic reflection imaging, JpGU meeting 2019, Chiba, Japan.

Yamashita, Y., Yakiwara, H., Asano, Y., Shimizu, H., Uchida, K., Hirano, S., Umakoshi, K., Miyamachi, H., Nakamoto, M., Fukui, M., Kamizono, M., Kanehara, H., Yamada, T., Shinohara, M., Obara, K. (2015). Migrating tremor off southern Kyushu as evidence for slow slip of a shallow subduction interface, *Science*, 348(6235), 676-679. <https://dx.doi.org/10.1126/science.aaa4242>

Yamashita, Y., Watanabe, S., Yamada, T., Shinohara, M., Matsushima, T. (2019b) Spatiotemporal variation of released seismic energy from shallow low-frequency tremor in Hyuga-nada, revealed by ocean bottom seismological observation, JpGU meeting 2019, Chiba, Japan

Yokota, Y., Ishikawa, T. (2020). Shallow slow slip events along the Nankai Trough detected by GNSS-A, *Science Advances* 6(3), eaay5786. <https://dx.doi.org/10.1126/sciadv.aay5786>

Yoshioka S. (2007) Difference in the maximum magnitude of interplate earthquakes off Shikoku and in the Hyuganada region, southwest Japan, inferred from the temperature distribution obtained from numerical modeling – The proposed Hyuganada triangle –, *Earth and Planetary Science Letters* 263 (2007) 309–322.

Zumberge, M., Hatfield, W., Wyatt, F. (2018). Measuring Seafloor Strain With an Optical Fiber Interferometer, *Earth and Space Science*, 5(8), 371-379. <https://dx.doi.org/10.1029/2018ea000418>

Rie Nakata
Earthquake Research Institute, University of Tokyo
 1-1-1 Yayoi, Bunkyo-ku, Tokyo, Japan
 T: +1 405 406 4172; E: rie.nakata.r@gmail.com

Education

2008-2012	Ph.D. in Geophysics Department of Earth Sciences, The University of Western Ontario
2003-2005	M. Eng. Department of Civil and Earth Resources Engineering, Kyoto University
1999-2003	B. Eng. Undergraduate School of Global Engineering, Kyoto University

Work experiences

2019-	Assistant Professor (tenured), Earthquake Research Institute, The university of Tokyo
2019	Visiting Scientist, Department of Earth, Atmospheric and Planetary Sciences, Massachusetts Institute of Technology
2017-2018	Visiting Researcher, ConocoPhillips School of Geology and Geophysics, The University of Oklahoma
2013-2018	Research Fellow, Centre for Energy Geoscience, School of Earth Environment, The University of Western Australia
2013	Post-doctoral fellow, Department of Earth Sciences, The University of Western Ontario

Publications

1. **Nakata, R.**, Lumley, D., Hampson, G., Nihei, K., Nakata, N., 2020, Waveform-based estimation of Q and scattering properties for zero-offset VSP data, *Geophysics*, submitted.
2. Tsuji, T., Minato, S., **Kamei, R.**, Tsuru, T., Kimura, G. 2017 Detachment fault from fully coupled plate interface; Insights from seismic profiles at the hypocenter of the 2016 Off-Mie earthquake in the Nankai Trough, submitted to *Earth and Planetary Science Letters*
3. **Kamei, R.**, Lumley, D. 2017 Full waveform inversion of repeating seismic events to estimate time-lapse velocity changes, *Geophysical Journal International*, 209(2), 1239-1264.
4. Lumley, D., King, A., Pevzner, R., Bona, A., Dautriat, J., Esteban, L., Hauser, T., Hoskin, T., Issa, N., **Kamei, R.**, Langhi, L., Miyoshi, T., Mueller, T., Potter, T., Sarout, J., Siggins, T., Shragge, J., Tertyshnikov, K., Urosevic, M., 2016, Feasibility and Design for Passive Seismic Monitoring at the SW Hub CO2 Geosequestration Site, Report for Australian National Low Emissions Coal Research & Development Project 7-0212-0203 (available from http://anlecrd.com.au/wp-content/uploads/2016/08/ANLEC-Project-7-0212-0203_Revised-Final-Report-24.06.2016.pdf).
5. **Kamei, R.**, Miyoshi, T., Pratt, R. G., Takanashi, M., Masaya, S., 2015, Application of waveform tomography to a crooked-line 2D land seismic data set, *Geophysics*, B125-B129
6. **Kamei, R.**, Nakata, N., Lumley D., 2015, Introduction to Microseismic Source Mechanisms, *The Leading Edge*, 876-880.
7. Gavin, L. J., Hoskin, T., Witten, B., Deeks, J., **Kamei, R.**, Markov, J., Shragge, J. 2014, Geophysical remote sensing of historical Aboriginal gravesites in southwestern Western Australia, *The Leading Edge*, 1348-1354.
8. Afanasiev, M., Pratt, R. G., **Kamei, R.**, 2014, Waveform-based simulated annealing of crosshole transmission data: A semi-global method for estimating seismic anisotropy, 199(3), 1586-1607
9. Tsuji, T., **Kamei, R.**, Pratt, R. G., 2014. Mega-splay fault characterization from pore pressure distribution in the Nankai seismogenic zone. , *Earth and Planetary Science Letters*, 396, 165-178

10. **Kamei, R.**, Pratt, R. G., Tsuji, T., 2014. On misfit functions for Laplace-Fourier waveform inversion, with applications to wide-angle OBS data. *Geophysical Prospecting* doi: 10.1111/1365-2478.12127
11. **Kamei, R.**, Pratt R. G., 2013, Inversion strategies for visco-acoustic waveform inversion *Geophysical Journal International*, 194 (2): 859-884.
12. **Kamei, R.**, Pratt, R. G, Tsuji, T., 2013, On Acoustic Waveform Tomography of wide-angle OBS data - Strategies for preconditioning and inversion. *Geophysical Journal International*: ggt165v1-ggt165.
13. **Kamei, R.**, Pratt, R. G., Tsuji, T., 2012. Waveform Tomography Imaging of a Megasplay Fault System in the Seismogenic Nankai Subduction Zone, *Earth and Planetary Science Letters*, 317-318, 343-353.
14. **Kamei, R.**, Hato, M., Matsuoka, T. 2005 Random heterogeneous model with bimodal velocity distribution for Methane Hydrate exploration, *Exploration Geophysics*, 36, 41-49.

GRANTS

- 2019-2020 *Waveform imaging of Eastern Iburi earthquake rupture area*, Tokyo Marine Memorial Institute, PI, JPY1M, with Kurashimo, E.
- 2019-2020 *Development of Waveform based methods*, U. Tokyo, PI, JPY 1.8M, with Morita, R., Mochizuki, K., Takeuchi, N., Nishida, K.
- 2019-2020 *Development of marine DAS acquisition system*, U. Tokyo, CI, JPY 80M, with Shinohara, N., Hirata, N., Mochizuki, M.
- 2019-2020 *Developing time-lapse full waveform inversion methods for cross-well monitoring data sets*, Japan Oil, Gas and Metal National Corporation, PI, \$71k with Nakata, N.
- 2017-2018 *Developing time-lapse full waveform inversion methods for cross-well monitoring data sets*, Japan Oil, Gas and Metal National Corporation (JOGMEC), CI, A\$97k, with Lumley, D., Miyoshi, T.
- 2016 *Predictive noise attenuation of VSP data for Q Estimation – Proof of Concept*, Chevron, CI, A\$20k, with Lumley, D.
- 2015-2016 *Elastic full waveform inversion for monitoring using field data and comparison with Acoustic FWI*, Japan Oil, Gas and Metal National Corporation (JOGMEC), PI, A\$90k, with Lumley, D., and Jang, U-G.
- 2013-2015 *Feasibility and design of robust passive seismic monitoring arrays for CO2 geosequestration*, Australian National Low Emissions Coal Research & Development, 2012, A\$1000k, with Lumley, D., et al.
- 2014-2015 *Full waveform inversion of VSP data for Q estimation*, Chevron Energy Technology, PI, A\$50k, with Lumley, D.
- 2014-2015 *Elastic full waveform inversion for S-wave velocity using vector potential*, Japan Oil, Gas and Metal National Corporation (JOGMEC), PI, A\$70k, with Lumley, D.,
- 2013-2014 *Advanced Imaging with Broadband Seismic Data*, Chevron Australia, A\$35k, with Lumley, D., Jang, U-G..
- 2012-2013 *Full waveform inversion of land seismic data*, Japan Oil, Gas and Metal National Corporation (JOGMEC), PI, C\$110k, with Pratt, R. G., Miyoshi, T.

HONOURS AND AWARDS

- 2013 Best paper, Japan Association for Petroleum Technology, Japan
 2010 Best presentation, 112th Meeting, Society of Exploration Geophysicists In Japan

Yoshitaka Hashimoto

Natural sciences Cluster, Research and Education Faculty, Kochi University
2-5-1 Akebono-cho, Kochi 780-8520, JAPAN
hassy@cc.kochi-u.ac.jp
+81-88-844-8318

Education

BSc Department of geological and mineralogical science, Faculty of Science, Hokkaido University (1996)
MSc Department of Earth and Planetary Science, Faculty of Science, Hokkaido University (1998)
PhD Department of Earth and Planetary Science, Faculty of Science, University of Tokyo (2001)

Work Experiences

Present position:

- Professor, Natural sciences Cluster, Research and Education Faculty, Kochi University, Kochi Japan
- Professor, Department of Global Environment and Disaster Prevention, Faculty of Science and Technology, Kochi University, Kochi, Japan
- Professor (concurrent), Center for Advanced Marine Core Research, Kochi University, Kochi, Japan
- Delegate, Japan Geoscience Union

Past Position:

2000-2001 Japan Society for the Promotion of Science Research fellow (DC2)
2001-2002 Japan Society for the Promotion of Science Research fellow (PD)
2002-2007 Kochi University Assistant Professor
2007-2009 JSPS postdoctoral fellowship for research abroad (University of Wisconsin –Madison)
2007- 2017 Kochi University Associate Professor
2016-2017 Guest researcher at GEOMAR, Germany

Publications Past five years:

Hashimoto, Y. and Eida, M., Quantitative estimation of fluid pressure ratio of shear vein in an onland accretionary complex, the Yokonami mélange, the Cretaceous Shimanto Belt, Kochi, southwest Japan, *Tectonophysics*, 2015, 665, 17-22.

Hashimoto, Y., et al., Changes in paleostress and its magnitude related to seismic cycles in the Cehlung-pu Fault, Taiwan, *Tectonics*, 2015, 34, 2418-2428.

Hamahashi, M., et al. (Hashimoto on the 10th.), Multiple damage zone structure of an exhumed seismogenic megasplay fault in a subduction zone - A study from the Nobeoka Thrust Drilling Project -, *Earth, Planets and Space*, 2015, 67:30.

Tonai, S., et al. (Hashimoto on the 3rd.), Complete 40 Ar resetting in an ultracataclasite by reactivation of a fossil seismogenic fault along the subducting plate interface in the Mugi Mélange of the Shimanto accretionary complex, southwest Japan. *Journal of Structural Geology*, 2016, 89, 19-29.

Kawasaki, R., et al. (Hashimoto on the 3rd.), Temporal stress variations along a seismogenic megasplay fault in the subduction zone: an example from the Nobeoka Thrust, southwestern Japan, *Island arc*, 2017, 26.

Hashimoto, Y., et al., Acoustic properties of deformed rocks at the Nobeoka thrust in the Shimanto Belt, Kyushu, Southwest Japan, Island arc, 2017, DOI: 10.1111/iar.12198.

Kameda, J., et al. (Hashimoto on the 6th.), Alteration and dehydration of subducting oceanic crust within subduction zones: Implications for décollement step-down and plate boundary seismogenesis, Earth planets and Space, 2017, 69:52.

Hamahashi, M., et al. (Hashimoto on the 4th.), Normal faulting and mass movement during ridge subduction inferred from porosity transition and zeolitization in the Costa Rica subduction zone, G3., 2017, 18, 2601-2616.

Hashimoto, Y., et al., Normal faults at depth with thrust faults in an exhumed accretionary complex, Kayo Formation, Okinawa islands, Japan, Geological Society of America Special Publications, 2018, 534, Doi:[https://doi.org/10.1130/2018.2534\(11\)](https://doi.org/10.1130/2018.2534(11))

Hamahashi, M. et al. (Hashimoto on the 4th.), Physical property anisotropy of foliated fault rocks: Study from the Nobeoka Thrust, Shimanto Belt, southwest Japan, Island Arc, 2018, DOI: 10.1111/iar.12257.

Jeppson, T., et al. (Hashimoto on the 4th.), Laboratory measurements quantifying elastic properties of accretionary wedge sediments: Implications for slip to the trench during the 2011 Mw 9.0 Tohoku-Oki earthquake, Geosphere, 2018

Hashimoto, Y., et al., Paleo-stress orientations and magnitudes from triaxial testing and stress inversion analysis in Nankai accretionary prism sediments, Progress in Earth and Planetary Science, 2019, 6, 3.

Kinoshita, M., et al. (Hashimoto on the 4th.), Geometrical dependence on the stress and slip tendency acting on the subduction megathrust of the Nankai seismogenic zone off Kumano, Prog. in Earth and Planetary Science, 2019, 6,7.

Kate Corry-Saavedra, et al. (Hashimoto on the 7th.), The Role of Dispersed Ash in Orbital-Scale Time Series Studies of Explosive Arc Volcanism: Insights from IODP Hole U1437B, Northwest Pacific Ocean, Int. Geol. Rev. 2019,

Kimura, G., et al. (Hashimoto on the 5th.), Origin of the early Cenozoic belt boundary thrust and Izanagi–Pacific ridge subduction in the western Pacific margin, Island Arc, 2019, DOI: 10.1111/iar.12320

Å. Fagereng, H.M. et al. (Hashimoto on the 13th.), Mixed deformation styles on a shallow subduction thrust, Hikurangi margin, New Zealand, Geology, 2019, DOI:<https://doi.org/10.1130/G46367.1>

Donald M. Fisher, et al. (Hashimoto on the 3rd.), K-Ar Dating of Fossil Seismogenic Thrusts in the Shimanto Accretionary Complex, Southwest Japan, Tectonics, 2019, DOI: 10.1029/2019TC005571

ICDP and IODP Project Participations

2004 ICDP Taiwan Chelung-pu Fault Drilling Project (TCDP) as a structural geologist and a clay mineral geochemist

2005 IODP Expedition 311 Cascadia gas hydrate as a sedimentologist

2007 IODP Expedition 315 NantroSEIZE as a sedimentologist

2010 IODP Expedition 333 Inputs coring 2 and heat flow as an offshore scientist

2011 IDOP Expedition 343 J-FAST as an offshore scientist

2012 IODP Expedition 344 CRISP-A2 as a physical property specialist

2018 IODP Expedition 375 Hikurangi subduction margin as a sedimentologist

Masataka Kinoshita

Professor, Ph.D.
 Earthquake Research Institute
 The University of Tokyo
 1-1-1 Yayoi, Bunkyo-ku Tokyo
 113-0032 JAPAN tel: +81-3-
 5841-5809
 masa@eri.u-tokyo.ac.jp

Education

Geophysical Institute, University of Tokyo B.S. Geophysics, 1985
 Earthquake Research Institute, University of Tokyo M.S. Geophysics, 1987
 Earthquake Research Institute, University of Tokyo D. Science, Geophysics, 1990

Work experiences

2015- Professor, Earthquake Research Institute, the University of Tokyo 2015
 Deputy Director, Ocean Drilling R&D, Japan Agency for Marie-Earth Sci. Tech.
 2012-2014 Director, Kochi Core Center, JAMSTEC
 2004-2011 Team Leader, IFREE, JAMSTEC
 2001-2003 Sub Leader, Dept. Deep Sea Res., JAMSTEC
 1997-2000 Associate Professor, Tokai University, Japan
 1992-1996 Assistant Professor, Tokai University, Japan
 1990-1991 Research Associate, Tokai University, Japan
 1995-1996 Visiting Scientist, Lamont-Doherty Earth Observatory
 2003-2015 Visiting Professor, Kochi University
 2013-2014 Visiting Professor, Kyoto University 2013-2014
 2015-Present Visiting Researcher, JAMSTEC

Publications (recent 5 years)

Shiraishi K., et al. (Kinoshita on the 12th.) (2020), Earth, Planets and Space, 70
 Kinoshita, M., et al. (2019), Progress in Earth and Planetary Science (*PEPS*), 6:7
 Miyakawa, A., M. Kinoshita, et al. (2019), *PEPS*, 6:8.
 Kinoshita, M., et al. (2018), MAR PETROL GEOL, 108, 368-376
 Tanikawa, W., et al. (Kinoshita on the 12th.) (2019), MAR PETROL GEOL, 108, 332-347
 Hirose, T., et al. (Kinoshita on the 13th.) (2019), MAR PETROL GEOL, 108, 148-355
 Ijiri, A., et al. (Kinoshita on the 6th.) (2019), MAR PETROL GEOL, 108, 377-388
 Hamada, Y., et al. (Kinoshita on the 14th.) (2019), MAR PETROL GEOL, 108, 356-367
 Gupta, L.P., et al. (Kinoshita on the 12th.) (2019) MAR PETROL GEOL, 108, 239-248
 Hamada, Y., et al. (Kinoshita on the 37th.) (2018), *PEPS*, 5:70
 Yamamoto, Y., et al. (Kinoshita on the 11th.) (2018), Geological Society, London, Special Publications, 477, 183-193
 Lin, W., et al. (Kinoshita on the 3rd.) (2018), Geology and Tectonics of Subduction Zone, Geological Society of America Books.
 Toki, T., M. Kinoshita, et al., (2017), Tectonophysics, 710–711, 88-96
 Hirono, T., et al. (Kinoshita on the 6th.) (2016), Sci. Rep. 6, 28184
 Kinoshita, M., et al. (2015), Earth, Planets and Space, 67, 16
 Lin, W., et al. (Kinoshita on the 3rd.) (2015), Tectonophysics, 692, 120-130
 Hino, R., et al. (Kinoshita on the 9th.) (2015), Earth, Planets and Space, 67:7

Projects lead/committed

- 2007-2019 IODP Nankai Trough Seismogenic Zone Experiments (NanTroSEIZE)
 2018-2020 PI, Grant-in-aid for Basic Research, Japan. “How the Chile Triple Junction generated the M9 earthquake? -A challenge from thermal investigation-”

Participation in scientific ocean drilling

- 2018 IODP Exp380, “NanTroSEIZE Stage 3: Frontal Thrust Long-Term Borehole Monitoring System (LTBMS)”, as a Co-chief scientist.
 2016 IODP Exp.370, “Temperature Limit of the Deep Biosphere off Muroto”, onboard as a T-Limit Project Coordination Team liaison and a temperature monitoring system PI.
 2010 IODP Exp. 326, “NanTroSEIZE Stage 3: Plate Boundary Deep Riser 1”, as a Co-chief Scientist.
 2009 IODP Exp. 319, “NanTroSEIZE Stage 2: NanTroSEIZE riser/riserless observatory”, as a Project management Team
 2007 IODP Exp. 314, “NanTroSEIZE Stage 1: LWD Transect”, as a co-chief scientist
 2001 ODP Leg196, “Nankai Trough Accretionary Prism: LWD and ACORK”, as an ACORK scientist.
 1991 ODP Leg139, “Middle Valley, Juan de Fuca Ridge”, as a physical properties specialist.

Participation in major research cruises

- | | |
|------------------|--|
| 2018 KH18-05 | Kuril Trench, Outer Rise Heat flow flow |
| 2018 KR18-04 | Nankai Trough, ROV dives to recover borehole temperature data |
| 2014 KR15-14 | Nankai Trough, ROV dives to measure borehole pressure |
| 2012 KR12-17 | Nankai Trough, ROV dives to measure borehole pressure |
| 2011 KR11-12 | Nankai Trough, ROV dives to measure borehole pressure |
| 2008 KY08-01 | Nankai Trough & Okinawa Trough, MGG survey |
| 2008 KR08-13 | Nankai Trough, ROV dives to measure borehole pressure |
| 2007 KR07-18 | Nankai Trough, ROV dives to measure borehole pressure |
| 2007 KY07-01 | Iheya hydrothermal field, mid-Okinawa Trough |
| 2006 KR06-10 | Nankai Trough, ROV dives to measure borehole pressure |
| 2005 KY05-14 | Nankai Trough & Okinawa Trough, MGG survey |
| 2004 YK04-05 | Nankai Trough, ROV dives to measure borehole pressure |
| 2002 KR02-10 | Nankai Trough, ROV dives to measure borehole pressure |
| 2002 NT02-09 | Suiyo Seamount, ROV survey for hydrothermal system |
| 2001 NT02-08 | Suiyo Seamount, ROV survey for hydrothermal system |
| 2000 K2K | Knipovich Ridge, heat flow |
| 1999 NGH99 | Nankai Trough, heat flow |
| 1997 SEPR97 | Deployment of long-term heat flow instrument using submersible Shinkai 6500 at EPR 17°S ridge crest |
| 1996 KAIKO-TOKAI | l'Atalante cruise (Japan-French cooperative survey on hydrological regime in the Nankai Trough) |
| 1994 MODE94 | Japan-U.S. cooperative diving investigation at TAG hydrothermal mound using submersible Shinkai-6500 |
| 1994 MODE94 | Japan-U.S. cooperative diving investigation at EPR 14-18°S using submersible Shinkai-6500 |
| 1990 HYDROMIN-II | Japan-Germany cooperative survey of hydrothermal field in the Mid-Okinawa Trough |
| 1990 Science 1 | Heat flow measurements in the East China Sea (Japan-China cooperative cruise) |
| 1990 HYDROMIN-I | Japan-Germany cooperative survey of hydrothermal field in the Mid-Okinawa Trough |

Yohei Hamada

Ph.D.

Japan Agency for Marine-Earth
Science and Technology, Kochi
200 Monobe-otsu Nankoku
Kochi 783-8502, JAPAN
tel: +81-88-878-2260
yhamada@jamstec.go.jp

Education

- 2008 B. S., Department of Physics, Faculty of Science, Osaka University
- 2010 M. S., Department of Earth and Space Science, Graduate School of Science, Osaka University
- 2013 D. S., Department of Earth and Planetary Science, Graduate School of Science, The University of Tokyo

Work experiences

- 2020- Researcher, Kochi Core Center, JAMSTEC
- 2014-2019 Researcher (II), Kochi Core Center, JAMSTEC
- 2013-2014 Research Fellow (PD) of the Japan Society for the Promotion of Science
Institute for Research on Earth Evolution, JAMSTEC
- 2010-2013 Research Fellow (DC1) of the Japan Society for the Promotion of Science
Department of Earth and Planetary Science, Graduate School of Science, The University of Tokyo

Publications (peer reviewed, recent 5 years)

- Kameda, J., and Hamada, Y. (2020), Geophys. Res. Lett., 47, 18, e2020GL088395
- Hamada, Y., et al. (2019), MAR PETROL GEOL, 108, 356–367.
- Kameda, J., et al. (Hamada on the 5th.) (2019), Earth, Planets and Space, 71, 131
- Yabe, S., et al. (Hamada on the 3rd.) (2019), Earth Planets Space, 71, 116
- Kitamura, M., et al. (Hamada on the 4th.) (2019), Geophys. Res. Lett., 46(19), 10791–10799
- Ijiri, A., et al. (Hamada on the 9th.) (2019), MAR PETROL GEOL, 108, 377-388
- Saito, S., et al. (Hamada on the 5th.) (2019), MAR PETROL GEOL, 108, 216-225
- Kinoshita, M., et al. (Hamada on the 10th.) (2019), MAR PETROL GEOL, 108, 368-376
- Tanikawa, W., et al. (Hamada on the 3rd.) (2019), MAR PETROL GEOL, 108, 332-347
- Hirose, T., et al. (Hamada on the 3rd.) (2019), MAR PETROL GEOL, 108, 148-355
- Gupta, L.P., et al. (Hamada on the 3rd.) (2019) MAR PETROL GEOL, 108, 239-248
- Tanikawa, W., et al. (Hamada on the 3rd.) (2019), Marine Geology, 415, 105962
- Hasegawa, R., et al. (Hamada on the 4th.) (2019), Prog. Earth Planet. Sci., 6, 36
- Miyakawa, A., et al. (Hamada on the 3rd.) (2019), Prog. Earth Planet. Sci., 6, 1
- Ota, Y., et al. (Hamada on the 16th.) (2019), GEOCHEM GEOPHY GEOSY, 20(1) 148–165
- Hamada, Y., et al. (2018), Prog. Earth Planet. Sci., 5, 70
- Hamahashi, M., et al. (2018), Island Arc, 27(5)
- Lin, W., et al. (Hamada on the 7th.) (2018), The Geological Society of America, 534, 35–50
- Hamada, Y., et al. (2018), Scientific Reports, 8, 2622

- Kawabata, K., et al., (2018), The Geological Society of America, 534, 141–154
 Ijiri, A., et al. (Hamada on the 5th.) (2018), Geochemical Journal, 52(4), 373–378
 Hamada, Y., et al. (2018), Island Arc, 2018;e12241
 Yamamoto, Y., Hamada, Y., et al. (2017), Tectonophysics, 710, 81–87
 Hashimoto, Y., et al. (Hamada on the 10th.) (2017), Island Arc, 26, 4
 Kawasaki, R., et al. (Hamada on the 8th.) (2017), Island Arc, 26, 3
 Kameda, J., et al. (Hamada on the 5th.) (2017), Earth, Planets and Space. 69:52
 Hoshino, T., and Hamada, Y. (2017), Jour. Bioscience and Bioengineering, 124(3), 359-364.
 Yamaguchi, A., et al. (Hamada on the 3rd.) (2017), Tectonophysics, 686, 24.
 Sanada, Y., et al. (Hamada on the 3rd.) (2016), 22 Formation Evaluation Symposium of Japan
 Hamada, Y., et al. (2015), Earth Planet and Space, 67, 39
 Lin, W., et al. (Hamada on the 3rd.) (2015), Jour. of Geosci. and Environ. Prot., 3, 72-79
 Kameda, J., et al. (Hamada on the 9th.) (2015), Geochem. Geophys. Geosy. 16, 2725–2742
 Hamahashi, M., Hamada, Y., et al. (2015), Earth, Planet and Space, 67:30

Projects lead/Grants

- 2021 (proposal submitted) Hyuga-nada, seismic reflection survey around Toi-SMT
 2020- PI, Grant-in-Aid for Scientific Research. “Experimental investigation for acquiring in-situ formation strength”
 2020 PI, Fukada geological Institute grant. “Basic evaluation of high-speed multipoint analysis in field survey of magnetic susceptibility and elemental composition”
 2017 PI, Sasakawa Scientific Research Grant. “Automatic identification of microfossils by machine learning to elucidate the history of fault activity”
 2015-2016 PI, Grant-in-Aid for Scientific Research. “Investigation of co-seismic chemical reaction”
 2013 PI, JSPS Research Fellow (PD). “Chemical reaction recorded in fault material and slip behaviour on plate subduction zone”
 2010-2012 PI, JSPS Research Fellow (PD). “Coseismic chemical reaction”

Participation in scientific ocean drilling

- 2018 IODP Exp358, ‘NanTroSEIZE Deep Riser Drilling: Nankai Seismogenic/Slow Slip Megathrust”, as Logging Specialist/Logging Staff Scientist.
 2016 Cross-ministerial Strategic Innovation Promotion Program, “Hydrothermal reservoir drilling program II in Okinawa Trough”, as Logging Specialist.
 2013 IODP Exp. 348, “NanTroSEIZE Stage 3: Plate Boundary Deep Riser 3”, as Logging Staff Scientist.
 2009 IODP Exp. 322, “NanTroSEIZE Stage 2: NanTroSEIZE subduction inputs”, as Physical Properties Specialist.

Participation in major research cruises

- 2015 Oil and Natural Gas Corporation Limited, “India National Gas Hydrate Program Expedition 02”, as Physical Properties Specialist/Logging Specialist.
 2008 YK08-04 Nankai Trough, Shinkai dives to collect seafloor sediments

Dr. Laura Wallace

Research Scientist
 Univ. of Texas, Institute for Geophysics
 J.J. Pickle Research Campus, Bldg. 196, 10100 Burnet Rd. (R2200)
 Austin, TX 78758-4445
 lwallace@utexas.edu

EDUCATION

<u>College/University</u>	<u>Major</u>	<u>Degree & Year</u>
Univ. of North Carolina-Chapel Hill	Geology	B.S. 1995
University of California –Santa Cruz	Earth Sciences	Ph.D. 2002

WORK EXPERIENCES

- 2012-present: Research Scientist, University of Texas Institute for Geophysics, Austin, TX
 2016-present: Principal Scientist, GNS Science, Lower Hutt, NZ (*joint appointment at UT and GNS*)
 2007-2012: Senior Scientist, GNS Science, Lower Hutt, New Zealand
 2002-2007: Research Scientist, GNS Science, Lower Hutt, New Zealand

Publications Most Closely Related to Proposal (out of 109 total):

- Wallace, L.M.** (2020), Slow Slip Events in New Zealand, Annual Review of Earth and Planetary Sciences (invited review article), doi.org/10.1146/annurev-earth-0717190055104.
- Barnes, P.M., **L.M. Wallace**, D.M. Saffer et al. (2020), Slow slip source characterized by lithological and geometric heterogeneity, *Science Advances*, 6, eaay3314.
- Wallace, L.M.**, M. Ikari, D. Saffer, H. Kitajima (2019), Slow motion earthquakes: Taking the pulse of slow slip events with Scientific Ocean Drilling, *Oceanography*, (invited Review article), 32(1), 106-118.
- Wallace, L.M.**, Saffer, D.M., Barnes, P.M., Pecher, I.A., Petronotis, K.E., LeVay, L.J., and the Expedition 372/375 Scientists, 2019. *Hikurangi Subduction Margin Coring, Logging, and Observatories*. Proceedings of the International Ocean Discovery Program, 372B/375: College Station, TX (International Ocean Discovery Program). <https://doi.org/10.14379/iodp.proc.372B375.2019>
- Warren Smith, E., B. Fry, **L. Wallace**, et al. (2019), Episodic stress and fluid pressure cycling in subducting oceanic crust during slow slip, *Nature Geosci.*, 10.1038/s41561-019-0367-x
- Wallace, L. M.**, Hreinsdóttir, S., Ellis, S., Hamling, I., D'Anastasio, E., & Denys, P. (2018). Triggered slow slip and afterslip on the southern Hikurangi subduction zone following the Kaikōura earthquake. *Geophysical Research Letters*, 45. <https://doi.org/10.1002/2018GL077385>
- Wallace, L.M.**, Y. Kaneko, S. Hreinsdottir, I. Hamling, Z. Peng, N. Bartlow, E. D'Anastasio, and B. Fry, 2017, Large-scale dynamic triggering of shallow slow slip enhanced by overlying sedimentary wedge, *Nature Geoscience*, 10, 765-770 doi: 10.1038/ngeo3021.
- Araki, E., D.M. Saffer, A. Kopf, **L.M. Wallace**, T. Kimura, Y. Machida, S. Ide (2017), Recurring and triggered slow slip events near the trench at the Nankai Trough subduction megathrust, *Science* 356, 1157-1160, doi: 10.1126/science.aan3120

- Wallace, L.M.**, S. C. Webb, Y. Ito, K. Mochizuki, R. Hino, S. Henrys, S. Schwartz, A. Sheehan, (2016), Slow slip near the trench at the Hikurangi subduction zone, *Science*, 352(6286), 701-704, doi: 10.1126/science.aaf2349.
- Wallace, L.M.**, E. Araki, D. Saffer, X. Wang, A. Roesner, A. Kopf, A. Nakanishi, W. Power, R. Kobayashi, C. Kinoshita, S. Toczko, T. Kimura, Y. Machida, and S. Carr (2016), Near-field observations of an offshore Mw 6.0 earthquake from an integrated seafloor and subseafloor monitoring network at the Nankai Trough, southwest Japan, *J. Geophys. Res.*, 121, doi: 10.1002/2016JB013417.
- Saffer, D.M. and **L.M. Wallace**, 2015, The Frictional, Hydrologic, Metamorphic, and Thermal Habitat of Shallow Slow Earthquakes, *Nature Geoscience*, 8, 594-600, doi:10.1038/ngeo2490.
- Mahony, S.H.; **Wallace, L.M.**; Miyoshi, M.; Villamor, P.; Sparks, R.S.J.; Hasenaka, T. 2011. Volcano-tectonic interactions during rapid plate-boundary evolution in the Kyushu region, SW Japan. *Geological Society of America bulletin*, 123(11/12): 2201-2223.
- Wallace, L. M.**, and J. Beavan (2010), Diverse slow slip behavior at the Hikurangi subduction margin, New Zealand, *J. Geophys Res.*, 115(B12402), doi:10.1029/2010JB007717.
- Wallace, L.M.**; Ellis, S.M.; Miyao, K.; Miura, S.; Beavan, R.J.; Goto, J. (2009), Enigmatic, highly active left-lateral shear zone in southwest Japan explained by aseismic ridge collision. *Geology*, 37(2): 143-146; doi: 10.1130/G25221A.1
- Wallace, L.M.**; et al. (2009), Characterizing the seismogenic zone of a major plate boundary subduction thrust : Hikurangi Margin, New Zealand. *Geochemistry geophysics geosystems*, 10(10): Q10006, doi:10.1029/2009GC002610

SYNERGISTIC ACTIVITIES

- 2018-present:** Member of the board of UNAVCO
- 2018:** Co-chief scientist for IODP Expedition 375
- 2014-2016:** Associate Editor for JGR-Solid Earth
- 2013:** Co-convenor and one of the principal organizers of the GeoPRISMS/NSF New Zealand Focus Site Implementation workshop, Wellington, NZ, April 15-17, 2013.
- 2011:** Co-convenor and local host of IODP workshop “Using Ocean Drilling Studies to Unlock the Secrets of Slow Slip Events”, held in Gisborne New Zealand, 1-3 August 2011.

MARINE RESEARCH CRUISE EXPERIENCE:

- 2019:** Voyage leader for an R/V Tangaroa cruise (TAN1907) to recover and redeploy seafloor geodetic instruments offshore the east coast of the North Island, New Zealand.
- 2018:** Co-chief scientist for IODP Expedition 375, on the JOIDES Resolution
- 2017:** Voyage leader for an R/V Tangaroa cruise (TAN1705) to recover and redeploy seafloor geodetic instruments offshore Gisborne and Mahia, and to undertake multicoring along the Hikurangi margin and offshore northeastern South Island to recover turbidite records from the Kaikoura earthquake.
- 2016:** Participated in IODP Expedition 365 aboard the D/V Chikyu
- 2015:** Chief Scientist on the R/V Revelle cruise (RR1509) to recover seafloor geodetic and seismological instruments offshore New Zealand (the HOBITSS project).
- 2014:** Undertook a marine geophysical deployment of seafloor pressure sensors offshore New Zealand, aboard the R/V Tangaroa (TAN1405)

Tianhaozhe Sun

Pacific Geoscience Centre
 Geological Survey of Canada
 9860 West Saanich Road, Sidney, British Columbia, Canada Phone: 1-250-3636699
 Email:tianhaozhe.sun@canada.ca

Education

Ph.D. in Geophysics (2011.09 – 2017.07)	School of Earth and Ocean Sciences, University of Victoria, Canada; GPA: 9.00/9.00 <i>Recipient of Governor General's Gold Medal for outstanding Ph.D. dissertation</i>
B.Sc. in Geophysics (2007.09 – 2011.06)	School of Ocean and Earth Sciences, Tongji University, China; GPA: 4.81/5.00 Rank: 1/19

Work experiences

2019.11-	Research Fellow	Geological Survey of Canada
2017.09-2019.10	Postdoctoral Scholar	Pennsylvania State University
2017.10-11	Visiting Scholar	GNS Science, New Zealand
2012, 2014	Graduate Teaching Assistant	University of Victoria

Professional service

2016-	Reviewer for Earth Planets Space, Earth Planet. Sci. Lett., JGR-Solid Earth, Geophys. Res. Lett., Scientific Drilling, Nonlinear Process. Geophys., Marine Geology, and Science Advances
2019	AGU's Outstanding Reviewer of 2019, JGR: Solid Earth
2020.05	Session convenor of JpGU-AGU joint meeting Session: The Japan Trench: Learning from the 2011 M=9 Tohoku-oki earthquake – a decade later
2019.12	Session convenor of AGU Fall meeting Session T028: Interplay between structure, fluids, and deformation processes at subduction zones
2019.05	Organization Committee member of Subduction Fluid Modeling Workshop, Minnesota
2016-2017	Organizer of weekly Geodynamics group meeting at Pacific Geoscience Centre (PGC), Geological Survey of Canada
2016.08	Primary convener of 13 th AOGS annual meeting (Beijing) Session SE25: Geophysics and Geology of Earthquakes Associated with Subduction Processes

Publications (peer reviewed)

- Sun, T.**, D. Saffer, and S. Ellis (2020), Mechanical and hydrological effects of seamount subduction on megathrust stress and slip, *Nat. Geosci.*, doi:10.1038/s41561-020-0542-0.
- Sun, T.**, S. Ellis, and D. Saffer (2020), Coupled evolution of deformation, pore pressure, and fluid flow in subduction forearcs, *J. Geophys. Res. Solid Earth*. doi:10.1029/2019JB019101.
- Brodsky, E. et al. (including **T. Sun**) (2019), The State of stress on the fault before, during, and after a major earthquake, *Annu. Rev. Earth Planet. Sci.*, Vol. 48.
- Wang, K., L. Brown, Y. Hu, K. Yoshida, J. He, and **T. Sun** (2019), Stable forearc stressed by a weak megathrust: Mechanical and geodynamic implications of stress changes caused by the M=9 Tohoku-oki Earthquake, *J. Geophys. Res. Solid Earth*, 124. Doi:10.1029/2018JB017043.
- Sun, T.**, K. Wang, and J. He (2018), Crustal deformation following great subduction earthquakes controlled by earthquake size and mantle rheology, *J. Geophys. Res. Solid Earth*, 123. Doi:10.1029/2017JB015242.

- Gao, D., K. Wang, T. L. Insua, M. Riedel, M. Sypus, and **T. Sun** (2018), Defining megathrust tsunami sources at Northernmost Cascadia, *Natural Hazards*, doi:10.1007/s11069-018-3397-6.
- Wang, K., **T. Sun**, L. Brown, R. Hino, T. Iinuma, S. Kodaira, and T. Fujiwara, Learning from crustal deformation associated with the M=9 2011 Tohoku-oki earthquake (2018), *Geosphere*, Thematic Issue: Subduction from Top to Bottom II, doi:10.1130/GES01531.1.
- Sun, T.**, E. Davis, K. Wang, and Y. Jiang (2017), Trench-breaching afterslip following deeper coseismic slip of the 2012 M_w 7.6 Costa Rica earthquake constrained by near-trench pressure and land-based geodetic observations, *Earth Planet. Sci. Lett.*, doi:10.1016/j.epsl.2017.09.021.
- Sun, T.**, K. Wang, T. Fujiwara, S. Kodaira, and J. He (2017), Large fault slip peaking at trench in the 2011 Tohoku-oki earthquake, *Nature Communications*, doi:10.1038/ncomms14044.
- Fujiwara, T., C. S. Ferreira, A. K. Bachmann, M. Strasser, G. Wefer, **T. Sun**, T. Kanamatsu, and S. Kodaira (2017), Seafloor displacement after the 2011 Tohoku-oki earthquake in the Northern Japan Trench examined by repeated bathymetric surveys, *Geophys. Res. Lett.*, doi:10.1002/2017GL075839.
- Sun, T.** and K. Wang (2015), Viscoelastic relaxation following subduction earthquakes and its effects on afterslip determination, *J. Geophys. Res. Solid Earth*, doi:10.1002/2014JB011707.
- Brown, L., K. Wang, and **T. Sun** (2015), Static stress drop in the M_w 9 Tohoku-oki earthquake: Heterogeneous distribution and low average value, *Geophys. Res. Lett.*, doi:10.1002/2015GL066361.
- Davis, E. E., H. Villinger, and **T. Sun** (2015), Slow and delayed deformation and uplift of the outermost subduction prism following ETS and seismogenic slip events beneath Nicoya Peninsula, Costa Rica, *Earth Planet. Sci. Lett.*, doi:10.1016/j.epsl.2014.11.015.
- Sun, T.**, K. Wang, T. Iinuma, R. Hino, J. He, H. Fujimoto, M. Kido, Y. Osada, S. Muira, Y. Ohta, and Y. Hu (2014), Prevalence of viscoelastic relaxation after the 2011 Tohoku-oki earthquake, *Nature*, doi:10.1038/nature13778.
- Sun, T.**, M. Xue, K. P. Le, Y. Zhang, and H. Xu (2013), Signatures of ocean storms on seismic records in South China Sea and East China Sea. *Mar. Geophys. Res.*, doi:10.1007/s11001-013-9204-6.
- * Co-authoring on the following publications as a member of “**Expedition 343 Scientists**”.
- Fulton, P. M. et al. (2013), *Science*, doi:10.1126/science.1243641.
- Chester, F. M. et al. (2013), *Science*, doi:10.1126/science.1243719.
- Ujiie, K. et al. (2013), *Science*, doi:10.1126/science.1243485.
- Lin, W. et al. (2013), *Science*, doi:10.1126/science.1229379.
- Rowe, C. D. et al. (2013), *Geology*, doi: 10.1130/G34556.1.
- Yang, T. et al. (2013), *Earth Planet Sci. Lett.*, doi:10.1016/j.epsl.2013.08.045.

ODP/IODP-related Experience

- 2018.03 Science Party member of R/V Kairei Cruise, responsible for downloading CORK pressure data from ODP borehole sites 808 and 1173 with ROV Kaiko
- 2018.01-02 Science Party member of **IODP Exp. 380**: Frontal Thrust Borehole Monitor System
- 2016.07 Science Party member of R/V Sikuliaq Cruise for deploying borehole seismic and geodetic observatories with ROV Jason in ODP borehole 1364A, responsible for retrieving fluid pressure data from previously installed CORK borehole observatory
- 2012.04-05 Science Party member of **IODP Exp. 343**: JFAST, responsible for supervising borehole observatory installation and conducting onboard measurements of physical properties of drill cores

Yusuke Yamashita

Disaster Prevention Research Institute, Kyoto University
Miyazaki Observatory, Research Center for Earthquake Prediction
Assistant Professor
3884 Kaeda, Miyazaki, 889-2161, Japan
+81-985-65-1161
yamac@rcep.dpri.kyoto-u.ac.jp

Education

B.Sc., Faculty of Science, Kagoshima University (04/2004-03/2008)
M.Sc., Graduate school of Science, Kyushu University (04/2008-03/2010)
Ph. D., Graduate school of Science, Kyushu University (04/2010-03/2013)

Work Experience

JSPS Research Fellowship for Young Scientists (DC2), Kyushu University (04/2012 – 03/2013)
JSPS Research Fellowship for Young Scientists (PD), Kyushu University (04/2013 – 03/2014)
Project Researcher, Earthquake Research Institute, The University of Tokyo (04/2014 – 07/2015)
Assistant Professor, Miyazaki Observatory, Disaster Prevention Research Institute, Kyoto University (07/2015 – present)

Publications (Peer-reviewed papers)

1. Iio, Y., S. Matsumoto, Y. Yamashita, et al. (2020), , *Earth Planets Space*, **72**(1), 42
2. Mitsuoka, A., A. Shito, S. Matsumoto, Y. Yamashita, et al. (2020), *J. Geophys. Res.*, **125** (9)
3. Tonegawa, T., Y. Yamashita, et al. (2020), *Geophys. J. Int.*, **222** (3), 1542-1554
4. Yamazaki, K., Y. Yamashita, S. Komatsu (2020), *Earth, Planets and Space*, **72**, 83
5. Nagano, A., Y. Yamashita, et al. (2019), *Marine Geophysical Research*, **40**, 525–539
6. Kano, M., et al. (Yamashita on the 28th.) (2018), *Seismological Res. Lett.*, **89** (4), 1566-1575
7. Matsumoto, S., Y. Yamashita, et al. (2018), *Geophys. Res. Lett.*, **45**, 2, 637-645
8. Katakami, S., Y. Yamashita, et al. (2017), *Geophys. Res. Lett.*, **44**, 19
9. Yakiwara, H., S. Hirano, Y. Yamashita, et al. (2017), *Jour. of Nature. Dis. Sci.*, **38**, 119-131
10. Aizawa K., et al. (Yamashita on the 30th.) (2017), *Earth, Planets and Space*, **69**, 4
11. Yamashita, Y., et al. (2015), *Science*, **348** (6235), 676-679, doi:10.1126/science.aaa4242
12. Matsumoto, S., et al. (Yamashita on the 10th.) (2015), *Earth, Planets and Space*, **67**, 172
13. Miyamachi, H., et al. (Yamashita on the 11th.) (2013), *Bull. Volcanolo. Soc. Japan*, **58**, 227-237
14. Matsumoto, S., et al. (Yamashita on the 5th.) (2013), *Earth, Planets and Space*, **65**, 323-329
15. Yamashita, Y., H. Shimizu, and K. Goto, (2012), *Geophys. Res. Lett.*, **39**, L08304
16. Okada, T., et al. (Yamashita on the 9th.) (2011), *Earth, Planets and Space*, **63**, 749-754
17. Iinuma, T., et al. (Yamashita on the 22nd.) (2009), *Geophys. Res. Lett.*, **36**, L20308

Grants

1. JSPS: KAKENHI (Grant-in-Aid for Young Scientists) (FY20-present: 20K14579), PI
2. Ministry of Education, Culture, Sports, Science and Technology (MEXT) of Japan, under its Earthquake and Volcano Hazards Observation and Research Program, (FY20-present), Co-I
3. JSPS: KAKENHI (Grant-in-Aid for Scientific Research (C)) (FY17-present), PI
4. JSPS: KAKENHI (Grant-in-Aid for Scientific Research on Innovative) (FY16-present), Co-I
5. Ministry of Education, Culture, Sports, Science and Technology (MEXT) of Japan, under its Earthquake and Volcano Hazards Observation and Research Program, (FY15-FY19), Co-I
6. Tokyo Marine Kagami Memorial Foundation (FY15-present), PI
7. JSPS: KAKENHI (Grant-in-Aid for Scientific Research (B)) (FY15-18), Co-I
8. JSPS: KAKENHI (Grant-in-Aid for Young Scientists (B)) (FY15-17), PI
9. JSPS: KAKENHI (Grant-in-Aid for JSPS Fellows) (FY12-13), PI

Cruise Experiment (from 2013)

1. *R/V Kaiyo-maru* No.3, September 2020, Chief Scientist (Hyuga-nada)
2. *T/S Nagasaki-maru*, July 2020 (NS058), Chief Scientist (off Kikai Island, Okinawa Trough)
3. *R/V Kaiyo-maru* No.3, January 2020, Chief Scientist (east of Tanegashima Island)
4. *R/V Tangaroa*, November 2019 (TAN1907) (the northern part of Hikurangi subduction zone) (International joint observation of Japan, New Zealand, and the United States)
5. *R/V Shinsei-maru*, September 2019 (KS-19-18), Co-Chief Scientist (Kumano-nada)
6. *T/S Nagasaki-maru*, August 2019 (NS035), Chief Scientist, (Koshiki Strait, Okinawa Trough)
7. *R/V Kaiyo-maru* No.3, September 2019, Chief Scientist (the Ryukyu Trench)
8. *T/S Nagasaki-maru*, April 2019 (NS025), Chief Scientist (Kikai Island)
9. *R/V Kaiyo-maru* No.2, February 2019, Chief Scientist (Hyuga-nada, Tanegashima island)
10. *R/V Kaiyo-maru* No.2, January 2019, Chief Scientist (Hyuga-nada)
11. *Tug Tsushima*, November 2018 (Aira caldera)
12. *R/V Tangaroa*, October 2018 (TAN1809) (Hikurangi subduction zone; International joint observation of Japan, New Zealand, and the United States)
13. *R/V Kaiyo-maru* No. 1, August 2018 (Hyuga-nada)
14. *T/S Nagasaki-maru*, August 2018 (NS011), Chief Scientist (Tokara Island, East China Sea)
15. *T/S Nagasaki-maru*, April 2018 (NS002), Chief Scientist (Koshiki Strait, East China Sea)
16. *R/V Kaiko-maru* No. 7, March 2018, Chief Scientist (Hyuga-nada)
17. *Tug Meijimaru* No.8, November 2017 (Aira caldera)
18. *R/V Kaiyo-maru* No.3, August 2017, Chief Scientist (Ryukyu Trench)
19. *R/V Yokosuka*, July 2017 (YK17-16C) (Tangegeashima Island)
20. *T/S Nagasaki-maru*, July 2017 (NS463), Co-Chief Scientist (Koshiki Strait, East China Sea)
21. *T/S Nagasaki-maru*, April 2017 (NS456), Co-Chief Scientist (Koshiki Strait, East China Sea)
22. *R/V Kaiyo-maru* No.7, March 2017, Chief Scientist (Hyuga-nada)
23. *R/V Kaiyo-maru* No.1, February 2017, Chief Scientist (Hyuga-nada)
24. *R/V Kaiyo-maru* No.3, September 2016, Chief Scientist (Ryukyu Trench)
25. *R/V Kaiyo-maru* No.3, August 2016, Chief Scientist (Ryukyu Trench)
26. *T/S Nagasaki-maru*, July 2016, Co-Chief Scientist (Tokara Island, East China Sea)
27. *T/S Nagasaki-maru*, April 2016, Co-Chief Scientist (Tokara Island)
28. *R/V Kaiyo-maru* No.3, January 2016, Chief Scientist (Hyuga-nada)
29. *R/V Kaiyo-maru* No.3, August-September 2015, Chief Scientist (Ryukyu Trench)
30. *T/S Nagasaki-maru*, April. 2015, Co-Chief Scientist (Tokara Island, East China Sea)
31. *R/V Kaiyo-maru* No.5, January 2015, Chief Scientist (Hyuga-nada, Ryukyu Trench)
32. *T/S Nagasaki-maru*, July 2014, Co-Chief Scientist, (Tokara Island)
33. *M/V Kaiko-maru* No.7, August 2014 (Japan Sea)
34. *R/V Kaiyo-maru* No.3, September-October 2013 (Sanriku)
35. *T/S Nagasaki-maru*, July 2013, Co-Chief Scientist (Hyuga-nada, East China Sea)
36. *T/S Nagasaki-maru*, April. 2013, Co-Chief Scientist (Hyuga-nada)

Eiichiro Araki

Research and Development Center for Earthquake and Tsunami, Japan Agency for Marine Earth Science and Technology

2-15 Natsushima-cho, Yokosuka, Kanagawa, 237-0061 JAPAN

Tel: +81-46-867-9334

Fax: +81-46-867-9343

E-mail: araki@jamstec.go.jp

Education

PhD in Geophysics, the University of Tokyo, March 2000.

Thesis: Geophysical nature of broadband seismic signals in deep oceans.

Master of Science in Geophysics, the University of Tokyo, March 1997

Thesis: Crustal and upper mantle structure beneath the Solomon oceanic island arc derived from natural earthquake records of ocean bottom seismometer array.

Work Experiences

2019 to date, Research Scientist, Institute for Marine-Geodynamics, JAMSTEC

2009 - 2019, Research Scientist, Research and Development Center for Earthquake and Tsunami, JAMSTEC

2006 – 2009, Researcher, DONET, Marine Technology Center, JAMSTEC

2004 – 2006, Researcher, IFREE, JAMSTEC.

2002-2003 Visiting researcher at Department of Terrestrial Magnetism,

Carnegie Institution of Washington

2001-2004 Researcher, Deep Sea Research Department, in JAMSTEC

2000 Contract Researcher in JAMSTEC

Membership of academic societies

The Seismological Society of Japan

American Geophysical Union

Seismological Society of America

Geophysical Exploration Society of Japan.

Recent publications

H. Matsumoto, T. Kimura, S. Nishida, Y. Machida & E. Araki. Experimental evidence characterizing pressure

- fluctuations at the seafloor-water interface induced by an earthquake. *Scientific Reports*, 2018, 8, doi: 10.1038/s41598-018-34578-2
- Y. Machida, E. Araki, et al. On the Accuracy of Quartz Pressure Sensor in the Seafloor Affected by Transport Condition. *IEEE JOURNAL OF OCEANIC ENGINEERING*, 2018, doi: 10.1109/JOE.2018.2855478
- S. Nishida, Y. Machida, E. Araki, et al. Level Adjustor of Mobile Pressure Calibrator for Ocean Bottom Pressure Gauge. *2018 OCEANS - MTS/IEEE Kobe Techno-Oceans (OTO)*, 2018, p. 1-4
- K. Suzuki, E. Araki, Narumi Takahashi. Detectability of crustal deformation by using ocean bottom pressure gauges deployed to DONET system. *OCEANS'18 MTS/IEEE Kobe / Techno-Ocean 2018*, 2018
- Matsumoto H., Aaraki E., Kawaguchi K. Experimental evaluation of initial characteristics of DONET pressure sensors. *MARINE TECHNOLOGY SOCIETY JOURNAL*, 2018, 52, 3, p. 109-119, doi: 10.4031/MTSJ.52.3.3
- Y. Machida, E. Araki, et al. Installation of a High Sensitivity Ocean Borehole Strainmeter in the Nankai Trough Under Severe Sea Current Conditions. *MAR. TECH. SOCIETY JOUR.*, 2018, 52, 3, p. 128-137
- T. Ohki, et al. (Araki on the 5th.) Probabilistic Cable Damage Risk Assessment Method for Seafloor Cabled 1 Observatory and its Application to Hydrothermal Fields. *MAR. TECH. SOC. JOUR.* 2018, 52, 3, p. 138-149
- Nakano, M., T. Hori, E. Araki, S. Kodaira, S. Ide, Shallow very-low-frequency earthquakes accompany slow slip events in the Nankai subduction zone, *Nature Communications* 9, 984, 2018.
- T. Tonegawa, E. Araki, et al. Sporadic low-velocity volumes spatially correlate with shallow very low frequency earthquake clusters. *Nature Communications*, 2017, 8, doi: 10.1038/s41467-017-02276-8
- Araki, E., et al. Recurring and triggered slow-slip events near the trench at the Nankai Trough subduction megathrust, *Science*, **356**, 1157–1160, 2017.
- Wallace, L. M., Araki, E., et al. Near-field observations of an offshore Mw 6.0 earthquake from an integrated seafloor and subseafloor monitoring network at the Nankai Trough, southwest Japan, *Jour. Geophys. Res.*, **121**, 8338–8351, 2016.
- K. Suzuki, et al. (Araki on the 6th.) Synchronous changes in the seismicity rate and ocean-bottom hydrostatic pressures along the Nankai trough: A possible slow slip event detected by the Dense Oceanfloor Network system for Earthquakes and Tsunamis (DONET). *Tectonophysics*, 2016, 680, p. 90-98
- Kaneda, Y., K. Kawaguchi, E. Araki, et al. Development and application of an advanced ocean floor network system for megathrust earthquakes and tsunamis. in *Seafloor Observatories*, 643–666, Springer, Heidelberg, Germany, 2015.
- Araki, E., and H. Sugioka, Calibration of deep sea differential pressure gauge, *JAMSTEC-R IFREE Special Issue*, November, 141 -148, 2009.
- Araki, E., et al. Aftershock distribution of the 26 December 2004 Sumatra-Andaman earthquake from ocean bottom seismographic observation, *Earth Planets Space*, 58, 113-119, 2006.
- Araki, E., M. Shinohara, S. Sacks, A. Linde, T. Kanazawa, H. Shiobara, H. Mikada, and K. Suyehiro, Improvement of seismic observation in the ocean by use of seafloor boreholes, *Bull. Seism. Soc. Am.*, 94, 678-690, 2004

Jonathan Ajo-Franklin
Rice University
ja62@rice.edu

Ake Fagereng
Cardiff University
fagerenga@cardiff.ac.uk

William Frank
MIT
wfrank@mit.edu

Satoshi Ide
University of Tokyo
ide@eps.s.u-tokyo.ac.jp

Gaku Kimura
Tokyo University of Marine Science and Technology
gakumu-eps.s@g.s.mail.u-tokyo.ac.jp

Greg Moore
University of Hawaii
gmoore@Hawaii.edu

Paola Vannucchi
Università degli Studi di Firenze
paola.vannucchi@unifi.it

Kelin Wang
Geological Survey of Canada
kelin.wang@canada.ca

Geoff Wheat
Moss Landing Marine Laboratories
wheat@mbari.org

Yasuhiro Yamada
JAMSTEC
yyamada@jamstec.go.jp

First Name	Last Name	Affiliation	Country	Role	Expertise
Demian	Saffer	University of Texas at Austin	United States	Other Proponent	Hydrogeology, Geomechanics
Yuzuru	Yamamoto	Kobe University	Japan	Other Proponent	Structural Geology
Yusuke	Yokota	University of Tokyo	Japan	Other Proponent	Geodesy
Takashi	Tonegawa	JAMSTEC	Japan	Other Proponent	Seismology
Mikiya	Yamashita	National Institute of Advanced Industrial Science and Technology, Japan Agency for Marine-Earth Science and Technology	Japan	Other Proponent	Seismic imaging and acquisition

IODP Site Forms

General Site Information

Section A: Proposal Information

Proposal Title:	Drilling and monitoring in Hyuga-Nada: Unveiling effects of ridge subduction on slow earthquakes
Date Form Submitted:	2020-10-09 01:27:08
Site-Specific Objectives with Priority (Must include general objectives in proposal)	Core and log sedimentary section in middle slope of wedge in the leading side of a subducting seamount for lithology and physical properties. Establish a borehole observatory to measure time series of pore fluid pressure, temperature and strain.
List Previous Drilling in Area:	

Section B: General Site Information

Site Name:	SKP-11A		Area or Location:	Western Pacific Ocean Nankai Trough, Hyuganada, Japan
If site is a reoccupation of an old DSDP/ODP Site, Please include former Site#:				Jurisdiction:
Latitude:	31.512		Distance to Land (km):	80
Longitude:	132.2959		Water Depth (m):	1980
Coordinate System:	WGS 84			
Priority of Site:	Primary <input checked="" type="checkbox"/>	Alternate <input type="checkbox"/>		

Section C: Operational Information

Proposed Penetration (m):

Sediments	Basement	Total Sediment Thickness (m)	Total Penetration (m)
700	0	10000	700

General Lithologies:

hemipelagic muds and turbidites: silts, sands, clays, ash layers	
--	--

Coring Plan (Specify or check):

APC to refusal and then XCB to TD; RCB if necessary
APC <input checked="" type="checkbox"/> XCB <input checked="" type="checkbox"/> RCB <input checked="" type="checkbox"/> Re-entry <input checked="" type="checkbox"/> PCS <input type="checkbox"/>

Wireline Logging Plan:

Standard Measurement		Special Tools	
Wireline Logging	<input type="checkbox"/>	Magnetic Susceptibility	<input type="checkbox"/>
Porosity	<input checked="" type="checkbox"/>	Borehole Temperature	<input type="checkbox"/>
Density	<input checked="" type="checkbox"/>	Formation Image (Acoustic)	<input type="checkbox"/>
Gamma Ray	<input checked="" type="checkbox"/>	VSP (walkaway)	<input type="checkbox"/>
Resistivity	<input checked="" type="checkbox"/>	LWD	<input checked="" type="checkbox"/>
Sonic (Δt)	<input checked="" type="checkbox"/>		
Formation Image (Res)	<input checked="" type="checkbox"/>		
VSP (zero offset)	<input type="checkbox"/>		
Formation Temperature & Pressure	<input type="checkbox"/>		
Other Measurements:		Other Tools:	

Estimated Days:

Drilling / Coring	Logging	Total On-Site
		0

Observatory Plan:

Longterm Borehole Observation Plan/Re-entry Plan:
Case and CORK for long-term borehole observatory.

Potential Harzards/Weather:

Shallow Gas	<input checked="" type="checkbox"/>	Complicated Seabed Condition	<input type="checkbox"/>	Hydrothermal Activity	<input type="checkbox"/>	Preferred weather window:						
Hydrocarbon	<input type="checkbox"/>	Soft Seabed	<input type="checkbox"/>	Landslide and Turbidity Current	<input type="checkbox"/>							
Shallow Water Flow	<input type="checkbox"/>	Currents	<input type="checkbox"/>	Gas Hydrate	<input checked="" type="checkbox"/>							
Abnormal Pressure	<input checked="" type="checkbox"/>	Fracture Zone	<input checked="" type="checkbox"/>	Diapir and Mud Volcano	<input type="checkbox"/>							
Man-made Objects (e.g. sea-floor cables, dump sites)	<input type="checkbox"/>	Fault	<input checked="" type="checkbox"/>	High Temperature	<input type="checkbox"/>							
H2S	<input type="checkbox"/>	High Dip Angle	<input type="checkbox"/>	Ice Conditions	<input type="checkbox"/>							
CO2	<input type="checkbox"/>											
Sensitive marine habitat (e.g. reefs, vents)												
Other:												

IODP Site Forms

Site Survey Detail

990-Full for Site SKP-11A Submitted 2020-10-09 01:27:08

Data Type	In SSDB	Details of available data and data that are still to be collected
1a High resolution seismic reflection (primary)	yes	Line: KPr2 Position 8756
1b High resolution seismic reflection (crossing)	yes	Line: HYU1 Position 13642 Data was acquired in 2020 Aug and we upload onboard processing result.
2a Deep penetration seismic reflection (primary)	yes	Line: KPr2 Position 8756
2b Deep penetration seismic reflection (crossing)	yes	Line: HYU1 Position 13642 Data was acquired in 2020 Aug and we upload onboard processing result.
3 Seismic Velocity	yes	Velocity file is only available for the primary line.
4 Seismic Grid		
5a Refraction (surface)		
5b Refraction (bottom)		
6 3.5 kHz		
7 Swath bathymetry		
8a Side looking sonar (surface)		
8b Side looking sonar (bottom)		
9 Photography or video		
10 Heat Flow		
11a Magnetics		
11b Gravity		
12 Sediment cores		
13 Rock sampling		
14a Water current data		
14b Ice Conditions		
15 OBS microseismicity		
16 Navigation		
17 Other		

IODP Site Forms

Environmental Protection

990-Full for Site SKP-11A Submitted 2020-10-09 01:27:08

Pollution & Safety Hazard	Comment
1. Summary of operations at site	LWD first, then APC to refusal and then XCB to TD; RCB if necessary, Case and CORK for long-term borehole observatory as shown on form 1.
2. All hydrocarbon occurrences based on previous DSDP/ODP/IODP drilling	No previous DSPPS/ODP/IODP drilling
3. All commercial drilling in this area that produced or yielded significant hydrocarbon shows	No previous commercial drilling
4. Indications of gas hydrates at this location	No BSR at this site
5. Are there reasons to expect hydrocarbon accumulations at this site?	No hydrocarbon accumulation
6. What "special" precautions will be taken during drilling?	No special precautions
7. What abandonment procedures need to be followed?	A long-term borehole observatory will be installed.
8. Natural or manmade hazards which may affect ship's operations	Cables
9. Summary: What do you consider the major risks in drilling at this site?	Unstable borehole because of deformed strata.

IODP Site Forms

Lithologies

990-Full for Site SKP-11A Submitted 2020-10-09 01:27:08

Subbottom depth (m)	Key reflectors, unconformities faults, etc	Age (My)	Assumed velocity (km/s)	Lithology	Paleo-environment	Avg. accum. rate(m/My)	Comments
0 - 700	Unconformity at 300 mbsf	Not available	2 km/s	hemipelagic muds and turbidites: silts, sands, clays, ash layers	Slope basin or trench fill	Not available	

Site Summary Form 6: Site SKP-11A (Primary) KPr2

Data files in SSDB:

- HYU1: HYU01m_mig.sgy (time, onboard)
- KPr2: KPr2_f mig.sgy (time)
KPr2_depth.sgy (depth)
- Velocity informaiton (KPr2)
- Depth-converted section (KPr2)

Interpretation

Red solid line = Fault (arrow indicate slip direction, normal or reverse)

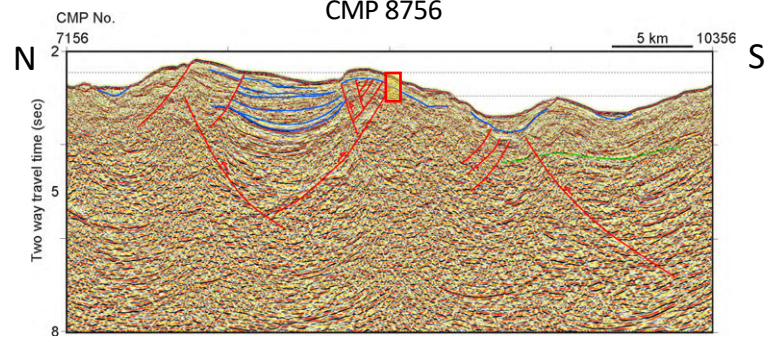
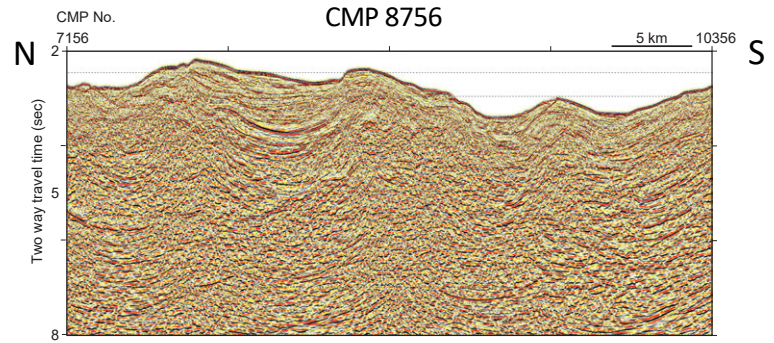
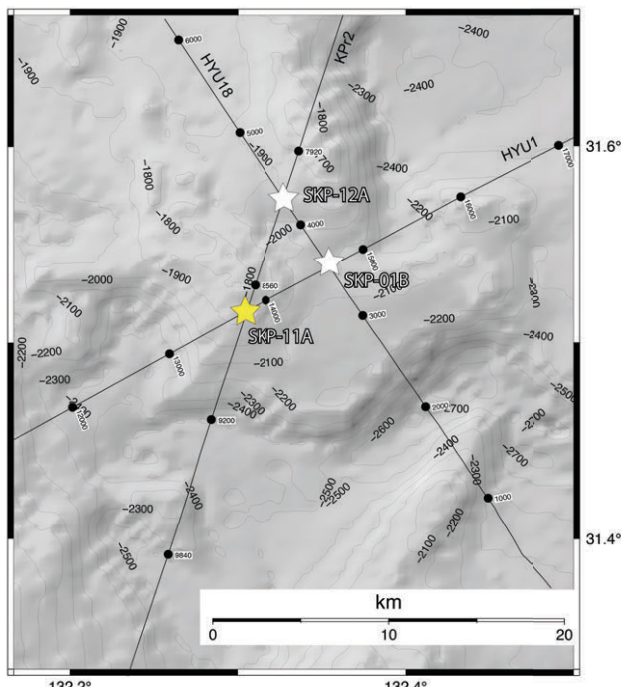
Red dashed line = Detachment

Pink line = Basement/Seamount/plate interface

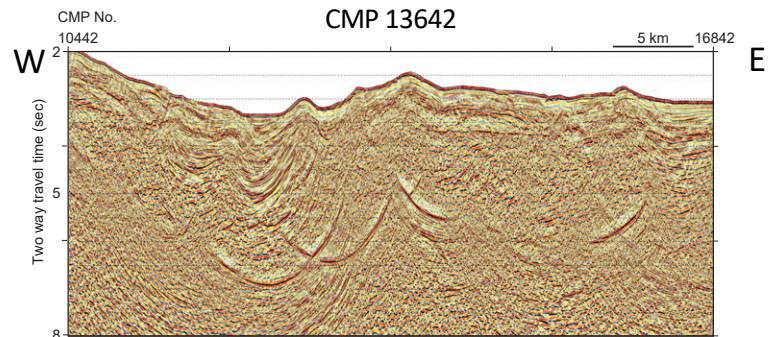
Green dashed line = BSR

Blue solid line = unconformity / lithology or facies boundary / prominent reflector

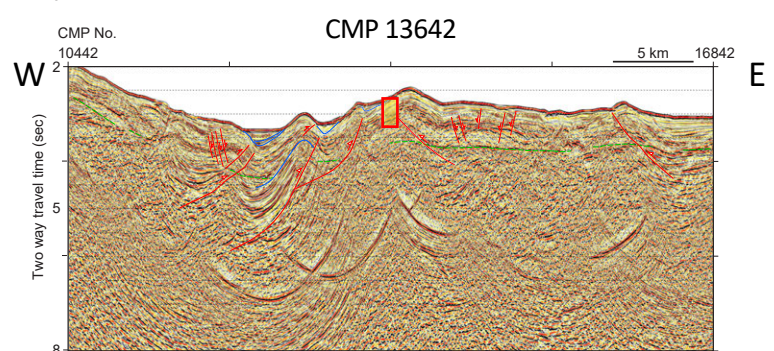
Black solid line = Multiples



HYU1



W



IODP Site Forms

General Site Information

Section A: Proposal Information

Proposal Title:	Drilling and monitoring in Hyuga-Nada: Unveiling effects of ridge subduction on slow earthquakes
Date Form Submitted:	2020-10-09 01:27:08
Site-Specific Objectives with Priority (Must include general objectives in proposal)	Core and log sedimentary section in middle slope of wedge in the leading side of a subducting seamount for lithology and physical properties. Establish a borehole observatory to measure time series of pore fluid pressure, temperature and strain.
List Previous Drilling in Area:	

Section B: General Site Information

Site Name:	SKP-01B		Area or Location:	Western Pacific Ocean Nankai Trough, Hyuganada, Japan
If site is a reoccupation of an old DSDP/ODP Site, Please include former Site#:	SKP-01A		Jurisdiction:	
Latitude:	31.5388		Distance to Land (km):	80
Longitude:	132.3542		Water Depth (m):	2090
Coordinate System:	WGS 84			
Priority of Site:	Primary <input type="checkbox"/>	Alternate <input checked="" type="checkbox"/>		

Section C: Operational Information

Proposed Penetration (m):

Sediments	Basement	Total Sediment Thickness (m)	Total Penetration (m)
700	0	10000	700

General Lithologies:

hemipelagic muds and turbidites: silts, sands, clays, ash layers	
--	--

Coring Plan (Specify or check):

APC to refusal and then XCB to TD; RCB if necessary
APC <input checked="" type="checkbox"/> XCB <input checked="" type="checkbox"/> RCB <input checked="" type="checkbox"/> Re-entry <input checked="" type="checkbox"/> PCS <input type="checkbox"/>

Wireline Logging Plan:

Standard Measurement		Special Tools	
Wireline Logging	<input type="checkbox"/>	Magnetic Susceptibility	<input type="checkbox"/>
Porosity	<input checked="" type="checkbox"/>	Borehole Temperature	<input type="checkbox"/>
Density	<input checked="" type="checkbox"/>	Formation Image (Acoustic)	<input type="checkbox"/>
Gamma Ray	<input checked="" type="checkbox"/>	VSP (walkaway)	<input type="checkbox"/>
Resistivity	<input checked="" type="checkbox"/>	LWD	<input checked="" type="checkbox"/>
Sonic (Δt)	<input checked="" type="checkbox"/>		
Formation Image (Res)	<input checked="" type="checkbox"/>		
VSP (zero offset)	<input type="checkbox"/>		
Formation Temperature & Pressure	<input type="checkbox"/>		
Other Measurements:		Other Tools:	

Estimated Days:

Drilling / Coring	Logging	Total On-Site
		0

Observatory Plan:

Longterm Borehole Observation Plan/Re-entry Plan:
Case and CORK for long-term borehole observatory.

Potential Harzards/Weather:

Shallow Gas	<input checked="" type="checkbox"/>	Complicated Seabed Condition	<input type="checkbox"/>	Hydrothermal Activity	<input type="checkbox"/>	Preferred weather window:						
Hydrocarbon	<input type="checkbox"/>	Soft Seabed	<input type="checkbox"/>	Landslide and Turbidity Current	<input type="checkbox"/>							
Shallow Water Flow	<input type="checkbox"/>	Currents	<input type="checkbox"/>	Gas Hydrate	<input checked="" type="checkbox"/>							
Abnormal Pressure	<input checked="" type="checkbox"/>	Fracture Zone	<input checked="" type="checkbox"/>	Diapir and Mud Volcano	<input type="checkbox"/>							
Man-made Objects (e.g. sea-floor cables, dump sites)	<input type="checkbox"/>	Fault	<input checked="" type="checkbox"/>	High Temperature	<input type="checkbox"/>							
H2S	<input type="checkbox"/>	High Dip Angle	<input type="checkbox"/>	Ice Conditions	<input type="checkbox"/>							
CO2	<input type="checkbox"/>											
Sensitive marine habitat (e.g. reefs, vents)												
Other:												

IODP Site Forms

Site Survey Detail

990-Full for Site SKP-01B Submitted 2020-10-09 01:27:08

Data Type	In SSDB	Details of available data and data that are still to be collected
1a High resolution seismic reflection (primary)	yes	Line: HYU1 Position 14647 Data were acquired in 2020 Aug and we upload onboard processing result.
1b High resolution seismic reflection (crossing)	yes	Line: HYU18 Position 3496 Data were acquired in 2020 Aug and we upload onboard processing result.
2a Deep penetration seismic reflection (primary)	yes	Line: HYU1 Position 14647 Data were acquired in 2020 Aug and we upload onboard processing result.
2b Deep penetration seismic reflection (crossing)	yes	Line: HYU18 Position 3496 Data were acquired in 2020 Aug and we upload onboard processing result.
3 Seismic Velocity	no	
4 Seismic Grid		
5a Refraction (surface)		
5b Refraction (bottom)		
6 3.5 kHz		
7 Swath bathymetry		
8a Side looking sonar (surface)		
8b Side looking sonar (bottom)		
9 Photography or video		
10 Heat Flow		
11a Magnetics		
11b Gravity		
12 Sediment cores		
13 Rock sampling		
14a Water current data		
14b Ice Conditions		
15 OBS microseismicity		
16 Navigation		
17 Other		

IODP Site Forms

Environmental Protection

990-Full for Site SKP-01B Submitted 2020-10-09 01:27:08

Pollution & Safety Hazard	Comment
1. Summary of operations at site	LWD first, then APC to refusal and then XCB to TD; RCB if necessary, Case and CORK for long-term borehole observatory as shown on form 1.
2. All hydrocarbon occurrences based on previous DSDP/ODP/IODP drilling	No previous DSPPS/ODP/IODP drilling
3. All commercial drilling in this area that produced or yielded significant hydrocarbon shows	No previous commercial drilling
4. Indications of gas hydrates at this location	BSR at 900 mbsf
5. Are there reasons to expect hydrocarbon accumulations at this site?	No hydrocarbon accumulation
6. What "special" precautions will be taken during drilling?	No special precautions
7. What abandonment procedures need to be followed?	A long-term borehole observatory will be installed.
8. Natural or manmade hazards which may affect ship's operations	Cables
9. Summary: What do you consider the major risks in drilling at this site?	Unstable borehole because of deformed strata.

IODP Site Forms

Lithologies

990-Full for Site SKP-01B Submitted 2020-10-09 01:27:08

Subbottom depth (m)	Key reflectors, unconformities faults, etc	Age (My)	Assumed velocity (km/s)	Lithology	Paleo-environment	Avg. accum. rate(m/My)	Comments
0 - 700	unconformity at 450 mbsf	Not avairable	2.0 km/s	hemipelagic muds and turbidites: silts, sands, clays, ash layers	slope basin or trench fill	Not avairable	

Site Summary Form 6: Site SKP-01B

Data files in SSDB:

- HYU1: HYU01m_mig.sgy (time, onboard)
- HYU18: HYU18_mig.sgy (time, onboard)

Interpretation

Red solid line = Fault (arrow indicate slip direction, normal or reverse)

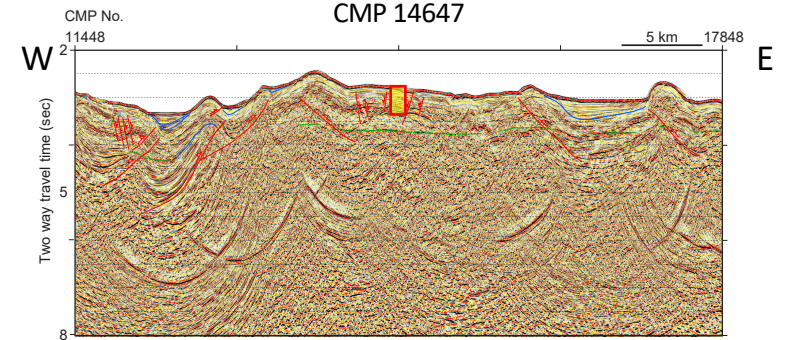
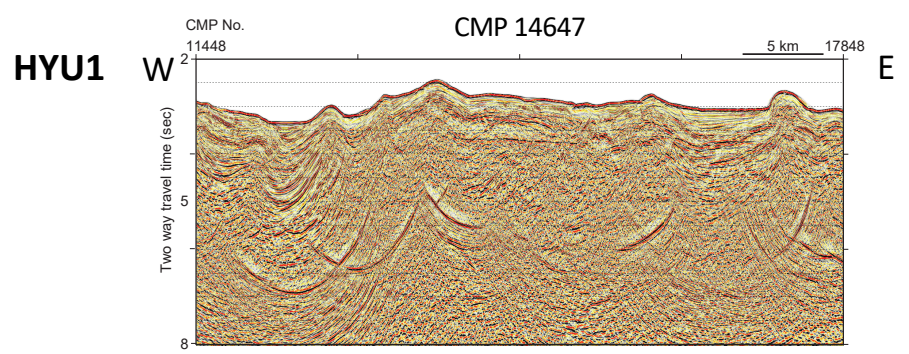
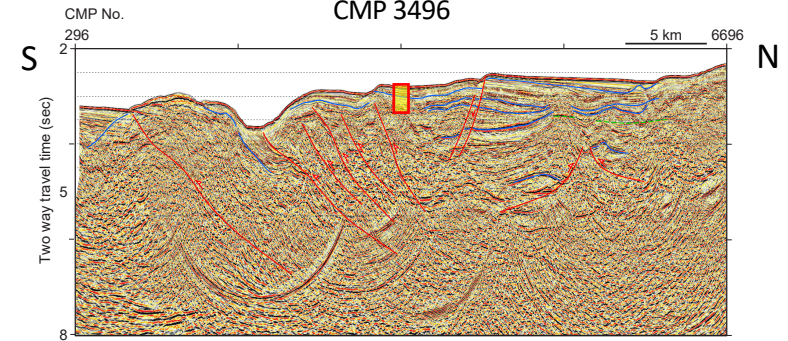
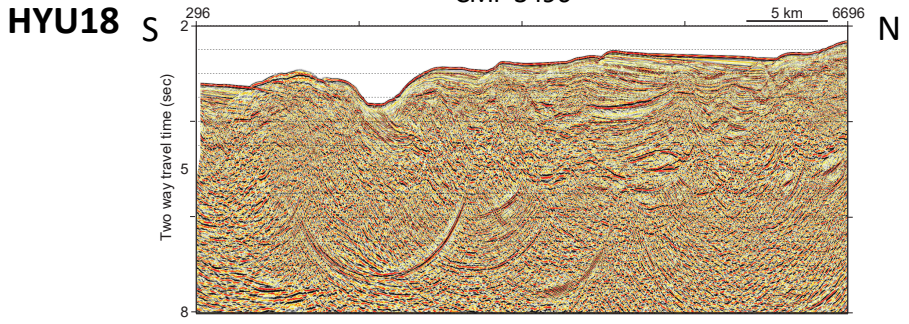
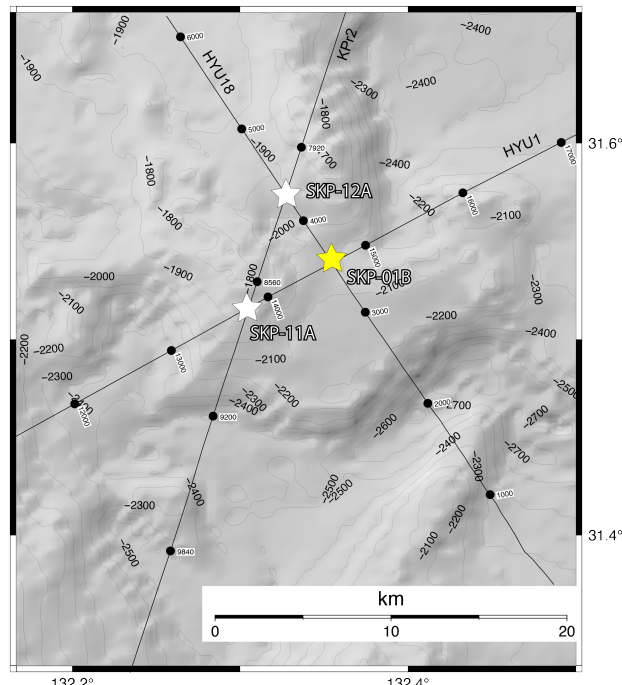
Red dashed line = Detachment

Pink line = Basement/Seamount/plate interface

Green dashed line = BSR

Blue solid line = unconformity / lithology or facies boundary / prominent reflector

Black solid line = Multiples



IODP Site Forms

General Site Information

Section A: Proposal Information

Proposal Title:	Drilling and monitoring in Hyuga-Nada: Unveiling effects of ridge subduction on slow earthquakes
Date Form Submitted:	2020-10-09 01:27:08
Site-Specific Objectives with Priority (Must include general objectives in proposal)	Core and log sedimentary section in middle slope of wedge in the leading side of a subducting seamount for lithology and physical properties. Establish a borehole observatory to measure time series of pore fluid pressure, temperature and strain.
List Previous Drilling in Area:	

Section B: General Site Information

Site Name:	SKP-12A		Area or Location:	Western Pacific Ocean Nankai Trough, Hyuganada, Japan
If site is a reoccupation of an old DSDP/ODP Site, Please include former Site#:				Jurisdiction:
Latitude:	31.5797		Distance to Land (km):	80
Longitude:	132.322		Water Depth (m):	2000
Coordinate System:	WGS 84			
Priority of Site:	Primary <input type="checkbox"/>	Alternate <input checked="" type="checkbox"/>		

Section C: Operational Information

Proposed Penetration (m):

Sediments	Basement	Total Sediment Thickness (m)	Total Penetration (m)
700	0	10000	700

General Lithologies:

hemipelagic muds and turbidites: silts, sands, clays, ash layers	
--	--

Coring Plan (Specify or check):

APC to refusal and then XCB to TD; RCB if necessary
APC <input checked="" type="checkbox"/> XCB <input checked="" type="checkbox"/> RCB <input checked="" type="checkbox"/> Re-entry <input checked="" type="checkbox"/> PCS <input type="checkbox"/>

Wireline Logging Plan:

Standard Measurement		Special Tools	
Wireline Logging	<input type="checkbox"/>	Magnetic Susceptibility	<input type="checkbox"/>
Porosity	<input checked="" type="checkbox"/>	Borehole Temperature	<input type="checkbox"/>
Density	<input checked="" type="checkbox"/>	Formation Image (Acoustic)	<input type="checkbox"/>
Gamma Ray	<input checked="" type="checkbox"/>	VSP (walkaway)	<input type="checkbox"/>
Resistivity	<input checked="" type="checkbox"/>	LWD	<input checked="" type="checkbox"/>
Sonic (Δt)	<input checked="" type="checkbox"/>		
Formation Image (Res)	<input checked="" type="checkbox"/>		
VSP (zero offset)	<input type="checkbox"/>		
Formation Temperature & Pressure	<input type="checkbox"/>		
Other Measurements:		Other Tools:	

Estimated Days:

Drilling / Coring	Logging	Total On-Site
		0

Observatory Plan:

Longterm Borehole Observation Plan/Re-entry Plan:
Case and CORK for long-term borehole observatory.

Potential Harzards/Weather:

Shallow Gas	<input checked="" type="checkbox"/>	Complicated Seabed Condition	<input type="checkbox"/>	Hydrothermal Activity	<input type="checkbox"/>	Preferred weather window:						
Hydrocarbon	<input type="checkbox"/>	Soft Seabed	<input type="checkbox"/>	Landslide and Turbidity Current	<input type="checkbox"/>							
Shallow Water Flow	<input type="checkbox"/>	Currents	<input type="checkbox"/>	Gas Hydrate	<input checked="" type="checkbox"/>							
Abnormal Pressure	<input checked="" type="checkbox"/>	Fracture Zone	<input checked="" type="checkbox"/>	Diapir and Mud Volcano	<input type="checkbox"/>							
Man-made Objects (e.g. sea-floor cables, dump sites)	<input type="checkbox"/>	Fault	<input checked="" type="checkbox"/>	High Temperature	<input type="checkbox"/>							
H2S	<input type="checkbox"/>	High Dip Angle	<input type="checkbox"/>	Ice Conditions	<input type="checkbox"/>							
CO2	<input type="checkbox"/>											
Sensitive marine habitat (e.g. reefs, vents)												
Other:												

IODP Site Forms

Site Survey Detail

990-Full for Site SKP-12A Submitted 2020-10-09 01:27:08

Data Type	In SSDB	Details of available data and data that are still to be collected
1a High resolution seismic reflection (primary)	no	
1b High resolution seismic reflection (crossing)	yes	Line: HYU18 Position 4372
2a Deep penetration seismic reflection (primary)	yes	Line: KPr2 Position 8124
2b Deep penetration seismic reflection (crossing)	yes	Line: HYU18 Position 4372
3 Seismic Velocity	yes	Velocity file is only available for the primary line.
4 Seismic Grid		
5a Refraction (surface)		
5b Refraction (bottom)		
6 3.5 kHz		
7 Swath bathymetry		
8a Side looking sonar (surface)		
8b Side looking sonar (bottom)		
9 Photography or video		
10 Heat Flow		
11a Magnetics		
11b Gravity		
12 Sediment cores		
13 Rock sampling		
14a Water current data		
14b Ice Conditions		
15 OBS microseismicity		
16 Navigation		
17 Other		

IODP Site Forms

Environmental Protection

990-Full for Site SKP-12A Submitted 2020-10-09 01:27:08

Pollution & Safety Hazard	Comment
1. Summary of operations at site	LWD first, then APC to refusal and then XCB to TD; RCB if necessary, Case and CORK for long-term borehole observatory as shown on form 1.
2. All hydrocarbon occurrences based on previous DSDP/ODP/IODP drilling	No previous DSPPS/ODP/IODP drilling
3. All commercial drilling in this area that produced or yielded significant hydrocarbon shows	No previous commercial drilling
4. Indications of gas hydrates at this location	No BSR at this site
5. Are there reasons to expect hydrocarbon accumulations at this site?	No hydrocarbon accumulation
6. What "special" precautions will be taken during drilling?	No special precautions
7. What abandonment procedures need to be followed?	A long-term borehole observatory will be installed.
8. Natural or manmade hazards which may affect ship's operations	Cables
9. Summary: What do you consider the major risks in drilling at this site?	Unstable borehole because of deformed strata.

IODP Site Forms

Lithologies

990-Full for Site SKP-12A Submitted 2020-10-09 01:27:08

Subbottom depth (m)	Key reflectors, unconformities faults, etc	Age (My)	Assumed velocity (km/s)	Lithology	Paleo-environment	Avg. accum. rate(m/My)	Comments
0 - 700	No event	Not available	2 km/s	hemipelagic muds and turbidites: silts, sands, clays, ash layers	slope basin or trench fill	Not available	

Site Summary Form 6: Site SKP-12A

KPr2

Data files in SSDB:

- HYU18: HYU18_mig.sgy (time, onboard)
- KPr2: KPr2_f mig.sgy (time)
KPr2_depth.sgy (depth)
- Velocity informaiton (KPr2)

Interpretation

Red solid line = Fault (arrow indicate slip direction, normal or reverse)

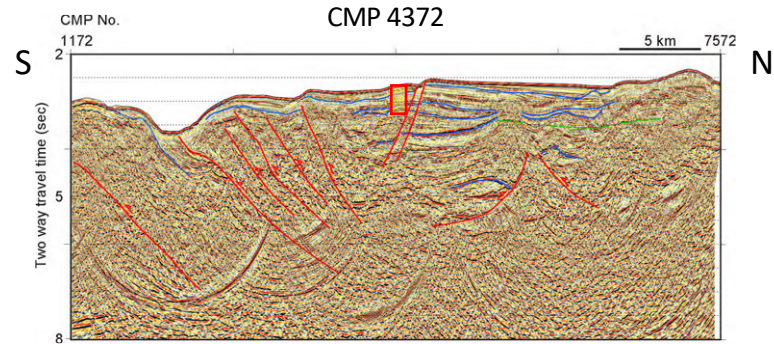
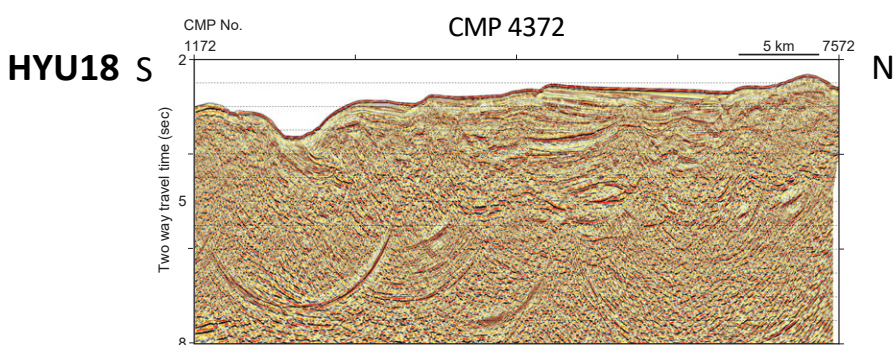
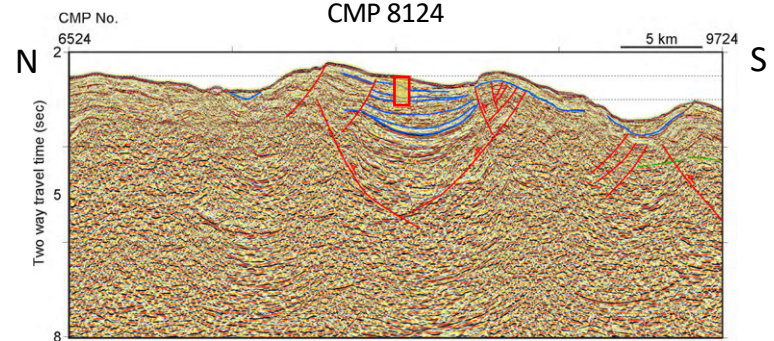
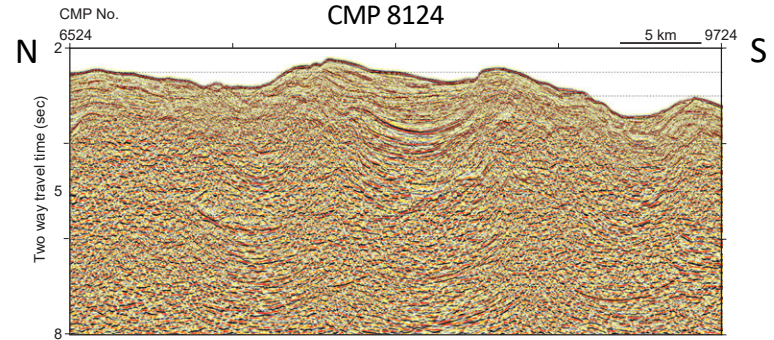
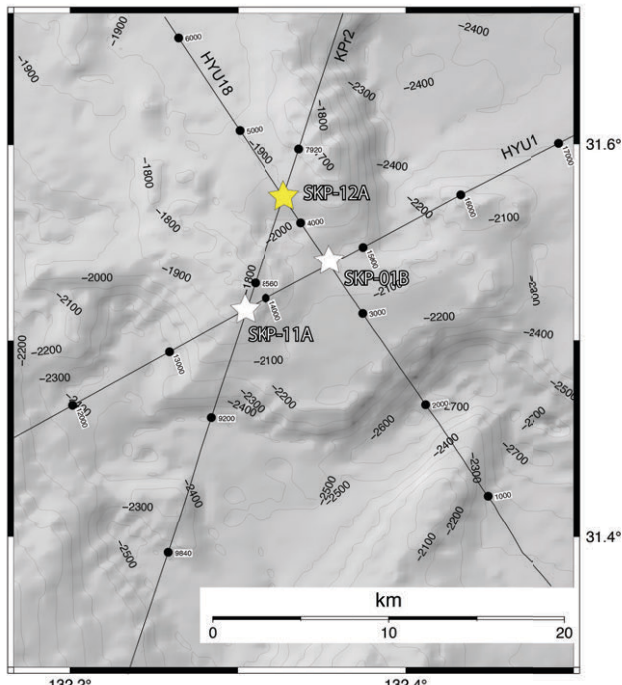
Red dashed line = Detachment

Pink line = Basement/Seamount/plate interface

Green dashed line = BSR

Blue solid line = unconformity / lithology or facies boundary / prominent reflector

Black solid line = Multiples



IODP Site Forms

General Site Information

Section A: Proposal Information

Proposal Title:	Drilling and monitoring in Hyuga-Nada: Unveiling effects of ridge subduction on slow earthquakes
Date Form Submitted:	2020-10-09 01:27:08
Site-Specific Objectives with Priority (Must include general objectives in proposal)	Core and log sedimentary section in middle slope of wedge in the western side of a subducting seamount for lithology and physical properties. Establish a borehole observatory to measure time series of pore fluid pressure, temperature and strain.
List Previous Drilling in Area:	

Section B: General Site Information

Site Name:	SKP-13A		Area or Location:	Western Pacific Ocean Nankai Trough, Hyuganada, Japan
If site is a reoccupation of an old DSDP/ODP Site, Please include former Site#:				
Latitude:	30.9057		Jurisdiction:	
Longitude:	132.2435		Distance to Land (km):	100
Coordinate System:	WGS 84		Water Depth (m):	2690
Priority of Site:	Primary <input checked="" type="checkbox"/>	Alternate <input type="checkbox"/>		

Section C: Operational Information

Proposed Penetration (m):

Sediments	Basement	Total Sediment Thickness (m)	Total Penetration (m)
800	0	4000	800

General Lithologies:

hemipelagic muds and turbidites: silts, sands, clays, ash layers	
--	--

Coring Plan (Specify or check):

APC <input checked="" type="checkbox"/>	XCB <input checked="" type="checkbox"/>	RCB <input checked="" type="checkbox"/>	Re-entry <input checked="" type="checkbox"/>	PCS <input type="checkbox"/>
---	---	---	--	------------------------------

Wireline Logging Plan:

Standard Measurement		Special Tools	
Wireline Logging	<input type="checkbox"/>	Magnetic Susceptibility	<input type="checkbox"/>
Porosity	<input checked="" type="checkbox"/>	Borehole Temperature	<input type="checkbox"/>
Density	<input checked="" type="checkbox"/>	Formation Image (Acoustic)	<input type="checkbox"/>
Gamma Ray	<input checked="" type="checkbox"/>	VSP (walkaway)	<input type="checkbox"/>
Resistivity	<input checked="" type="checkbox"/>	LWD	<input checked="" type="checkbox"/>
Sonic (Δt)	<input checked="" type="checkbox"/>		
Formation Image (Res)	<input checked="" type="checkbox"/>		
VSP (zero offset)	<input type="checkbox"/>		
Formation Temperature & Pressure	<input type="checkbox"/>		
Other Measurements:	Other Tools:		

Estimated Days:

Drilling / Coring	Logging	Total On-Site
		0

Observatory Plan:

Longterm Borehole Observation Plan/Re-entry Plan:
Case and CORK for long-term borehole observatory.

Potential Harzards/Weather:

Shallow Gas	<input checked="" type="checkbox"/>	Complicated Seabed Condition	<input type="checkbox"/>	Hydrothermal Activity	<input type="checkbox"/>	Preferred weather window:						
Hydrocarbon	<input type="checkbox"/>	Soft Seabed	<input type="checkbox"/>	Landslide and Turbidity Current	<input type="checkbox"/>							
Shallow Water Flow	<input type="checkbox"/>	Currents	<input type="checkbox"/>	Gas Hydrate	<input checked="" type="checkbox"/>							
Abnormal Pressure	<input checked="" type="checkbox"/>	Fracture Zone	<input checked="" type="checkbox"/>	Diapir and Mud Volcano	<input type="checkbox"/>							
Man-made Objects (e.g. sea-floor cables, dump sites)	<input type="checkbox"/>	Fault	<input checked="" type="checkbox"/>	High Temperature	<input type="checkbox"/>							
H2S	<input type="checkbox"/>	High Dip Angle	<input type="checkbox"/>	Ice Conditions	<input type="checkbox"/>							
CO2	<input type="checkbox"/>											
Sensitive marine habitat (e.g. reefs, vents)												
Other:												

IODP Site Forms

Site Survey Detail

990-Full for Site SKP-13A Submitted 2020-10-09 01:27:08

Data Type	In SSDB	Details of available data and data that are still to be collected
1a High resolution seismic reflection (primary)	yes	Line: KR0114-8 Position 6906
1b High resolution seismic reflection (crossing)	no	Line: KPr1 Position 4379
2a Deep penetration seismic reflection (primary)	yes	Line: KR0114-8 Position 6906
2b Deep penetration seismic reflection (crossing)	no	Line: KPr1 Position 4379
3 Seismic Velocity	yes	
4 Seismic Grid		
5a Refraction (surface)		
5b Refraction (bottom)		
6 3.5 kHz		
7 Swath bathymetry		
8a Side looking sonar (surface)		
8b Side looking sonar (bottom)		
9 Photography or video		
10 Heat Flow		
11a Magnetics		
11b Gravity		
12 Sediment cores		
13 Rock sampling		
14a Water current data		
14b Ice Conditions		
15 OBS microseismicity		
16 Navigation		
17 Other		

IODP Site Forms

Environmental Protection

990-Full for Site SKP-13A Submitted 2020-10-09 01:27:08

Pollution & Safety Hazard	Comment
1. Summary of operations at site	LWD first, then APC to refusal and then XCB to TD; RCB if necessary, Case and CORK for long-term borehole observatory as shown on form 1.
2. All hydrocarbon occurrences based on previous DSDP/ODP/IODP drilling	No previous DSPPS/ODP/IODP drilling
3. All commercial drilling in this area that produced or yielded significant hydrocarbon shows	No previous commercial drilling
4. Indications of gas hydrates at this location	BSR at 750 mbsf
5. Are there reasons to expect hydrocarbon accumulations at this site?	No hydrocarbon accumulation
6. What "special" precautions will be taken during drilling?	No special precautions
7. What abandonment procedures need to be followed?	A long-term borehole observatory will be installed.
8. Natural or manmade hazards which may affect ship's operations	No other hazards
9. Summary: What do you consider the major risks in drilling at this site?	Unstable borehole because of deformed strata.

IODP Site Forms

Lithologies

990-Full for Site SKP-13A Submitted 2020-10-09 01:27:08

Subbottom depth (m)	Key reflectors, unconformities faults, etc	Age (My)	Assumed velocity (km/s)	Lithology	Paleo-environment	Avg. accum. rate(m/My)	Comments
0 - 800	unconformity at 600 mbsf	Not available	2 km/s	hemipelagic muds and turbidites: silts, sands, clays, ash layers	slope basin or trench fill	Not available	

Site Summary Form 6: Site SKP-13A (Primary) KPr1

Data files in SSDB:

- KPr1:KPr1_fmig.sgy (time)
KPr1_depth.sgy (depth)
- KR0114-8: kr01-14-8_mig_f.sgy (time)
kr01-14-8_200_podm_fin.sgy (depth)
- Velocity information

Interpretation

Red solid line = Fault (arrow indicate slip direction, normal or reverse)

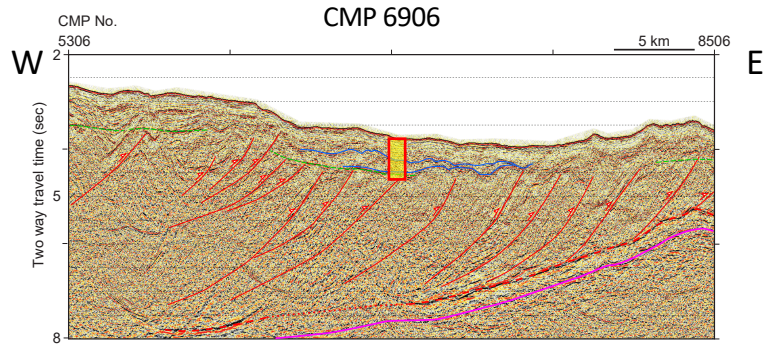
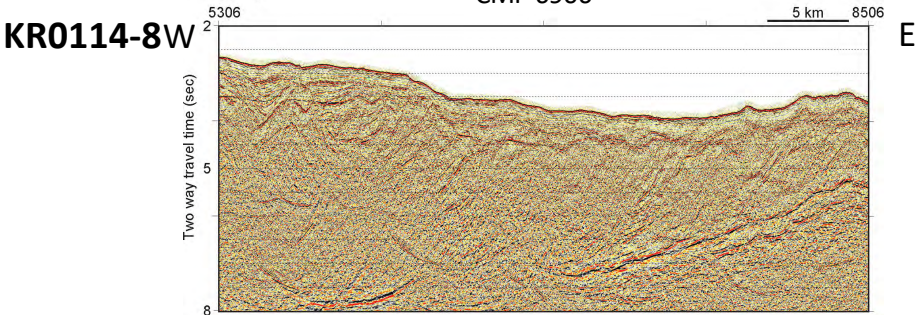
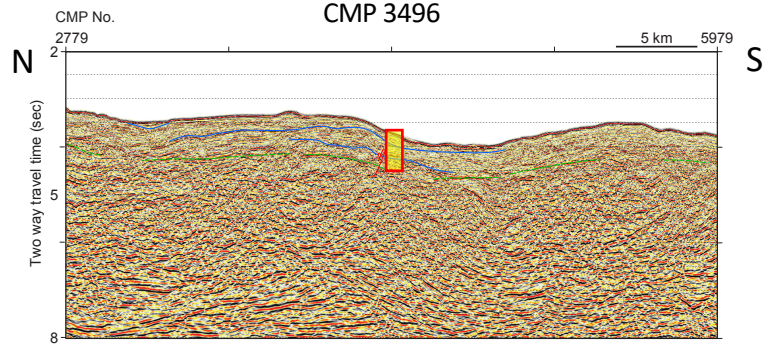
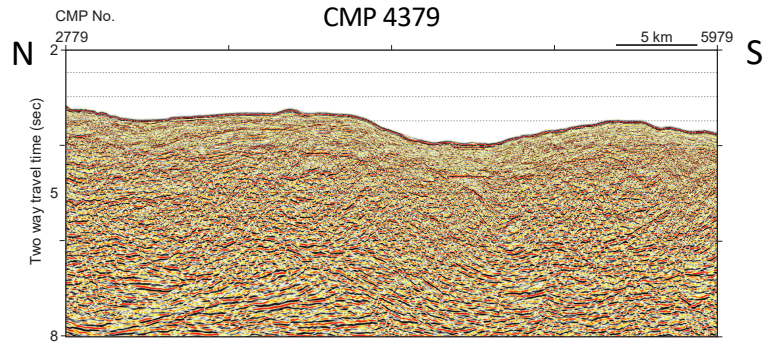
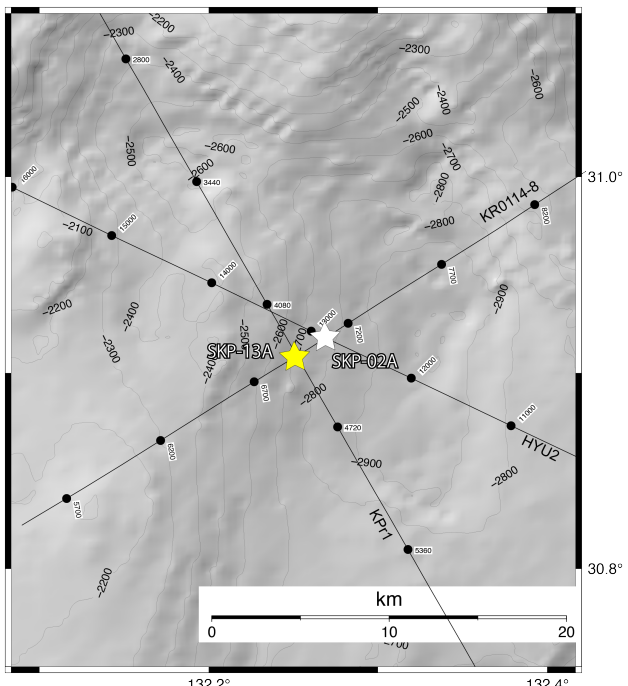
Red dashed line = Detachment

Pink line = Basement/Seamount/plate interface

Green dashed line = BSR

Blue solid line = unconformity / lithology or facies boundary / prominent reflector

Black solid line = Multiples



IODP Site Forms

General Site Information

Section A: Proposal Information

Proposal Title:	Drilling and monitoring in Hyuga-Nada: Unveiling effects of ridge subduction on slow earthquakes
Date Form Submitted:	2020-10-09 01:27:08
Site-Specific Objectives with Priority (Must include general objectives in proposal)	Core and log sedimentary section in middle slope of wedge in the western side of a subducting seamount for lithology and physical properties. Establish a borehole observatory to measure time series of pore fluid pressure, temperature and strain.
List Previous Drilling in Area:	

Section B: General Site Information

Site Name:	SKP-02A		Area or Location:	Western Pacific Ocean, Nankai Trough, Hyuga-Nada, Japan
If site is a reoccupation of an old DSDP/ODP Site, Please include former Site#:				
Latitude:	30.9152		Jurisdiction:	
Longitude:	132.2612		Distance to Land (km):	80
Coordinate System:	WGS 84		Water Depth (m):	2815
Priority of Site:	Primary <input type="checkbox"/>	Alternate <input checked="" type="checkbox"/>		

Section C: Operational Information

Proposed Penetration (m):

Sediments	Basement	Total Sediment Thickness (m)	Total Penetration (m)
800	0	3700	800

General Lithologies:

hemipelagic muds and turbidites: silts, sands, clays, ash layers	N/A
--	-----

Coring Plan (Specify or check):

APC to refusal and then XCB to TD; RCB if necessary
APC <input checked="" type="checkbox"/> XCB <input checked="" type="checkbox"/> RCB <input checked="" type="checkbox"/> Re-entry <input checked="" type="checkbox"/> PCS <input type="checkbox"/>

Wireline Logging Plan:

Standard Measurement		Special Tools	
Wireline Logging	<input type="checkbox"/>	Magnetic Susceptibility	<input type="checkbox"/>
Porosity	<input checked="" type="checkbox"/>	Borehole Temperature	<input type="checkbox"/>
Density	<input checked="" type="checkbox"/>	Formation Image (Acoustic)	<input type="checkbox"/>
Gamma Ray	<input checked="" type="checkbox"/>	VSP (walkaway)	<input type="checkbox"/>
Resistivity	<input checked="" type="checkbox"/>	LWD	<input checked="" type="checkbox"/>
Sonic (Δt)	<input checked="" type="checkbox"/>		
Formation Image (Res)	<input checked="" type="checkbox"/>		
VSP (zero offset)	<input type="checkbox"/>		
Formation Temperature & Pressure	<input type="checkbox"/>		
Other Measurements:		Other Tools:	

Estimated Days:

Drilling / Coring	Logging	Total On-Site
		0

Observatory Plan:

Longterm Borehole Observation Plan/Re-entry Plan:
Case and CORK for long-term borehole observatory.

Potential Harzards/Weather:

Shallow Gas	<input checked="" type="checkbox"/>	Complicated Seabed Condition	<input type="checkbox"/>	Hydrothermal Activity	<input type="checkbox"/>	Preferred weather window:						
Hydrocarbon	<input type="checkbox"/>	Soft Seabed	<input type="checkbox"/>	Landslide and Turbidity Current	<input type="checkbox"/>							
Shallow Water Flow	<input type="checkbox"/>	Currents	<input type="checkbox"/>	Gas Hydrate	<input checked="" type="checkbox"/>							
Abnormal Pressure	<input checked="" type="checkbox"/>	Fracture Zone	<input checked="" type="checkbox"/>	Diapir and Mud Volcano	<input type="checkbox"/>							
Man-made Objects (e.g. sea-floor cables, dump sites)	<input type="checkbox"/>	Fault	<input checked="" type="checkbox"/>	High Temperature	<input type="checkbox"/>							
H2S	<input type="checkbox"/>	High Dip Angle	<input type="checkbox"/>	Ice Conditions	<input type="checkbox"/>							
CO2	<input type="checkbox"/>											
Sensitive marine habitat (e.g. reefs, vents)												
Other:												

IODP Site Forms

Site Survey Detail

990-Full for Site SKP-02A Submitted 2020-10-09 01:27:08

Data Type	In SSDB	Details of available data and data that are still to be collected
1a High resolution seismic reflection (primary)	no	Line: KR0114-8 Position 7120
1b High resolution seismic reflection (crossing)	yes	Line: HYU2 Position 12885 Data were acquired in 2020 Aug and we upload onboard processing result.
2a Deep penetration seismic reflection (primary)	yes	Line: KR0114-8 Position 7120
2b Deep penetration seismic reflection (crossing)	yes	Line: HYU2 Position 12885 Data were acquired in 2020 Aug and we upload onboard processing result.
3 Seismic Velocity	yes	Velocity file is only available for the primary line.
4 Seismic Grid		
5a Refraction (surface)		
5b Refraction (bottom)		
6 3.5 kHz		
7 Swath bathymetry		
8a Side looking sonar (surface)		
8b Side looking sonar (bottom)		
9 Photography or video		
10 Heat Flow		
11a Magnetics		
11b Gravity		
12 Sediment cores		
13 Rock sampling		
14a Water current data		
14b Ice Conditions		
15 OBS microseismicity		
16 Navigation		
17 Other		

IODP Site Forms

Environmental Protection

990-Full for Site SKP-02A Submitted 2020-10-09 01:27:08

Pollution & Safety Hazard	Comment
1. Summary of operations at site	LWD first, then APC to refusal and then XCB to TD; RCB if necessary, Case and CORK for long-term borehole observatory as shown on form 1.
2. All hydrocarbon occurrences based on previous DSDP/ODP/IODP drilling	No previous DSPPS/ODP/IODP drilling
3. All commercial drilling in this area that produced or yielded significant hydrocarbon shows	No previous commercial drilling
4. Indications of gas hydrates at this location	No BSR at this site
5. Are there reasons to expect hydrocarbon accumulations at this site?	No hydrocarbon accumulation
6. What "special" precautions will be taken during drilling?	No special precautions
7. What abandonment procedures need to be followed?	A long-term borehole observatory will be installed.
8. Natural or manmade hazards which may affect ship's operations	No other hazards
9. Summary: What do you consider the major risks in drilling at this site?	Unstable borehole because of deformed strata.

IODP Site Forms

Lithologies

990-Full for Site SKP-02A Submitted 2020-10-09 01:27:08

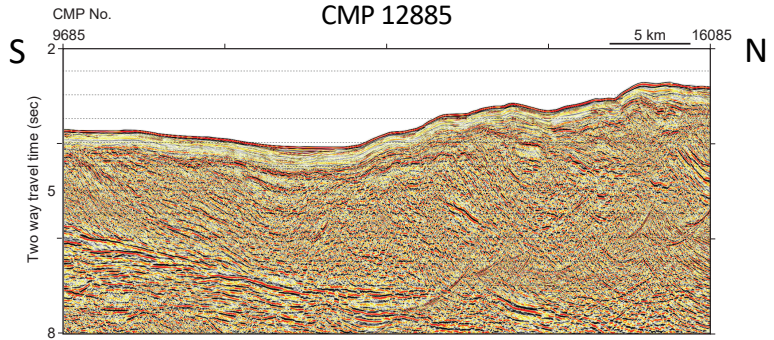
Subbottom depth (m)	Key reflectors, unconformities faults, etc	Age (My)	Assumed velocity (km/s)	Lithology	Paleo-environment	Avg. accum. rate(m/My)	Comments
0 - 800	Unconformity at 400 mbsf	Not available	2 km/s	hemipelagic muds and turbidites: silts, sands, clays, ash layers	Slope basin or trench fill	Not available	

Site Summary Form 6: Site SKP-02A

Data files in SSDB:

- HYU2: HYU02m_mig.sgy (time, onboard)
- KR0114-8: kr01-14-8_mig_f.sgy (time)
kr01-14-8_200_podm_fin.sgy (depth)
- Velocity informaiton (KR0114-8)

HYU2



Interpretation

Red solid line = Fault (arrow indicate slip direction, normal or reverse)

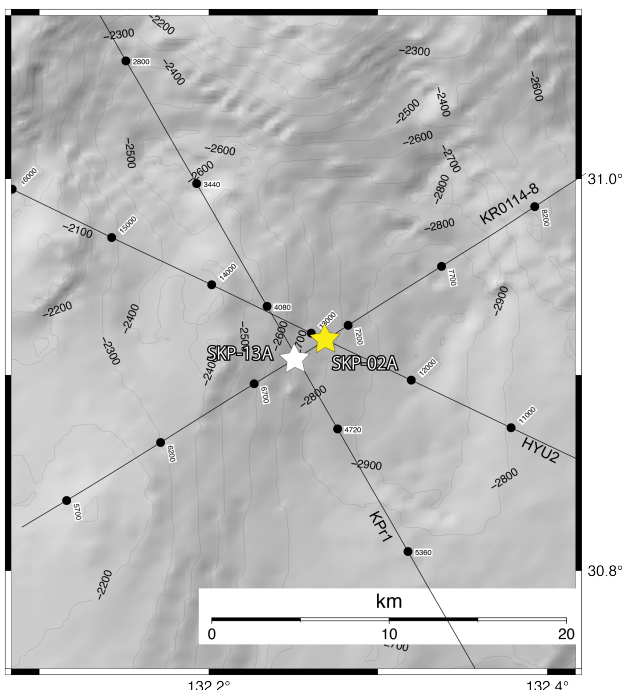
Red dashed line = Detachment

Pink line = Basement/Seamount/plate interface

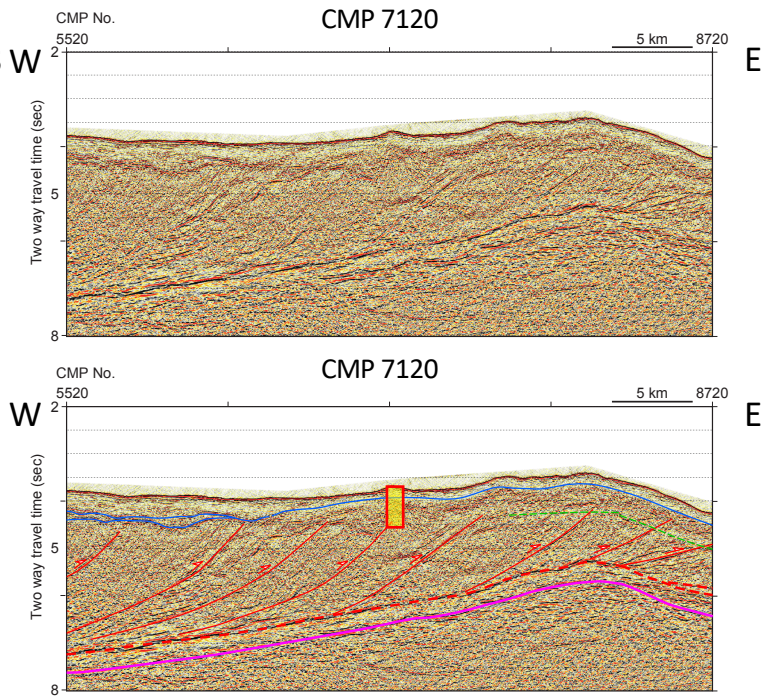
Green dashed line = BSR

Blue solid line = unconformity / lithology or facies boundary / prominent reflector

Black solid line = Multiples



KR0114-8 W



IODP Site Forms

General Site Information

Section A: Proposal Information

Proposal Title:	Drilling and monitoring in Hyuga-Nada: Unveiling effects of ridge subduction on slow earthquakes
Date Form Submitted:	2020-10-09 01:27:08
Site-Specific Objectives with Priority (Must include general objectives in proposal)	Core and log sedimentary section in a middle slope of wedge at the top of a subducting seamount for lithology and physical properties.
List Previous Drilling in Area:	

Section B: General Site Information

Site Name:	SKP-14A		Area or Location:	Western Pacific Ocean Nankai Trough, Hyuganada, Japan
If site is a reoccupation of an old DSDP/ODP Site, Please include former Site#:				Jurisdiction:
Latitude:	31.0144		Distance to Land (km):	111
Longitude:	132.4401		Water Depth (m):	2940
Coordinate System:	WGS 84			
Priority of Site:	Primary <input checked="" type="checkbox"/>	Alternate <input type="checkbox"/>		

Section C: Operational Information

Proposed Penetration (m):

Sediments	Basement	Total Sediment Thickness (m)	Total Penetration (m)
900	0	1900	900

General Lithologies:

hemipelagic muds and turbidites: silts, sands, clays, ash layers	
--	--

Coring Plan (Specify or check):

APC to refusal and then XCB to TD; RCB if necessary
APC <input checked="" type="checkbox"/> XCB <input checked="" type="checkbox"/> RCB <input checked="" type="checkbox"/> Re-entry <input type="checkbox"/> PCS <input type="checkbox"/>

Wireline Logging Plan:

Standard Measurement		Special Tools	
Wireline Logging	<input type="checkbox"/>	Magnetic Susceptibility	<input type="checkbox"/>
Porosity	<input checked="" type="checkbox"/>	Borehole Temperature	<input type="checkbox"/>
Density	<input checked="" type="checkbox"/>	Formation Image (Acoustic)	<input type="checkbox"/>
Gamma Ray	<input checked="" type="checkbox"/>	VSP (walkaway)	<input type="checkbox"/>
Resistivity	<input checked="" type="checkbox"/>	LWD	<input checked="" type="checkbox"/>
Sonic (Δt)	<input checked="" type="checkbox"/>		
Formation Image (Res)	<input checked="" type="checkbox"/>		
VSP (zero offset)	<input type="checkbox"/>		
Formation Temperature & Pressure	<input type="checkbox"/>		
Other Measurements:		Other Tools:	

Estimated Days:

Drilling / Coring	Logging	Total On-Site
		0

Observatory Plan:

Longterm Borehole Observation Plan/Re-entry Plan:

Potential Harzards/Weather:

Shallow Gas	<input checked="" type="checkbox"/>	Complicated Seabed Condition	<input type="checkbox"/>	Hydrothermal Activity	<input type="checkbox"/>	Preferred weather window:
Hydrocarbon	<input type="checkbox"/>	Soft Seabed	<input type="checkbox"/>	Landslide and Turbidity Current	<input type="checkbox"/>	
Shallow Water Flow	<input type="checkbox"/>	Currents	<input type="checkbox"/>	Gas Hydrate	<input checked="" type="checkbox"/>	
Abnormal Pressure	<input checked="" type="checkbox"/>	Fracture Zone	<input checked="" type="checkbox"/>	Diapir and Mud Volcano	<input type="checkbox"/>	
Man-made Objects (e.g. sea-floor cables, dump sites)	<input type="checkbox"/>	Fault	<input checked="" type="checkbox"/>	High Temperature	<input type="checkbox"/>	
H2S	<input type="checkbox"/>	High Dip Angle	<input type="checkbox"/>	Ice Conditions	<input type="checkbox"/>	
CO2	<input type="checkbox"/>					
Sensitive marine habitat (e.g. reefs, vents)						
Other:						

IODP Site Forms

Site Survey Detail

990-Full for Site SKP-14A Submitted 2020-10-09 01:27:08

Data Type	In SSDB	Details of available data and data that are still to be collected
1a High resolution seismic reflection (primary)	yes	Line: KR0114-8 Position 8692
1b High resolution seismic reflection (crossing)	yes	Line: HDNT96 Position 44534
2a Deep penetration seismic reflection (primary)	yes	Line: KR0114-8 Position 8692
2b Deep penetration seismic reflection (crossing)		
3 Seismic Velocity	yes	
4 Seismic Grid		
5a Refraction (surface)		
5b Refraction (bottom)		
6 3.5 kHz		
7 Swath bathymetry		
8a Side looking sonar (surface)		
8b Side looking sonar (bottom)		
9 Photography or video		
10 Heat Flow		
11a Magnetics		
11b Gravity		
12 Sediment cores		
13 Rock sampling		
14a Water current data		
14b Ice Conditions		
15 OBS microseismicity		
16 Navigation		
17 Other		

IODP Site Forms

Environmental Protection

990-Full for Site SKP-14A Submitted 2020-10-09 01:27:08

Pollution & Safety Hazard	Comment
1. Summary of operations at site	LWD first, then APC to refusal and then XCB to TD; RCB if necessary as shown on form 1.
2. All hydrocarbon occurrences based on previous DSDP/ODP/IODP drilling	No previous DSPPS/ODP/IODP drilling
3. All commercial drilling in this area that produced or yielded significant hydrocarbon shows	No previous commercial drilling
4. Indications of gas hydrates at this location	BSR at 750 mbsf
5. Are there reasons to expect hydrocarbon accumulations at this site?	No hydrocarbon accumulation
6. What "special" precautions will be taken during drilling?	No special precautions
7. What abandonment procedures need to be followed?	Open hole
8. Natural or manmade hazards which may affect ship's operations	No other hazards
9. Summary: What do you consider the major risks in drilling at this site?	Unstable borehole because of deformed strata.

IODP Site Forms

Lithologies

990-Full for Site SKP-14A Submitted 2020-10-09 01:27:08

Subbottom depth (m)	Key reflectors, unconformities faults, etc	Age (My)	Assumed velocity (km/s)	Lithology	Paleo-environment	Avg. accum. rate(m/My)	Comments
0 - 900	unconformity at 400 mbsf	Not available	2 km/s	hemipelagic muds and turbidites: silts, sands, clays, ash layers	slope basin or trench fill	Not available	

Site Summary Form 6: Site SKP-14A (Primary) HDNT96 N

Data files in SSDB:

- HDNT96: HDNT096_mig5_sc1_fin.sgy (time)
HDNT096_dep_obsvel_1m_15km.sgy (depth)
- KR0114-8: kr01-14-8_mig_f.sgy (time)
kr01-14-8_200_podm_fin.sgy (depth)
- Velocity information

Interpretation

Red solid line = Fault (arrow indicate slip direction, normal or reverse)

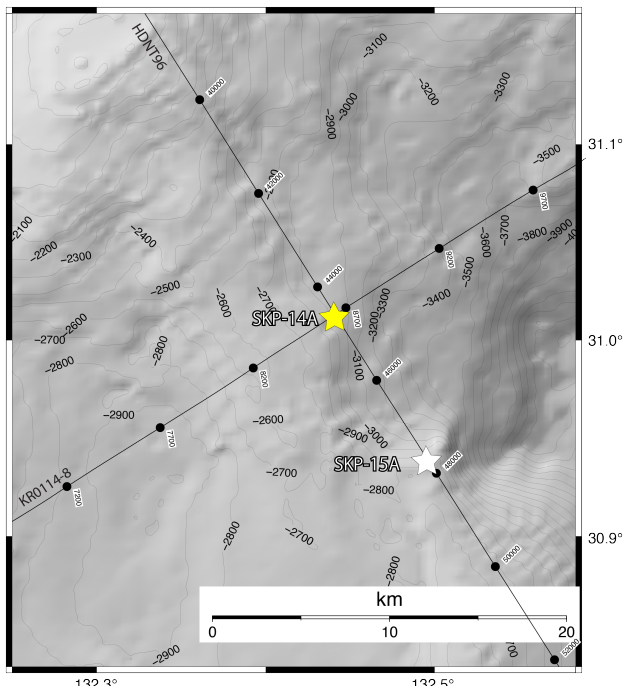
Red dashed line = Detachment

Pink line = Basement/Seamount/plate interface

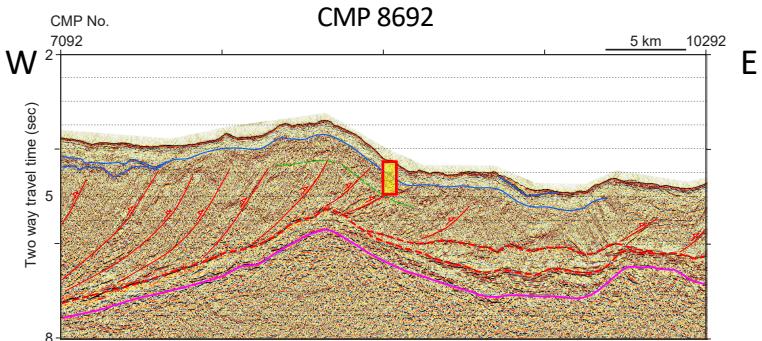
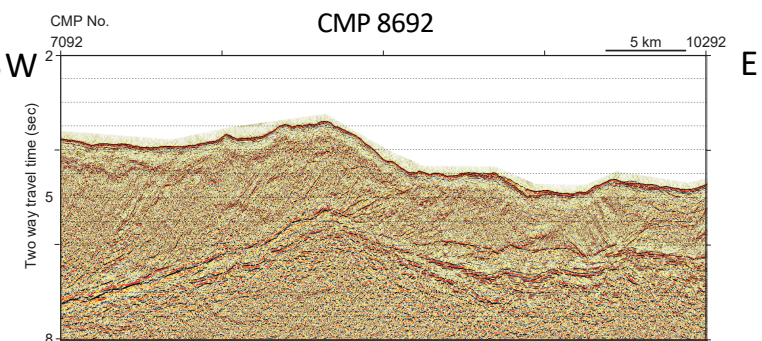
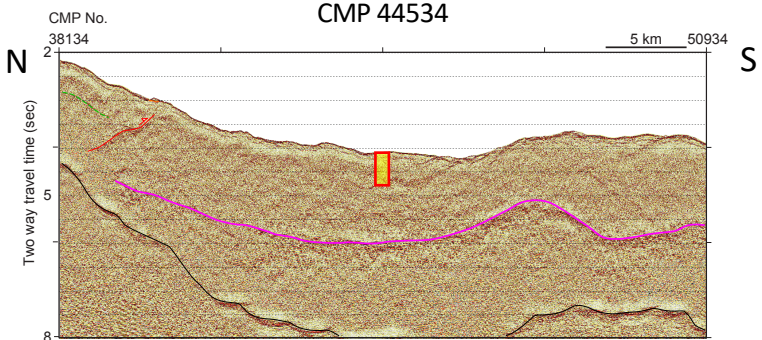
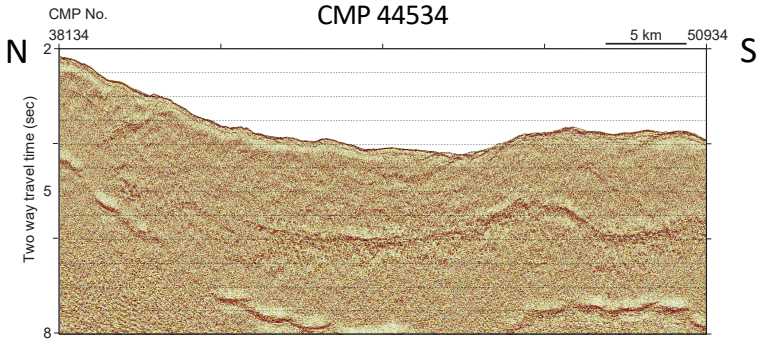
Green dashed line = BSR

Blue solid line = unconformity / lithology or facies boundary / prominent reflector

Black solid line = Multiples



KR0114-8 W



IODP Site Forms

General Site Information

Section A: Proposal Information

Proposal Title:	Drilling and monitoring in Hyuga-Nada: Unveiling effects of ridge subduction on slow earthquakes
Date Form Submitted:	2020-10-09 01:27:08
Site-Specific Objectives with Priority (Must include general objectives in proposal)	Core and log sedimentary section in a middle slope of wedge at the top of a subducting seamount for lithology and physical properties.
List Previous Drilling in Area:	

Section B: General Site Information

Site Name:	SKP-15A		Area or Location:	Western Pacific Ocean Nankai Trough, Hyuganada, Japan
If site is a reoccupation of an old DSDP/ODP Site, Please include former Site#:				Jurisdiction:
Latitude:	30.9434		Distance to Land (km):	119
Longitude:	132.4925		Water Depth (m):	2880
Coordinate System:	WGS 84			
Priority of Site:	Primary <input type="checkbox"/>	Alternate <input checked="" type="checkbox"/>		

Section C: Operational Information

Proposed Penetration (m):

Sediments	Basement	Total Sediment Thickness (m)	Total Penetration (m)
900	0	1800	900

General Lithologies:

hemipelagic muds and turbidites: silts, sands, clays, ash layers	
--	--

Coring Plan (Specify or check):

APC to refusal and then XCB to TD; RCB if necessary
APC <input checked="" type="checkbox"/> XCB <input checked="" type="checkbox"/> RCB <input checked="" type="checkbox"/> Re-entry <input type="checkbox"/> PCS <input type="checkbox"/>

Wireline Logging Plan:

Standard Measurement		Special Tools	
Wireline Logging	<input type="checkbox"/>	Magnetic Susceptibility	<input type="checkbox"/>
Porosity	<input checked="" type="checkbox"/>	Borehole Temperature	<input type="checkbox"/>
Density	<input checked="" type="checkbox"/>	Formation Image (Acoustic)	<input type="checkbox"/>
Gamma Ray	<input checked="" type="checkbox"/>	VSP (walkaway)	<input type="checkbox"/>
Resistivity	<input checked="" type="checkbox"/>	LWD	<input checked="" type="checkbox"/>
Sonic (Δt)	<input checked="" type="checkbox"/>		
Formation Image (Res)	<input checked="" type="checkbox"/>		
VSP (zero offset)	<input type="checkbox"/>		
Formation Temperature & Pressure	<input type="checkbox"/>		
Other Measurements:		Other Tools:	

Estimated Days:

Drilling / Coring	Logging	Total On-Site
		0

Observatory Plan:

Longterm Borehole Observation Plan/Re-entry Plan:

Potential Harzards/Weather:

Shallow Gas	<input checked="" type="checkbox"/>	Complicated Seabed Condition	<input type="checkbox"/>	Hydrothermal Activity	<input type="checkbox"/>	Preferred weather window:
Hydrocarbon	<input type="checkbox"/>	Soft Seabed	<input type="checkbox"/>	Landslide and Turbidity Current	<input type="checkbox"/>	
Shallow Water Flow	<input type="checkbox"/>	Currents	<input type="checkbox"/>	Gas Hydrate	<input checked="" type="checkbox"/>	
Abnormal Pressure	<input checked="" type="checkbox"/>	Fracture Zone	<input checked="" type="checkbox"/>	Diapir and Mud Volcano	<input type="checkbox"/>	
Man-made Objects (e.g. sea-floor cables, dump sites)	<input type="checkbox"/>	Fault	<input checked="" type="checkbox"/>	High Temperature	<input type="checkbox"/>	
H2S	<input type="checkbox"/>	High Dip Angle	<input type="checkbox"/>	Ice Conditions	<input type="checkbox"/>	
CO2	<input type="checkbox"/>					
Sensitive marine habitat (e.g. reefs, vents)						
Other:						

IODP Site Forms

Site Survey Detail

990-Full for Site SKP-15A Submitted 2020-10-09 01:27:08

Data Type	In SSDB	Details of available data and data that are still to be collected
1a High resolution seismic reflection (primary)	yes	Line: HDNT96 Position 47515
1b High resolution seismic reflection (crossing)		
2a Deep penetration seismic reflection (primary)	no	
2b Deep penetration seismic reflection (crossing)		
3 Seismic Velocity	yes	
4 Seismic Grid		
5a Refraction (surface)		
5b Refraction (bottom)		
6 3.5 kHz		
7 Swath bathymetry		
8a Side looking sonar (surface)		
8b Side looking sonar (bottom)		
9 Photography or video		
10 Heat Flow		
11a Magnetics		
11b Gravity		
12 Sediment cores		
13 Rock sampling		
14a Water current data		
14b Ice Conditions		
15 OBS microseismicity		
16 Navigation		
17 Other		

IODP Site Forms

Environmental Protection

990-Full for Site SKP-15A Submitted 2020-10-09 01:27:08

Pollution & Safety Hazard	Comment
1. Summary of operations at site	LWD first, then APC to refusal and then XCB to TD; RCB if necessary as shown on form 1.
2. All hydrocarbon occurrences based on previous DSDP/ODP/IODP drilling	No previous DSPPS/ODP/IODP drilling
3. All commercial drilling in this area that produced or yielded significant hydrocarbon shows	No previous commercial drilling
4. Indications of gas hydrates at this location	No BSR at this site
5. Are there reasons to expect hydrocarbon accumulations at this site?	No hydrocarbon accumulation
6. What "special" precautions will be taken during drilling?	No special precautions
7. What abandonment procedures need to be followed?	Open hole
8. Natural or manmade hazards which may affect ship's operations	No other hazards
9. Summary: What do you consider the major risks in drilling at this site?	Unstable borehole because of deformed strata.

IODP Site Forms

Lithologies

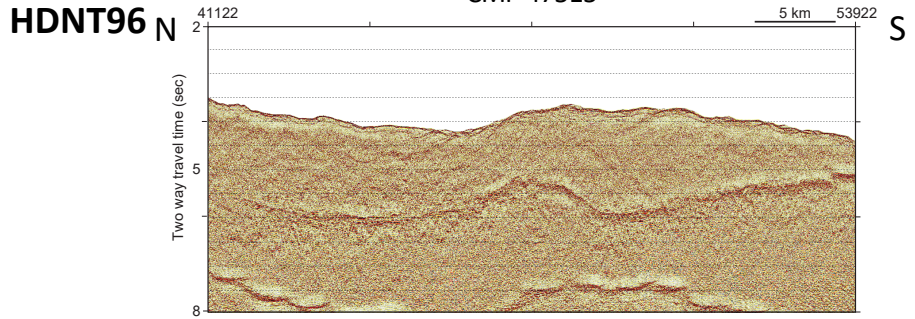
990-Full for Site SKP-15A Submitted 2020-10-09 01:27:08

Subbottom depth (m)	Key reflectors, unconformities faults, etc	Age (My)	Assumed velocity (km/s)	Lithology	Paleo-environment	Avg. accum. rate(m/My)	Comments
0 - 900	No event	Not available	2 km/s	hemipelagic muds and turbidites: silts, sands, clays, ash layers	slope basin or trench fill	Not available	

Site Summary Form 6: Site SKP-15A

Data files in SSDB:

- HDNT96: HDNT096_mig5_sc1_fin.sgy (time)
HDNT096_dep_obsvel_1m_15km.sgy (depth)
- Velocity information



Interpretation

Red solid line = Fault (arrow indicate slip direction, normal or reverse)

Red dashed line = Detachment

Pink line = Basement/Seamount/plate interface

Green dashed line = BSR

Blue solid line = unconformity / lithology or facies boundary / prominent reflector

Black solid line = Multiples

